Multimolecular adaptor protein complexes in B cell receptor signaling

Dissertation
for the award of the degree
"Doctor rerum naturalium"
of the Georg-August-Universität Göttingen

within the doctoral program Molecular Biology of Cells
of the Georg-August University School of Science (GAUSS)

submitted by
Julius Kühn

from **Frankfurt am Main**

Göttingen 2015

Thesis Committee

Prof. Dr. Jürgen Wienands, Department of Cellular and Molecular Immunology, University Medical Center Göttingen

Prof. Dr. Blanche Schwappach, Department of Molecular Biology, University Medical Center Göttingen

Prof. Dr. Henning Urlaub, Bioanalytical Mass Spectrometry, Max Planck Institute for Biophysical Chemistry

Members of the Examination Board

Referee: Prof. Dr. Jürgen Wienands, Department of Cellular and Molecular Immunology, University Medical Center Göttingen

2^{nd} Referee: Prof. Dr. Blanche Schwappach, Department of Molecular Biology, University Medical Center Göttingen

Further members of the Examination Board

Prof. Dr. Henning Urlaub, Bioanalytical Mass Spectrometry, Max Planck Institute for Biophysical Chemistry

Prof. Dr. Michael Thumm, Department of Cellular Biochemistry, University Medical Center Göttingen

Prof. Dr. Dieter Kube, Department for Hematology and Oncology, University Medical Center Göttingen

Prof. Dr. Uwe Groß, Department of Medical Microbiology, University Medical Center Göttingen

Date of oral examination: 28^{th} of May 2015

Declaration of academic honesty

Herewith I declare that I prepared the doctoral thesis "Multimolecular adaptor protein complexes in B cell receptor signaling" on my own with no other sources and aids than indicated.

Göttingen, 13^{th} of April 2015

Julius Kühn

Table of Contents

1 Summary

The activation of B cells is the crucial step of the humoral immune response. This process is controlled by the B cell receptor (BCR) signaling pathway which is initiated by antigen recognition. An elaborated and detailed understanding of this pathway is of great interest given that its misregulation is involved in the genesis of leukemia and immunodeficiencies. The adaptor protein SLP65 is a key regulator in BCR signaling. After phosphorylation of its tyrosine residues, SLP65 serves as assembly site for enzymes and facilitates their mutual activation. The activation of SLP65 by phosphorylation is a multi-step process that requires SH3 domain-binding proline motifs within SLP65. These motifs mediate the interaction of SLP65 with the adaptor protein CIN85. While it was known at the beginning of my doctoral thesis project that the SLP65-CIN85 interaction supports the function of SLP65 in the BCR pathway, the underlying mechanism remained totally unclear. The elucidation of this mechanism constitutes the aim of my doctoral thesis.

By a genetic approach including chimeric proteins I could localize the effector function of CIN85 in its C-terminal coiled-coil (CC) domain. To get insight into the function of the CIN85-CC, I determined the protein interactome of CIN85 by SILAC-based mass spectrometry and investigated membrane lipid binding by biochemical means. Next, I focused on the structure of the CIN85-CC in cooperation with Prof. C. Griesinger's group. By NMR-spectroscopy, we obtained the result that the CIN85-CC forms a stable trimer. In further genetic experiments, I determined that oligomerization of SLP65 is essential for its function in the BCR signaling pathway. Because CIN85 forms a trimer with nine SLP65 binding sites, it provides the required oligomerization by simultaneous binding of several SLP65 molecules . Furthermore, I found out that the SLP65 N-terminus is a pre-requisite for efficient SLP65 oligomerization. As the N-terminus targets SLP65 to intracellular membranes, I could identify vesicles as the platform for SLP65-oligomerization by CIN85. Because CIN85 and its homolog CD2AP interact with several other proteins in the same manner as with SLP65, this mechanism is likely a general biological principle of action for the CIN85-family adaptor proteins.

2 Introduction

2.1 Discovery of antibodies and B cells: a story of 130 years

The immune system is the crucial line of defense of every multicellular organism against pathogens and cancer development. Antibodies are soluble proteins that recognize and fight pathogens specifically. They play a key role for an effective immune response. The importance of molecules with antibody-like function can be seen from the fact that they are found in all vertebrates from lamprey on (reviewed in [28]).

The discovery of antibodies is closely linked to the discovery of the immune system itself. The first scientific approach to understand the immunizing factors of our body were made in the ending 18^{th} century. Edward Jenner discovered that a human being was protected from smallpox infection after the application of the relatively harmless cowpox virus (*vaccinia*) (reviewed in [193]). This was the birth of the procedure nowadays known as vaccination.

The key discoveries for the evolvement of immunology as a science were made in the second half of the 19^{th} and the beginning of the 20^{th} century (reviewed in [22] and [156]). They are linked to names like Louis Pasteur (first rabies vaccination), Emil von Behring, Paul Ehrlich and Ilja Metchnikow. Two fundamental concepts were developed in this time: There was the finding of Behring and Kitasato that diphtheria-infected children could be cured by the application of the serum of diphtheria-infected rabbits (serotherapy). The phenomenon was called *humoral immunity*, pathogen resistance transferred by liquid (*humor* in Latin). This concept was postulated, amongst others, by P. Ehrlich, who proposed the "side chain theory". Receptors ("side chains") on the cell surface would recognize a pathogenic structure which would lead to the secretion of soluble components that have the ability to neutralize pathogens. The other concept, strongly promoted by I. Metchnikow and others, based on phagocytosis (Ancient Greek for "devouring by a cell"). It was observed that specific cells can internalize, phagocytose, pathogens like bacteria. The process of phagocytosis was termed *cellular immunity* because it was conferred by cells, not by serum. The two concepts of humoral and cellular immunity were initially seen contradictory. The insight that both of them can be unified developed only later on.

The components of the humoral immune response, i.e. the serum molecules that could transfer immunity between individuals, remained enigmatic for a long time. The molecules we know today as "antibodies", a term used by P. Ehrlich already in 1891, were also called "fixatives" or "sensitizing substances" (I. Metchnikow) at the beginning. Their astonishing abilities to cause blood agglutination, bacterial lysis, and systemic protection of the organism at the same time led to confusion about their nature and origin. Until the 1940s, it was widely believed that phagocytotic cells were also responsible for antibody production. This picture was challenged when M. Bjørneboe and H. Gormsen described the production of antibodies by plasma cells and proposed that lymphocytes and plasma cells could be involved in the generation of antibodies. The antibody production by plasma cells was later confirmed by experiments

by A. Fagraeus and others. On the other hand, antibody production by lymphocytes was shown by N. Jerne and A. Nordin. The question of the origin of plasma cells was still open until the 1960s, when it could be shown by J. Gowans that plasma cells originate from lymphocytes which led to a conclusive theory of the cellular source of antibodies.

Lymphocytes, already discovered in the late 19^{th} century by A. Maximow, P. Ehrlich and others, could not be assigned to an exact immunological function for a long time period. J. Murphy succeeded in showing their importance for the immune response already in the 1910s, but their mechanistic role remained completely unknown. In 1965, M. Cooper could classify lymphocytes according to the origin of their development in T-lymphocytes (development in the **T**hymus) and B-lymphocytes (development in the **B**ursa fabricii in chicken, in the bone marrow in mammals) (reviewed in [27]). His work could also identify B-lymphocytes to be responsible for antibody production. T-lymphocytes have been shown to play an essential role for cellular immunity and possess a supportive role in B-lymphocyte-mediated production of antibodies.

Having established the cellular framework of antibody production, it was possible to investigate the molecular mechanisms in detail. This was especially facilitated by the development of new biochemical and genetic methods, most notably protein sequencing and polymerase chain reaction. One burning question that had occurred in this time was how the immense repertoire of diverse antibodies against virtually every pathogenic structure was generated. Germ-line coding of a myriad of different antibodies would overextend the limits of the human genome. The model of DNA recombination was developed in the 1970s by S. Tonegawa and others to explain this phenomenon (see section 2.2.1 for details).

The new methods enabled the identification of proteins and genes that are necessary for B cell function. The recognition tool of B cells for their specific pathogen-derived target structure, the antigen, was identified to be a membrane-associated antibody, termed B cell receptor (BCR). This sensing of the antigen presence is essential for the activation of a B cell and hence the whole humoral immune response. The details of molecular processes involved in BCR-signal propagation have been studied since at least three decades, yet there remain riddles and open questions that are still waiting to be solved.

2.2 Current understanding of BCR structure and signaling

2.2.1 Structure of antibodies and BCR

The BCR consist of an antibody molecule containing a transmembrane domain and the two associated signaling chains Igα (CD79a) and Igβ (CD79b) [21, 146]. The Igα-Igβ heterodimer associates with the membrane-anchored antibody by non-covalent interactions [21, 187, 139]. In general, the BCR allows the B cell to detect the presence of its antigen by antigen binding of the antibody part and subsequent transduction of this signal by the signaling chains. The molecular structure of an antibody, or immunoglobulin

(Ig), molecule was elucidated in the 1960, mainly by works of R. Porter and G. Edelman (reviewed in [188] and [162]). An immunoglobulin molecule consists of two Ig heavy chains and two Ig light chains. They form a Y-shaped ensemble with individual chains interlinked by disulfide bridges. The two heavy chains are linked by a varying number of disulfide bridges, while each light chain is linked to one heavy chain by usually one disulfide bridge [101]. The antibody molecule can be separated in two functionally distinct regions: the variable (V) domains which is responsible for antigen binding and the constant (C) domains which exhibits the effector functions of the antibody. Each chain of the antibody consists of several immunoglobulin super-family (IgSF) domains. IgSF domains display a characteristic fold of two sandwiched β-sheets, linked by one disulfide bridge. The N-terminal IgSF domain of each Ig chain is the V domain. The following C-terminal IgSF domains are C domains. Ig light chains contain only one C domain, while Ig heavy chains contain three or four C domains, depending on the antibody class. The first (CH1) and the second (CH2) domain surround a spacer region which forms a "hinge", resulting in the Y-shaped structure of an antibody shown in Figure 2.1.

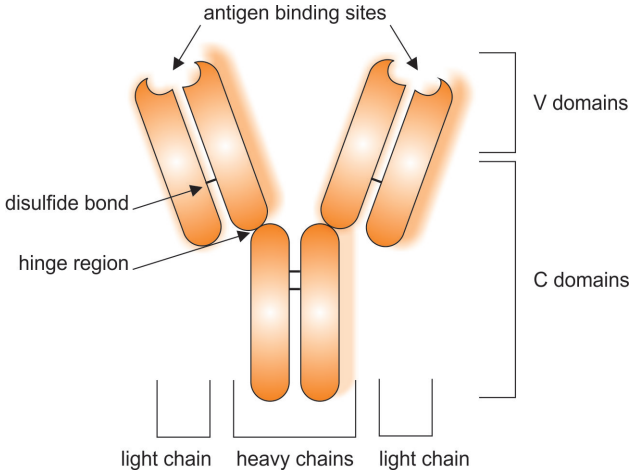

Fig. 2.1: Schematic structure of an antibody molecule. An antibody consists of two Ig light and to Ig heavy chains. The chains are linked by disulfide bridges. The structure of an antibody resembles an "Y" due to the hinge region between the C domains CH1 and CH2. The antigen binding sites are located within the V domains, the N-terminal IgSF domain of each chain. The following IgSG domains, the C domains (three for IgG), provide binding sites for Fc receptors and complement components.

The entire repertoire of immunoglobulins has the ability to bind to a nearly all occuring antigenic patterns, despite the structural heterogeneity of the antigens. This variety is enabled by genomic DNA-recombination of the multigene family coding Ig heavy and light chains. The V domain is encoded by V, D, and J gene segments, while the C domains are encoded by whole exons. The V, D, and J segments are arranged by DNA-recombination to constitute a complete V domain. Because the genome contains

multiple different versions of each segment, this enables a large combinatorial diversity of V domains. Imprecise segment arrangement, the introduction of single point mutations, and the presence of two different Ig light chains, termed κ and λ, can further enlarge the antibody repertoire. Altogether, the number of potentially produced immunoglobulin molecules can be estimated to exceed 10^{16}. The really observed repertoire of antibodies and BCRs is nevertheless more limited. B cells undergo positive and negative selection processes during their development (reviewed in [37]). Furthermore, the fate of a B cell depends on the presence of its antigen. Generally, B cells that encounter their antigen start to proliferate. Thereby they can out-compete other B cells, a process termed clonal selection by F. M. Burnet (reviewed in [140]).

In contrast to the huge diversity of the V domains, the C domains of an antibody are germ-line encoded without further modifications. The C domains of an Ig heavy chain can originate from nine different CH genes, defining the human antibody classes. The CH region of each class can be linked to an arranged V domain by DNA recombination in a process termed class switch recombination. The CH region undergoes alternative splicing so that the same transcript can encode for a soluble antibody or a membrane bound BCR.

2.2.2 Antibody function

In humans, there exist the five antibody classes IgA (subclasses IgA1 and IgA2), IgD, IgE, IgG (subclasses IgG1-IgG4) and IgM. They differ in their structure and as a result also in their biologic functions. The effector functions of an antibody are determined by the C-terminal IgSF-domains of its Ig heavy chain. The domains CH2-CH3 (for IgG, IgD and IgA) or CH2-CH4 (for IgM and IgE) represent the Fc (Fragment crystallizable) part of an antibody. The Fc part mediates the antibody effector function because it provides the ability to cause antibody-dependent cellular cytotoxicity (ADCC) or complement-dependent cytotoxicity (CDC). ADCC is mediated by Fc receptors (FcRs) that bind to the Fc part of an antibody. Many cells of the immune system, e.g. monocytes and macrophages, display Fc receptors on their surface. This allows them to recognize antibody-coated structures like a pathogen cell and attack them by phagocytosis or lysis due to cytotoxin secretion. By means of CDC, antibodies can target cells for destruction by the complement system. The complement component C1q has the ability to bind to Fc parts and to initiate the lysis of the antibody coated cell. Both processes, ADCC and CDC, depended on the glycosylation pattern of the Fc part. Besides these effector functions, antibodies can also directly neutralize their antigen. They can e.g. inhibit the cell entry of a pathogen by masking a protein structure involved in this process or prevent the effect of toxins.

The membrane-bound form of IgM is the first BCR expressed in the B cell development and it is found on all naïve B cells. Analogously, the secreted form of IgM is the first immunoglobulin produced in an immune response. It forms a pentamer that has a high ability to work by CDC. As IgM antibodies

originate normally from cells that did not experience extended affinity maturation in a germinal center reaction, their affinity towards the antigen is low compared to other antibody classes. The pentameric nature of IgM can compensate for this by an increased avidity.

The IgD-BCR is expressed on naïve B cells and originates from the same mRNA as the IgM-BCR by alternative splicing. The serum levels of soluble IgD are extremely low. Its physiological function is not yet clarified.

Monomeric IgG antibodies display the main portion of immunoglobulins in the serum. Because IgG originates from class switching during a germinal center reaction, IgG antibodies have usually undergone affinity maturation and possess a high affinity towards their antigen. This makes them efficient neutralizers for toxins and viruses. The Fc part of IgG binds to a variety of FcγRs present on many cell types of the immune system, thus IgG mediates ADCC most efficiently. In comparison to the IgM- and IgD-BCR, the IgG-BCR has an additional cytoplasmatic motif, the immunoreceptor tail tyrosine (ITT) motif that contributes to BCR signaling in addition to Igα and Igβ [41].

IgA antibodies are the most abundant immunoglobulins at mucosal surfaces. They are mainly present as monomers in the serum, but as dimers in the mucosa. IgA can act through neutralization of antigens, preventing the uptake of pathogens at mucosal surfaces. It can also cause ADCC by binding to the FcαR which is present e.g. on neutrophiles.

The level of soluble IgE antibodies is very low. They are implicated in the defense against parasites and the triggering of allergies. IgE binds to the FcϵR on mast cells with an extraordinary high affinity. Like the IgG-BCR, the IgE-BCR possesses an ITT motif [41].

2.2.3 Activation of BCR signaling by antigen binding: still partially a mystery

Despite the structure of the BCR molecule is known in very detail, the oligomerization state of the BCR in resting cells is still under debate (reviewed in [134]) . It has been found that the BCR is mainly mobile and monomeric without stimulation by antigen binding [183]. Contradictory, it was reported that the BCR is present on resting cells as a signaling inactive dimer or higher oligomer [198]. Also the change of the oligomerization state after antigen binding is seen controversially. According to the most established model, signaling-inactive BCR monomers are physically crosslinked by encountering their antigen which leads in turn to the formation of oligomeric signaling-active BCR complexes, described as microclusters (reviewed in [134]). On the other hand, the dissociation activation model proposes the presence of signaling-inactive oligomers which would dissociate after antigen encounter, forming signaling active monomers [198, 85].

Regardless which model of BCR activation might fit best to reality, the next essential step after the antigen encounter is the phosphorylation of the immunoreceptor tyrosine-based activation motifs (ITAMs) in the BCR-signaling chains Igα and Igβ. One ITAM consist of the sequence YXXI/LX_7YXXI/L that

is present once the Igα tail and once in the Igβ tail [145]. The kinases of the Src-family, mainly Lyn, and the spleen tyrosine kinase (Syk) have been found to be implicated in ITAM phosphorylation [32, 85]. The exact triggering of the ITAM phosphorylation process remains partially unclear. Changes in BCR conformation as well as a changed lipid environment of BCR oligomers seem to play a role (reviewed in [134]). The tyrosine phosphorylation of the ITAMs creates binding sites for the tandem SH2 domains of Syk [191, 45]. The interaction of Syk with the phosphorylated ITAMs leads to an enhancement of the Syk kinase activity [150]. This activation of Syk is essential for BCR signaling because Syk phosphorylates the adaptor protein SLP65, also called BLNK [47]. The complex of the two adaptor proteins SLP65 and CIN85 is a key signaling transducing element for the BCR and the focus of this doctoral thesis.

2.3 SLP65: A central adaptor molecule for BCR signaling

Adaptor proteins is a term commonly used for proteins that possess no inherent enzymatic activity but contain protein-protein or protein-lipid interaction domains. These can influence biological processes by targeting ligands to specific subcellular localizations, regulate their enzymatic activities allosterically, or enable the formation of protein complexes (reviewed in [95]). Adaptor proteins determine the spatial and temporal organization of protein complexes in cells to a large extent (reviewed in [52]). Enzymes and adaptor proteins cannot be strictly separated because many enzymes possess also adaptor protein properties.

The adaptor SH2-domain containing leukocyte protein of 65 kDa (SLP65), also called B cell linker (BLNK), B cell adaptor containing SH2 domain (BASH) or B cell activation (bca) gene product, was identified as a protein heavily phosphorylated upon BCR stimulation [192, 47, 51, 49]. SLP65 is essential for both, B cell development and activation [47, 195, 78, 110]. It is phosphorylated by Syk, but not by the Tec-family kinase Btk [47]. For chicken SLP65, nine phosphorylated tyrosine residues can be detected, seven of which are conserved in human SLP65 [122].

While the lack of SLP65 leads always to severe impairment of B cell development and function, the degree of this impairment depends on the investigated species. In the chicken B cell line DT40, SLP65 deficiency abolishes completely Ca^{2+} mobilization upon BCR stimulation [75]. In contrast, there is still Ca^{2+} mobilization detectable in SLP65-deficient mice, even if it is reduced compared to wildtype mice [127, 78]. This remaining Ca^{2+} signaling is attributed to the complementation of SLP65 by other adaptors expressed in mouse B cells, like SLP76 [170], or alternative pathways of Ca^{2+} mobilization, e.g. CD19 signaling ([38] and reviewed in [95]. As a result of an impaired B cell development, SLP65-deficient mice show reduced B cell numbers [127]. The immune response to T-cell-independent antigens is abolished [197]. Human patients with SLP65-deficiency show a severe immunodeficiency, they do not have mature B cells and suffer from agammaglobulinemia [110].

SLP65 mediates Ca^{2+} influx by assembly of the Ca^{2+} initiation complex, consisting of Bruton's ty-

rosine kinase (Btk), phospholipase C-γ2 (PLC-γ2), and SLP65 itself [97].
Btk is a protein tyrosine kinase [142]. Mutations in the Btk gene lead to immunodeficiency in form of X-linked agammaglobulinemia (XLA) [185, 123]. On cellular level, impaired Btk activation results in reduction of BCR-induced Ca^{2+} signaling [141]. Btk has been shown to be activated by two mechanisms upon BCR stimulation. Firstly, Btk is recruited to the plasma membrane by its binding to the membrane lipid PIP_3 which is produced after BCR stimulation [151]. Secondly, Btk is additionally activated by tyrosine phosphorylation in its activation loop, carried out by Src-family kinases like Lyn [143]. By its SH2 domain, Btk can bind to the phospho-tyrosine (pY) 96 of SLP65 [62, 171]. This association is crucial for Btk function [172]. On one hand, it can promote Btk activity by bringing Btk to the proximity of Lyn and Syk what might lead to phosphorylation of the Btk activation loop [7]. On the other hand, the binding to SLP65 facilitates the interaction of Btk with its substrate PLC-γ2 [62, 97].

PLC-γ2 is activated by phosphorylation by Syk [175] and Btk [46]. This phosphorylation processes are dependent on the presence of phosphorylated SLP65 that serves as a platform for the assembly of the PLC-γ2-Btk complex (Ca^{2+} initiation complex) [75, 96]. The SH2 domains of PLC-γ2 bind to pY178 and pY189 of SLP65 [47, 76]; its C2 domain binds to pY119 [39]. It has been shown that SLP65 assembles Btk and PLC-γ2 in *cis*, as both proteins have to be bound to the same SLP65 molecule [24]. After full activation, PLC-γ2 cleaves the plasma membrane lipid phosphatidylinositol-4,5-bisphosphate (PIP_2) into the second messenger molecules inositol trisphosphate (IP_3) and diacyl-glycerol (DAG) [69]. IP_3 binds to the IP_3 receptor in the membrane of the endoplasmic reticulum (ER), resulting in the release of Ca^{2+} from the ER lumen to the cytosol by the opening of ion channels (reviewed in [11]). The emptying of the ER Ca^{2+} reservoir leads in turn to the Stromal interaction molecule (STIM)-mediated opening of store-operated Ca^{2+} channels (SOCs) in the plasma membrane. This results in the influx of extracellular Ca^{2+} (reviewed in [105] and [155]).

The influx of Ca^{2+} and the generation of DAG initiate signaling cascades that lead in the end to the activation of a variety of transcription factors. The elevated intracellular Ca^{2+} concentration is crucial for the activation and nuclear translocation of the transcription factors NfκB and NFAT [4]. Furthermore, high Ca^{2+} levels cooperate with DAG binding to activate the protein kinase C-β (PKC-β) ([120]. PKC-β phosphorylates the protein CARD11, followed by the activation of the Inhibitor of κB kinase (IKK) and the nuclear translocation of the transcription factor NfκB ([132], reviewed in [163]).
The DAG-mediated activation of PKC-β triggers as well signaling pathways leading to the activation of the mitogen-activated protein kinases (MAPKs) JNK and p38 [56, 61]. DAG provides also a docking site for RasGRP proteins [29]. This leads in turn to activation of the MAPK pathway via Ras, resulting in the activation of different transcription factors by the extracellular signal-regulated kinase (ERK) [61]. ERK can alternatively be activated by an adaptor function of SLP65 independent of the Ca^{2+}

initiation complex. SLP65 binds the adaptor Grb2 which mediates the recruitment of the protein SOS. SOS activates Ras and initiates MAPK activation [192, 47, 5]. The MAPKs activate many transcription factors that play a role in lymphocyte activation, proliferation, and differentiation (reviewed in [148] and [113]). Figure 2.2 gives an overview of the described signaling pathways initiated by BCR stimulation and mediated by SLP65.

Depending on the developmental stage of the B cell and other extracellular signals, BCR signaling can support activation and proliferation, but under certain circumstances also anergy or apoptosis (e.g. in autoreactive B cells) (reviewed in [118]).
As an upstream event for all of the described pathways, the phosphorylation of SLP65 is a key step for BCR signaling. While the signaling pathways downstream of SLP65 are quite well understood, there is still one unsolved problem regarding this molecule itself. It is unclear how SLP65 is translocated from the cytosol to the plasma membrane upon BCR stimulation. The adaptor protein homolog of SLP65 in T cells, SLP76, has been shown to be targeted to the plasma membrane by binding to the membrane protein LAT via the adaptor GADS [103]. However, for SLP65 no such membrane anchor could be identified yet. The question of SLP65 membrane recruitment requires a closer look at the SLP65 domain structure and its multiple interactions.

2.4 The SLP65 regions and their functions

SLP65 consists of a positively charged N-terminal region, a central proline rich region and a C-terminal SH2 domain (Figure 2.3).

The N-terminal region of SLP65 has been described to form a leucine zipper which associates presumably with a membrane protein to provide SLP65 membrane anchoring [87]. In contrast, our analyses pointed to the direction that the N-terminus is not primarily a protein-protein-interaction-mediating leucine zipper but a lipid interaction module. It anchors SLP65 to membranes, dependent on their curvature [40, 136]. The N-terminus is crucially required for the translocation of SLP65 to the plasma membrane. It has been shown that the SLP65 N-terminus can be substituted by a lipid binding device, namely a myristoylation signal [87] or the membrane anchoring domain of TIRAP [67, 18].
The C-terminal SH2 domain of SLP65 is essential for the anchoring of SLP65 to the plasma membrane and the BCR [2]. It binds to the non-ITAM pY204 in the tail of Igα [42, 79]. However, in a chimeric CD8-Igα/CD8-Igβ model, the SLP65-Igα interaction was partially dispensable, questioning its relevance for SLP65 membrane and BCR recruitment under all conditions [135]. Consistent with this observation, transgenic mice with a Y-to-F exchange of Y204 of Igα showed that the SLP65-Igα interaction is only important for T-cell-independent immune responses [129]. The SH2 domain does also bind to the kinase HPK1 [184, 154] and Syk. The Syk-SLP65 interaction can occur without Syk phosphorylation [2].

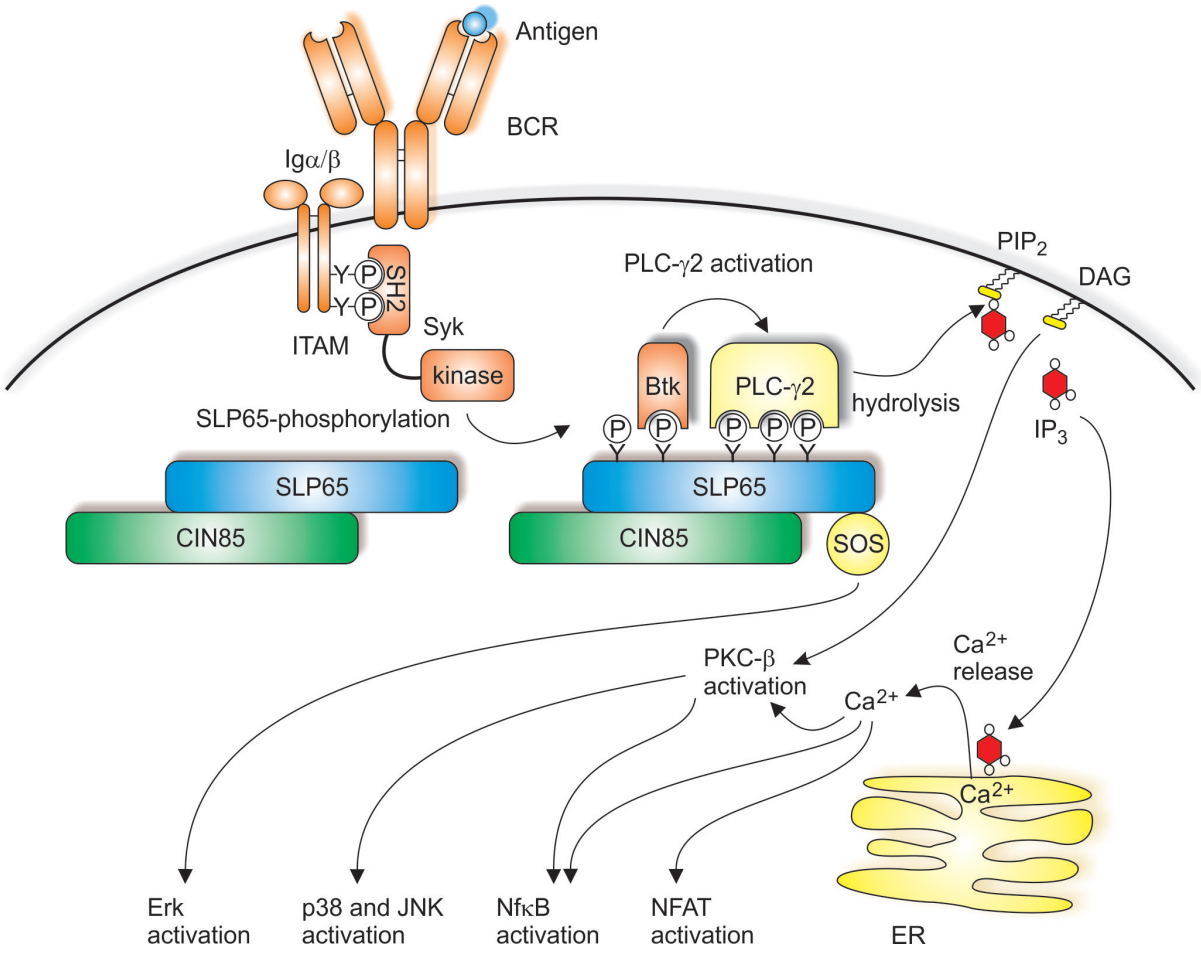

Fig. 2.2: Overview of the SLP65 functions in BCR signaling. The BCR is activated by binding to its antigen. This leads to phosphorylation of two tyrosines residues in the ITAM motif which display a binding site for the SH2 domain of the kinase Syk. Activated Syk phosphorylates the adaptor protein SLP65 which is in a steady complex with the adaptor CIN85. After its phosphorylation, SLP65 constitutes a platform for the assembly of the kinase Btk and the lipase PLC-γ2, resulting in PLC-γ2 activation. PLC-γ2 hydrolyzes the membrane lipid PIP_2 to produce the second messengers DAG and IP_3. IP_3 mediates the influx of Ca^{2+} from the ER to the cytosol. DAG initiates the activation of the kinase PKC-β, this process is enhanced by the elevated Ca^{2+} concentration. PKC-β activation and Ca^{2+} influx trigger signaling cascades that lead in the end to the activation of the transcription factors NFAT, NfκB and of the MAP kinases p38 and JNK. The activation of the MAP kinase Erk is triggered either by SOS, a molecules recruited by SLP65 via Grb2, or alternatively by DAG via the recruitment of RasGRP (not depicted). The activation of transcription factors and MAP kinases changes the transcriptional program of the B cell and may promote activation and proliferation, but also anergy, depending on other extracellular signals.

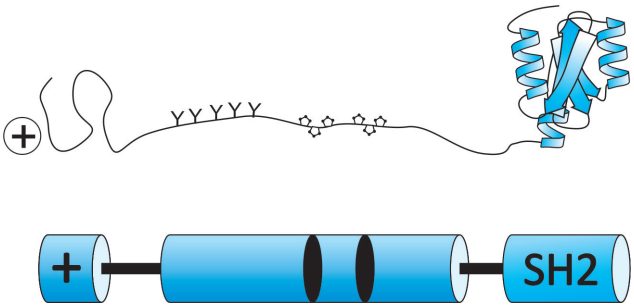

Fig. 2.3: Schematic domain structure of SLP65. SLP65 possesses a positively charged N-terminal region (aa 1-45, labeled by +). The following region of the protein is proline rich (aa 46-345, not labeled). This region contains two PXXXPR motifs as binding sites for CIN85 (aa 242-247 and 307-312, depited by black ovals). The C-terminus of the protein forms a SH2 domain (aa 346-453, SH2). The upper image displays the known secondary structure elements in SLP65. Y represents a tyrosine residue that is phosphorylated upon BCR stimulation. The pentagons represent proline residues of the two CIN85 binding sites.

The central proline rich region (PRR) of SLP65 contains the tyrosine residues that are phosphorylated upon BCR stimulation and several proline-containing interaction motifs [121]. Three motifs with the consensus sequence PXXXPR have been shown to interact with SH3 domains of the adaptor protein CIN85 [122]. The second and third of these three motifs are responsible for the interaction of SLP65 with CIN85, while the first motif is dispensable [122]. The SLP65-CIN85 interaction is required for efficient SLP65 plasma membrane recruitment and phosphorylation and hence for the induction of Ca^{2+} mobilization [121]. So the SLP65-CIN85 interaction constitutes a third functionality that is important for SLP65 plasma membrane recruitment, besides SLP65 N-terminus and SH2 domain.

2.5 CIN85: a multi-domain adaptor protein with still mysterious functions

The human Cbl-interacting protein of 85 kDa (CIN85) has been cloned and characterized by Take, Watanabe and colleagues. [176, 189]. Simultaneously, its homolog in rats was cloned by Gout and colleagues and Bögler and colleagues who termed the protein Regulator of ubiquitous kinase (Ruk) respectively SH3 domain containing gene expressed in tumorigenic astrocytes (SETA) [55, 15]. From the beginning on, CIN85 was characterized as an adaptor protein binding to the ubiquitin E3 ligase c-Cbl [176]. Together with its homolog CD2AP, it forms a family of adaptor proteins [176, 55]. Its domain structure was elucidated very soon after the cloning of the gene on the basis of bioinformatics [176, 189]. CIN85 has three N-terminal SH3 domains followed by a proline-rich region (PRR) and a C-terminal coiled-coil (CC) domain (Figure 2.4). The structure prediction could be confirmed by NMR spectroscopy studies. The structure of all three SH3 domains is known ([1, 133]. Structure and oligomerization state of the CC were solved in a collaboration of C. Griesinger's and our group (see 4.10).

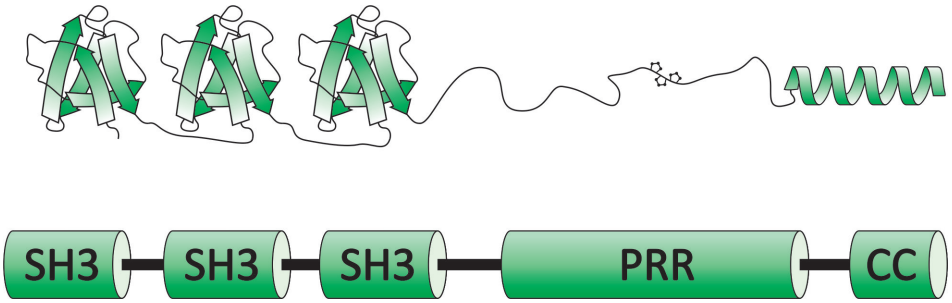

Fig. 2.4: Schematic domain structure of CIN85. CIN85 possesses three N-terminal SH3 domains (aa 1-328, SH3), followed by a proline-rich region (aa 329-599, PRR). The C-terminal part of CIN85 consists of a coiled-coil domain (aa 600-665, CC). The upper image displays the known secondary structure elements in CIN85.The pentagons represent proline residues of the intramolecular SH3 domain binding site within the PRR.

CIN85 is an ubiquitously expressed protein that occurs in several isoforms [55]. The largest isoform contains all the domains described above, while the other isoforms lack one, two, or all three SH3 domains ([19, 44, 108]. The SH3 domains of CIN85 bind to atypical proline motifs containing the consensus sequence PXXXPR (X= any aa) [92, 94]. They have also been shown to bind to ubiquitin ([13, 168]. The proline-rich region of CNI85 has been implicated to have an autoregulatory function. It can bind to the first and second SH3 domain of CIN85 ([92, 17]. This intramolecular interaction can compete with the SH3-domain-PRR-mediated interaction of CIN85 with PI3K p85-α [17]. The CC can mediate homo-oligomerization of CIN85 as well as association with the CIN85-homolog CD2AP [189, 16, 48]. The CC has also been described to mediate membrane association by phosphatidic acid (PA) binding [200]. CIN85 has been reported to interact with various proteins (reviewed in [64]). As adaptor protein, CIN85 is thought to exert its functions by bringing its interaction partners in spatial proximity. Mass spectrometric screens show that the CIN85 SH3 domains are redundant in their specificity [65, 20], at least under *in vitro* conditions. Corresponding to this finding, it was shown biochemically that one CIN85 protein can cluster several c-Cbl molecules [92]. While the knowledge of CIN85 structure and of its interaction partners increased, the exact cellular functions of CIN85 were less clear and sometimes controversial. The binding to SLP65 and c-Cbl was reported already in 2000 [189], and it was speculated that these interactions might influence PLC-γ2 activity in B cells. Nevertheless, the focus of CIN85 function was on its role for Epidermal growth factor receptor (EGFR) signaling for the next decade [166, 92, 91]. Upon the c-Cbl-mediated recruitment of CIN85 to the activated EGFR, CIN85 is described to cluster c-Cbl and endophilin molecules via interaction of their respective proline motifs with the CIN85 SH3 domains [166]. By this mechanism, CIN85 recruitment has been shown to promotes receptor internalization of the activated EGFR and other receptor tyrosine kinases [166, 131, 174]. However, the importance of CIN85 for EGFR endocytosis was negated by other reports ([63, 70, 77] and is regarded controversially (reviewed in [64]). Besides the endocytotic processes itself, the intracellular trafficking of the endocytosed EGFR has been reported to depend on SH3-mediated interactions of CIN85 with various interaction partners

[199, 161]. Also CIN85-tyrosine phosphorylation has been reported to influence intracellular EGFR trafficking [160].

The subcellular localization of CIN85 is still under dispute. CIN85 has been observed to be present in endosomes, COPI-coated vesicles or peripheral structures as lamellipodia and invadopodia, depending on the cell type and the CIN85 expression level [200, 63, 157, 117]. It is possible that the subcellular localization of CIN85 is determined by its respective binding partners in the investigated model systems. The functions attributed to CIN85 depend mainly on its ligands. Because many of them are known to participate either in endocytosis or in Golgi-apparatus-linked vesicular transport, it is likely that CIN85 has an influence on these processes [64]. There have been some studies on the CIN85 function in immune cells. CIN85 has been shown to interact with the cytoplasmic tail of the receptor CD2 [16]. In T cells, CIN85 can link CD2 to the cytoskeleton by binding to the actin capping protein CapZ. This influences potentially the TCR-induced cytoskeleton reorganization [71]. CIN85 has also been implicated to stabilize CD2 expression at the plasma membrane [179]. In neutrophils, CIN85 has been reported to be recruited to the activated FcγRIIa and to promote internalization and degradation of this receptor in a c-Cbl dependent manner [107].

CIN85 has also been implicated in the signaling of the FcϵRI in mast cells, a receptor that belongs to the Multichain immune recognition receptor (MIRR) family, as BCR and TCR [134]. It was shown that CIN85 contributes to endocytosis and intracellular trafficking of the FcϵRI. Overexpression of CIN85 accelerated the FcϵRI internalization, impairing the FcϵRI-mediated degranulation of mast cells [112]. Furthermore, CIN85-overexpression reduced the level of Syk in mast cells, thereby diminishing also PLC-γ phosphorylation and Ca^{2+} influx upon FcϵRI stimulation. [130]. In contrast to the inhibitory effect of CIN85 on the FcϵRI, the knockdown of CIN85 in the chicken B cell line DT40 led to an impaired BCR signaling, especially if it was done in cells deficient for the CIN85 homolog CD2AP [121]. This suggests that CIN85 might be a positive regulator in BCR signaling. No effect of CIN85 on BCR endocytosis was found [119, 18]. It has further been demonstrated that CIN85 interacts with the phosphatase SHIP1 in B cells, leading to the hypothesis that CIN85 might downregulate BCR signaling by recruiting this negative regulator to the activated BCR [20].

So the overall image of existing literature suggested that CIN85 might be a negative as well as a positive regulator of BCR signaling. Nevertheless, it was clear that the interaction of CIN85 with SLP65 had an enhancing effect on the BCR signaling cascade [121]. The aim of my doctoral thesis was to elucidate the mechanism by which CIN85 supports SLP65, gaining thereby general insight into the CIN85 function.

2.6 Aim of this study

Plasma membrane recruitment and phosphorylation of the adaptor protein SLP65 are crucial key steps of the BCR signaling and hence efficient B cell activation. These processes have been shown to depend on the interaction of SLP65 with the other adaptor protein CIN85. Nevertheless, it was totally unclear how the interaction with CIN85 contributes to SLP65 function. The aim of my doctoral thesis was the elucidation of the molecular mechanism by which CIN85 supports the function of SLP65 in BCR signaling.

To get inside into CIN85 function in B cells, I dealt with the following specific questions:

1. Does CIN85 possess protein or lipid ligands to target SLP65 to specific subcellular compartments? The CIN85 protein interactome was investigated by mass spectrometric analysis. Membrane association was assessed by subcellular fractionation experiments and lipid binding studies.

2. Which domains of CIN85 are essential for its support of SLP65? Can CIN85 binding be substituted by equipping SLP65 directly with additional functional domains? These points were addressed genetically by the generation of chimeric proteins and subsequent analysis of their functionality in the BCR pathway.

3. Can the structure of CIN85 explain its function? The structure of the C-terminal CIN85 coiled-coil domain was elucidated in cooperation with Prof. C. Griesinger's group . With this knowledge, the influence of single amino acids for CIN85 function could be examined.

3 Material and methods

3.1 Material

3.1.1 Instruments

Tab. 3.1: Instruments used in this study

Name	**Manufacturer**
Agarose Gelelectrophoresis System	Peqlab
Balance BP61	Sartorius
Balance H95	Sartorius
Balch homogenizer	MPI BPC, Göttingen
BioPhotometer	Eppendorf
Cell culture incubator HeraCell 150 CO_2	Heraeus
Cell disruption vessel 45 ml	Parr Instrument
Chemi Lux Gel Imager	Intas Science Imaging
Confocal laser scanning microscope TCS SP2	Leica Microsystems
Countess cell counter	Invitrogen
Electrophoresis power supply EPS 301	Amersham BioSciences
Electrophoresis System Hoefer SE600	Amersham
Flow cytometer LSR II	Becton Dickinson
Freezer Platilab 340	Angelantoni Industrie
GenePulser II electroporation system	Bio-Rad Laboratories
Ice machine	Ziegra
Incubation shaker Unitron	Infors
Incubator Kelvitron t	Heraeus
Laminar flow cabinet HERA safe	Heraeus
Light microscope TELAVAL 31	Zeiss
LSR II	BD Biosciences
Magnetic stirrer M21/1	Framo Gerätetechnik
Mastercycler epgradient	Eppendorf
Microcentrifuge 5415D	Eppendorf
Microcentrifuge 5417R	Eppendorf
Microplate reader PowerWave 340	BioTek
Mini PROTEAN Tetra Cell	Bio-Rad
Multifuge 3SR	Heraeus
NanoDrop 2000	Thermo Scientific

Name	Manufacturer
pH-Meter inoLab	WTW
Pipettes	Eppendorf
Rocking shaker	Neolab
Rotor SW40 Ti	Beckman
Rotor SW41 Ti	Beckman
Semiphor Transphor Unit TE77	Amersham Bioscience
Shaker 3006	GFL
Sonicator	Bandelin Sonoplus
Sorvall RC 3B Plus	Sorvall
Thermomixer comfort	Eppendorf
Ultracentrifuge Optima L-70k	Beckman
Ultracentrifuge Optima LE 80k	Beckman
UV-illuminator	Intas systems
Vortex Genie 2	Scientific industries
Water bath	GFL
Water Purification System Milli-Q	Millipore, Sartorius

3.1.2 Software

Tab. 3.2: Software used in this study

Name	Manufacturer	Application
Chemostar professional	Intas	Immunoblot documentation
Coreldraw	Corel Corporation	Graphic editing
FACSDiva	BD Biosciences	Flow cytometry recording
Flowjo	Treestar	Flow cytometry analysis
ImageJ	W. Rasband	Image processing
Leica confocal software	Leica	Microscopy image processing
LaTeX	L. Lamport	Text processing
Microsoft office2010	Microsoft	Text processing
pDraw32	Acaclone software	DNA sequence information processing

3.1.3 Consumables

Tab. 3.3: Consumables used in this study

Name	**Manufacturer**
Blotting Paper Whatman	GE Healthcare
CELLSTAR 96 well suspension culture plates	Greiner bio-one
CELLSTAR dishes 60 mm, 100 mm, 145 mm	Greiner bio-one
CELLSTAR serological pipettes 2 ml, 5 ml, 10 ml, 25 ml	Greiner bio-one
CELLSTAR tubes, 15 ml, 50 ml	Greiner bio-one
Cyro.S tubes	Greiner bio-one
Dialysis tubing SERVAPOR	Serva
Dishes for bacteria, 92 mM	Sarstedt
Filter tips	Greiner bio-one
Microscope imaging chambers, 4 wells	Lab Tek
Nitrocellulose membrane Hybond ECL	Amersham Biosciences
Parafilm	American National Can
PCR tubes, 0.2 ml	Sarstedt
Photometer cuvettes	Roth
Pierce centrifuge columns	Thermo scientific
Pipette tips	Greiner bio-one
Reaction tubes, 1.5 ml, 2 ml	Greiner bio-one
Scalpel	B. Braun
Sterile filter Filtropur, S 0.2 and S 0.45	Sarstedt
Syringe Omnifix ,1 ml	B. Braun
Syringes, 5 ml, 10 ml	BD Biosciences
Tubes for flow cytometry, 5 ml	Sarstedt
Tubes, 14 ml	Greiner bio-one
Ultracentrifugation tubes 9/16 x 3 3/4”	Beckman
Vivaspin 500	Sartorius

3.1.4 Chemicals and reagents

Tab. 3.4: Chemicals and reagents used in this study

Name	**Manufacturer**
Acetic acid (HOAc)	Roth
Acrylamide/bis-Acrylamide Rotiphorese Gel 30	Roth
Agar-Agar	Roth
Agarose	Peqlab
Ammonium persulfate (APS)	Roth
Ampcillin	Roth
L-Arginine:HCl ($^{13}C_6$)	Cambridge Isotope Lab.
Bleomycin (Bleocin)	Merck
Bovine serum albumin (BSA)	Serva
Brom-chlor-indoxyl-β-D-galactosid (X-gal)	Roth
Bromophenol blue	Merck
Bovine serum albumin (BSA) solution	NEB
Calcium chloride ($CaCl_2$)	Merck
Chicken serum	Sigma
Coomassie Brilliant Blue R-250	Roth
Dimethyl sulfoxide (DMSO)	Roth
DNA Ladder GeneRuler 1kb	Fermentas
Deoxynucleoside triphosphate (dNTP) mix	NEB
Dithiothreitol (DTT)	Roth
n-Dodecyl β-D-maltoside	Sigma-Aldrich
Ethylenediaminetetraacetic acid (EDTA)	Roth
Ethanol	Roth
Ethidium Bromide	Roth
Fetal Calf Serum (FCS), dialyzed	PAN Biotech
Fetal Calf Serum (FCS)	Biochrom
D-Glucose	Roth
Glycerol	Roth
Glycine	Roth
Hydrogen peroxide (H_2O_2)	Roth
Hydrochloric acid (HCl)	Roth
4-(2-hydroxyethyl)-1-piperazineethanesulfonic acid (HEPES)	Roth
Hexadimethrine bromide (polybrene)	Sigma-Aldrich

Name	**Manufacturer**
Igepal CA-630 (NP40)	Sigma-Aldrich
Immersion oil	Merck
INDO-1 AM	Life technologies
Invisorb Spin Plasmid Mini Two	Invitek
Isopropyl-β-D-thiogalactopyranoside (IPTG)	Roth
Isopropanol	Roth
Kanamycin	Roth
Luminol	Sigma-Aldrich
L-Lysine:2HCl (4,4,5,5-D_4)	Cambridge Isotope Lab.
µMACS GFP Tagged Protein Isolation kit	Miltenyi
Magnesium acetate ($Mg(OAc)_2$)	Roth
Magnesium chloride ($MgCl_2$)	Roth
Methanol (MeOH)	Roth
NEBuffers 1,2,3,4,cut smart	NEB
NuPAGE LDS sample buffer	Invitrogen
NuPAGE sample reducing reagent	Invitrogen
Phosphatidic acid (PA) coated beads	Echelon
p-Coumaric acid	Sigma-Aldrich
Penicillin	Sigma-Aldrich
Phusion HF reaction buffer	NEB
Pluronic F-127	Life technologies
Potassium chloride (KCl)	Roth
Potassium dihydrogen phosphate (KH_2PO_4)	Merck
Prestained Protein Marker Broad Range	NEB
Protease Inhibitor Cocktail P2714	Sigma-Aldrich
Protein A/G agarose beads	Santa Cruz
Protino Ni-IDA 1000	Macherey-Nagel
Pure Yield Plasmid Midiprep System	Promega
Puromycin	InvivoGEN
Sodium acetate (NaOAc)	Roth
Sodium azide (NaN_3)	Roth
Sodium chloride (NaCl)	Roth
Sodium dodecyl sulfate (SDS)	Roth
Sodium fluoride (NaF)	Roth
di-Sodium hydrogen phosphate (Na_2HPO_4)	Roth

Name	Manufacturer
Sodium hydroxide (NaOH)	Roth
Sodium orthovanadate (Na_3VO_4)	Sigma-Aldrich
Strep-Tactin Superflow high capacity	IBA
Strep-tag elution buffer	IBA
Streptomycin	Sigma-Aldrich
Sucrose	Roth
T4 DNA Ligase buffer	NEB
Tetramethylethylenediamine (TEMED)	Roth
TOPO TA Cloning Kit	Invitrogen
Trans-IT	Mirus
Tris(hydroxymethyl)-aminomethane (Tris)	Roth
Triton X-100	Roth
Trypsin	Gibco
Trypton/Pepton	Roth
Tween 20	Roth
Wizard SV Gel and PCR clean up Kit	Promega
Yeast extract	Roth

3.1.5 Buffers and solutions

Tab. 3.5: Buffers and solutions used in this study. All %-indications refer to weight per volume.

Name	Composition
Antibody dilution solution	1% BSA, 0.01% $NaNa_3$ in TBS-T
Blotting buffer	48 mM Tris, 39 mM glycine, 0.0375% SDS, 0.001% NaN3, 20% MeOH
Cell lysis buffer	50 mM Tris, 50 mM NaCl, 5 mM NaF, 1 mM Na_3VO_4, 1:50 Protease Inhibitor, 0.5% NP40, pH 8.0
Cell lysis buffer for strep-tag AP	Cell lysis buffer + 0.5% n-dodecyl β-D-maltoside
Coomassie staining solution	40% MeOH, 10% HOAc, 0.1% Coomassie Brilliant Blue R-250
DNA loading buffer (6x)	60 mM EDTA, 10 mM Tris/HCl, 60% glycerol, 0.03% Bromophenol blue, pH 7.6
ECL solution composition	4 ml ECL solution A, 400 µl ECL solution B, 1.2 µl H_2O_2 (30%)
ECL solution SA	100 mM Tris/HCl, 0.28 mM Luminol, pH 8.6

Name	Composition
ECL solution SB	6.7 mM p-coumaric acid in 100% DMSO
Homogenization buffer	250 mM Sucrose, 20 mM KCl, 25 mM HEPES, 2.5 mM $Mg(OAc)_2$, 2.5 mM DTT, 1:50 Protease Inhibitor, pH 7.4
Krebs-Ringer solution with $CaCl_2$	140 mM NaCl, 10 mM D-Glucose, 10 mM HEPES, 4 mM KCl, 1 mM $MgCl_2$, 1 mM $CaCl_2$, pH 7.4
Laemmli loading buffer (5x)	500 mM DTT, 150 mM Tris/HCl, 50% Glycerol, 15% SDS, 0.05% Bromophenol blue, pH 6.8
Lew buffer	300 mM NaCl, 50 mM NaH_2PO_4, pH 8.0
PBS	137 mM NaCl, 2.4 mM KCl, 4.3 mM Na_2HPO_4, 1.4 mM KH_2PO_4, pH 7.4
Resolving gel solution	375 mM Tris/HCl, 10% Acrylamide/bis-Acrylamide, 0.1% APS, 0.1% TEMED, pH 8.8
SDS-PAGE running buffer	192 mM glycine, 25 mM Tris, 0.1% SDS
Stacking gel solution	125 mM Tris/HCl, 4.8% Acrylamide/bis-Acrylamide, 0.1% APS, 0.1% TEMED, pH 6.8
TAE buffer	40 mM Tris/HOAc, 10 mM NaOAc, 1 mM EDTA, pH 7.8
TBS-T	137 mM NaCl, 20 mM Tris, 0.1% Tween20, pH 7.6
Western blot blocking solution	5% BSA, 0.01% NaN_3 in TBS-T

3.1.6 Antibodies

Tab. 3.6: Antibodies used in this study

Name	Manufacturer
α-Akt, rabbit monoclonal (C73H10)	Cell signaling technologies
α-Blnk, mouse monoclonal (2B11)	BD Biosciences
α-chicken IgM, mouse (M4)	Bethyl Laboratories
α-CIN85, rabbit polyclonal (C6115)	Sigma-Aldrich
α-Clathrin heavy chain, mouse monoclonal (23/Clathrin)	BD Biosciences
α-GFP, mouse monoclonal (7.1+13.1)	Roche
α-GM130, mouse monoclonal (35/GM130)	BD Biosciences
α-Grb2, mouse monoclonal (81/GRB2)	BD Biosciences
α-HA, rat monoclonal (3F10)	Roche
α-human IgM, $F(ab')_2$ Fragment, mouse	Jackson Immune Research Lab.
α-LAMP1, mouse monoclonal (H4A3)	BD Biosciences
α-Lyn, mouse monoclonal (42/Lyn)	BD Biosciences

Name	Manufacturer
α-Rab5, mouse monoclonal (621.1)	Synaptic Systems
α-α-Tubulin, mouse monoclonal (B512)	Sigma-Aldrich
α-VAMP7, rabbit polyclonal (LS-B88839)	LifeSpan BioSciences
α-mouse IgG (HRP-conjugated), goat	Southern biotech
α-rabbit IgG (HRP-conjugated), goat	Southern biotech

3.1.7 Enzymes

Tab. 3.7: Enzymes used in this study

Name	Manufacturer
AgeI HF	NEB
Alkaline phosphatase, calf intestinal (CIP)	NEB
BamHI HF	NEB
BglII	NEB
ClaI	NEB
DpnI	NEB
HindIII HF	NEB
NdeI	NEB
NotI HF	NEB
Phusion High-Fidelity DNA Polymerase	NEB
PvuI	NEB
T4 DNA ligase	NEB
Taq PCR Master Mix	Qiagen
XhoI	NEB

3.1.8 Media

Tab. 3.8: Media used in this study

Name	Manufacturer/Composition
RPMI-1640	Merck
DMEM	Merck
SILAC RPMI-1640 Medium	Thermo Scientific
Lysogeny broth (LB medium)	10 g/L trypton/Pepton, 5 g/L yeast extract, 10 g/L NaCl
LB-Agar	15 g Agar-Agar in 1L LB medium

3.1.9 PCR Primers

Tab. 3.9: Oligonucleotides used as PCR primers in this study. All oligonucleotides were manufactured by MWG-Biotech.

Name	Sequence
BglII SLP65 fw	TAATAGATCT CGACAAGCTT AATAAAATAA CCGTCC
CD2AP CC fw Bam	TTCAGGATCC CATGGAAATC AAAGCTAAAG TGGA
CD2AP CC Nde fw	TTCACATATG ATGGAAATCA AAGCTAAAG
CD2AP rev Bam ME frame	AAAAAAGCTG TCCTGTCTTC GGATCCACTT
Cin CC 631 Not rev	TATGCGGCCG CTCATTTCTG CTGGTCCTTC ATGGTCT
Cin CC 632 Bgl fw	TTCAAGATCT CATGCGAGAG ATTAAACAGT TATTGTCT
Cin CC Bam 631 rev	CGAGGGATCC TTCTGCTGGT CCTTCATGGT CT
Cin CC Bgl fw	TTCAAGATCT CATGGAAGGA AAACCAAAGA TGGAGCCT
Cin PR/CC Not rev with stop	ATGCGGCCGC TCATTTTGAT TGTAGAGCTT TCTT
CIN85 CC fw Nde	TTCGCATATG GAAGGAAAAC CAAAGATGGA GCCT
CIN85 CC fwd Bam	AAAGGATCCA CCATGGAAGG AAAACCAAAG ATGGAGCCT
CIN85 CC rev Xho with stop	TTCGCTCGAG TTATTTGATT GTAGAGCTTT CTT
Cin85 PR/CC Bam fw	TTCGTGGATC CCATGGACTT TGAAAAGGAA GGG
Cin85 PR/CC Rev	CGAGGGATCC TTTGATTGTA GAGCTTTCTT
Cin85 SH3 rev	CGAGGGATCC GGTGGAAGTA ACTTCACGAA
Cin85SH3 ATG Blg fw	TTCGTAGATC TCATGGTGGA GGCCATAGTG GA
CinCC L619A fw	ACACAGGTCC GCGAGGCGAG GAGCATCATC GAGAC
CinCC L619A rev	GTCTCGATGA TGCTCCTCGC CTCGCGGACC TGTGT
CinCC L619K fw	ACACAGGTCC GCGAGAAGAG GAGCATCATC GAGAC

Name	Sequence
CinCC L619K rev	GTCTCGATGA TGCTCCTCTT CTCGCGGACC TGTGT
CinPR Bam rev	CGAGGGATCC ATCTTTGGTT TTCCTTCCGT
HAtag Cin CC Bgl fw	TTCAAGATCT CATGTACCCA TACGACGTCC CAGACTACGC TGAAGGAAAA CCAAAGATGG AGCCT
hSlp rev stop Xho	TTCTCTCGAG TTATGAAACT TTAACTGCAT
hSLP65woStopAge	ATATACCGGT GGATCTGAAA CTTTAACTGC ATACTTCAG
M13fw	GTAAAACGAC GGCCAG
M13rev	CAGGAAACAG CTATGAC
NotI SLP65 rev	TAATGCGGCC GCTTATGAAA CTTTAACTGC ATACTTCAG
Overlap slpCinCC 632 fw	AAGTATGCAG TTAAAGTTTC ACGAGAGATT AAACAGTTAT TGTCT
Overlap slpCinCC632 rev	AGACAATAAC TGTTTAATCT CTCGTGAAAC TTTAACTGCA TACTT
pEGFPN1 for	GTCGTAACAA CTCCGCCC
pEGFPN1 rev	GTCCAGCTCG ACCAGGATG
pMSCVfw	CCCTTGAACC TCCTCGTTCG ACC
pMSCVrev	CAGACGTGCT ACTTCCATTT GTC
Raf1 PA Bam fw	TTCAGGATCC CATGAGGAAT GAGGTGGCTG TTCT
Raf1 PA Bam rev	TGAAGGATCC CCTGATCCCT CGCACCACTG GGTCAC
SCOC CC Bam fw	TTCAGGATCC CATGATGAAT GCCGACATGG AT
SCOC CC Bam rev	TGAAGGATCC TTACGTTTGG ATTTGGTATC G
SCOC E93V K97L fwd	GCCGAAAATC AGGTGGTACT GGAGGAATTA ACCCGTCTGA TCAAC
SCOC E93V K97L rev	GTTGATCAGA CGGGTTAATT CCTCCAGTAC CACCTGATTT TCGGC
SCOC N125L N132V fw	TGCCGTAAAA GAGGAGCTTC TGAAACTGAA AAGTGAGGTT CAAGTGCTGG GC
SCOC N125L N132V rev	GCCCAGCACT TGAACCTCAC TTTTCAGTTT CAGAAGCTCC TCTTTTACGG CA

Name	Sequence
Slp dN (46) Bam ATG fw	TTCGGGATCC CATGAGTGTT CCTCGAAGGG ACTACG
Slp dN (46) Bgl ATG fw	TTCGAGATCT CATGAGTGTT CCTCGAAGGG ACTACG
Slp EcoRI rev	AAGTGAATTC TTATGAAACT TTAACTGCAT A
SLP65CIN85CC OL fw	AAGTATGCAG TTAAAGTTTC AGAAGGAAAA CCAAAGATGG AGCCT
SLP65CIN85CC OL rev	AGGCTCCATC TTTGGTTTTC CTTCTGAAAC TTTAACTGCA TACTT
SLP65CIN85PRR OL fw	AAGTATGCAG TTAAAGTTTC AGACTTTGAA AAGGAAGGGA AT
SLP65CIN85PRR OL rev	ATTCCCTTCC TTTTCAAAGT CTGAAACTTT AACTGCATAC TT
Slp76 Age rev	TGAAACCGGT GGGTACCCTG CAGCATGCGT TAA
Slp76 Bam fw	TTCAGGATCC CGCACTGAGG AATGTGCCC
slpdN Bam fw frVB	TTCAGGATCC AGTGTTCCTC GAAGGGACTA CG
Slprev fl Xho mit Stop	TTCGCTCGAG TTATGAAACT TTAACTGCAT A
T7	TAATACGACT CACTATAGG

3.1.10 Plasmids

Tab. 3.10: Basic plasmids used in this study

Name	Source,description	Application
pCit-N1	Dr. M. Engelke, based on pEGFP-N1 (BD Biosciences Clontech), eGFP exchanged for Citrine	Cloning, addition of Citrine tag to chimeric proteins
pET 16b TEV	Dr. S. Becker	Expression of recombinant His-tagged proteins
pCR2.1	Invitrogen	TA cloning
pABESpuro N-One-Strep	Dr. V. Bremes	Expression of electroporated cDNA in eukaryotic cells, includes N-terminal strep-tag

Name	Source,description	Application
pMSCV puro	BD Biosciences Clontech	Expression of retrovirally transduced cDNA in eukaryotic cells
pMSCV puro plus NotI-cutting site	Dr. M. Engelke, based on pMSCV puro, Not cleavage site added	Expression of retrovirally transduced cDNA in eukaryotic cells
pMSCV bleo plus NotI-cutting site	This thesis, puromycin resistance cassette exchanged for bleomycin resistance cassette (with ClaI and HindIII restriction sites)	Expression of retrovirally transduced cDNA in eukaryotic cells
pMSCV puro NCit	Dr. M. Engelke, based on pMSCV puro, Citrine added,	Expression of retrovirally transduced cDNA in eukaryotic cells, includes N-terminal Citrine tag

Tab. 3.11: Plasmid constructs used in this study. All proteins originated from human, with exception of VAMP7 (chicken). The plasmid were prepared for this thesis, if not indicated otherwise. The numbers indicate the amino acid position in the protein. General abbreviations: SLP65-ΔN means SLP65 aa 46-456. SLP65-M2,3 means SLP65 with amino acid exchanges R247A and R312A.

Name	Description	Source
pCitN1 SLP65-ΔN	SLP65-ΔN, C-terminal Citrine tag	
pCitN1 SLP65-ΔN-M2,3	SLP65-ΔN-M2,3, C-terminal Citrine tag	
pCitN1 SLP65-M2,3	SLP65-M2,3, C-terminal Citrine tag	
pCitN1 SLP65-wt	SLP65-wt, C-terminal Citrine tag	
pCitN1 SLP65-ΔN RL	SLP65-ΔN R372L, C-terminal Citrine	Dr. M. Engelke
pCitN1 SLP76	SLP76, C-terminal Citrine	
pABES puro N-OneStrep CD2AP	N-terminal Strep tag, CD2AP	Dr. V. Bremes

Name	Description	Source
pABES puro N-OneStrep CIN85	N-terminal Strep tag, CIN85	Dr. V. Bremes
pABES puro N-OneStrep CIN85 CC SLP65-ΔN	N-terminal Strep tag, CIN85 594-665, SLP65-ΔN	
pCR2.1 CD2AP CC	CD2AP 568-639	
pCR2.1 CIN85 CC L619A SLP65-ΔN-M2,3	CIN85 594-665 L619A, SLP65-ΔN-M2,3	
pCR2.1 CIN85 CC L619K SLP65-ΔN-M2,3	CIN85 594-665 L619K, SLP65-ΔN-M2,3	
pCR2.1 CIN85 CC SLP65-ΔN-M2,3	CIN85 594-665, SLP65-ΔN-M2,3	
pCR2.1 CIN85 PRR	CIN85 329-599	
pCR2.1 CIN85 PRR/CC	CIN85 329-665	
pCR2.1 CIN85 SH3	CIN85 1-328	
pCR2.1 Raf PA	Raf1 391-426	
pCR2.1 SCOC CC	SCOC 78-159	
pCR2.1 SCOC CC Tetramer	SCOC 78-159 N125L/N132V	
pCR2.1 SCOC CC Trimer	SCOC 78-159 E93V/K97L	
pET16b CD2AP CC SLP65-ΔN	N-terminal His tag, CD2AP 568-639, SLP65-ΔN	
pET16b CIN85 CC	N-terminal His tag, CIN85 594-665	
pET16b CIN85 CC L619K	N-terminal His tag, CIN85 594-665 L619K	
pET16b CIN85 CC L619K SLP65-ΔN	N-terminal His tag, CIN85 594-665 L619K, SLP65-ΔN	
pET16b CIN85 CC SLP65-ΔN	N-terminal His tag, CIN85 594-665, SLP65-ΔN	
pET16b SLP65-ΔN	N-terminal His tag, SLP65-ΔN	S. Pirkuliyeva
pET16b SLP65-wt	N-terminal His tag, SLP65-wt	S. Pirkuliyeva
pET28a SCOC CC Strep Tag	SCOC 78-159, C-terminal Strep tag	Dr. K. Kühnel
pHCMV-VSV-G	coding for VSV glycoprotein	Dr. V. Bremes
pMSCV bleo Cerulean VAMP7	N-terminal Cerulean, chicken VAMP7	Dr. M. Engelke

Name	Description	Source
pMSCV bleo HA CIN85 CC L619K SLP65-ΔN-M2,3	N-terminal HA tag, CIN85 594-665 L619K, SLP65-ΔN-M2,3	
pMSCV bleo HA CIN85 CC SLP65-ΔN-M2,3	N-terminal HA tag, CIN85 594-665, SLP65-ΔN-M2,3	
pMSCV bleo NCit SLP65-ΔN-M2,3 CIN85 CC 594-631	N-terminal Citrine, SLP65-ΔN-M2,3, CIN85 594-631	
pMSCV bleo VC	Venus 156-239	Dr. M. Engelke
pMSCV bleo VC SLP65-ΔN	Venus 156-239, SLP65-ΔN	
pMSCV bleo VC SLP65-ΔN-M2,3	Venus 156-239, SLP65-ΔN-M2,3	
pMSCV bleo VC SLP65-ΔN-RL	Venus 156-239, SLP65-ΔN R372L	
pMSCV puro CD2AP CC SLP65-ΔN CCit	CD2AP 568-639, SLP65-ΔN, C-terminal Citrine	
pMSCV puro CD2AP CC SLP65-ΔN-M2,3 CCit	CD2AP 568-639, SLP65-ΔN-M2,3, C-terminal Citrine	
pMSCV puro CD2AP CC	CD2AP 568-639	
pMSCV puro CIN85 CC 594-631 SLP65-ΔN-M2,3 CCit	CIN85 594-631, SLP65-ΔN-M2,3, C-terminal Citrine	
pMSCV puro CIN85 CC 594-631	CIN85 594-631	
pMSCV puro CIN85 CC 632-665 SLP65-ΔN-M2,3 CCit	CIN85 632-665, SLP65-ΔN-M2,3, C-terminal Citrine	
pMSCV puro CIN85 CC 632-665	CIN85 632-665	
pMSCV puro CIN85 CC SLP65-ΔN-RL CCit	CIN85 594-665, SLP65-ΔN R372L, C-terminal Citrine	
pMSCV puro CIN85 PRR SLP65-ΔN CCit	CIN85 329-599, SLP65-ΔN, C-terminal Citrine	

Name	Description	Source
pMSCV puro CIN85 PRR SLP65-ΔN-M2,3 CCit	CIN85 329-599, SLP65-ΔN-M2,3, C-terminal Citrine	
pMSCV puro CIN85 PRR	CIN85 329-599	
pMSCV puro CIN85 PRR/CC SLP65-ΔN CCit	CIN85 329-665, SLP65-ΔN, C-terminal Citrine	
pMSCV puro CIN85 PRR/CC SLP65-ΔN-M2,3 CCit	CIN85 329-665, SLP65-ΔN-M2,3, C-terminal Citrine	
pMSCV puro CIN85 PRR/CC	CIN85 329-665	
pMSCV puro CIN85 SH3 SLP65-ΔN CCit	CIN85 1-328, SLP65-ΔN, C-terminal Citrine	
pMSCV puro CIN85 SH3 SLP65-ΔN-M2,3 CCit	CIN85 1-328, SLP65-ΔN-M2,3, C-terminal Citrine	
pMSCV puro CIN85 SH3	CIN85 1-328	
pMSCV puro CIN85CC L619K SLP76	CIN85 594-665 L619K, SLP76, C-terminal Citrine	
pMSCV puro CIN85CC SLP76	CIN85 594-665, SLP76, C-terminal Citrine	
pMSCV puro NCit CIN85 CC 594-631 SLP65-ΔN-M2,3	N-terminal Citrine, CIN85 594-631, SLP65-ΔN-M2,3	
CIN85 CC 632-665	CIN85 632-665	
pMSCV puro NCit CIN85 CC 632-665 SLP65-ΔN-M2,3	N-terminal Citrine, CIN85 632-665, SLP65-ΔN-M2,3	
CIN85 CC 594-631	CIN85 594-631	
pMSCV puro NCit CIN85 CC L619K SLP65-ΔN-M2,3	N-terminal Citrine, CIN85 594-665 L619K, SLP65-ΔN-M2,3	
pMSCV puro NCit CIN85 CC SLP65-ΔN-M2,3	N-terminal Citrine, CIN85 594-665, SLP65-ΔN-M2,3	
pMSCV puro NCit SLP65-ΔN CIN85 PRR/CC	N-terminal Citrine, SLP65-ΔN, CIN85 329-665	

Name	Description	Source
pMSCV puro NCit SLP65-ΔN-M2,3 CIN85 CC 594-631	N-terminal Citrine, SLP65-ΔN-M2,3 CIN85 594-631	
pMSCV puro NCit SLP65-ΔN-M2,3 CIN85 CC	N-terminal Citrine, SLP65-ΔN-M2,3, CIN85 594-665	
pMSCV puro NCit SLP65-ΔN-M2,3 CIN85 PRR/CC	N-terminal Citrine, SLP65-ΔN-M2,3, CIN85 329-665	
pMSCV puro NCitrin SLP65-ΔN	N-terminal Citrine tag, SLP65-ΔN	Dr. V. Bremes
pMSCV puro NCitrin SLP65-wt	N-terminal Citrine tag, SLP65-wt	Dr. V. Bremes
pMSCV puro PH SLP65-ΔN CCit	PLC-δ PH domain, SLP65-ΔN, C-terminal Citrine tag	
pMSCV puro PH SLP65-ΔN-M2,3 CCit	PLC-δ PH domain, SLP65-ΔN-M2,3, C-terminal Citrine tag	
pMSCV puro PLC d PH	PLC-δ PH domain	Dr. M. Engelke
pMSCV puro Raf PA SLP65-ΔN	Raf1 391-426, SLP65-ΔN	
pMSCV puro SCOC CC SLP65-ΔN CCit	SCOC 78-159, SLP65-ΔN, C-terminal Citrine	
pMSCV puro SCOC CC SLP65-ΔN-M2,3 CCit	SCOC 78-159, SLP65-ΔN-M2,3, C-terminal Citrine	
pMSCV puro SCOC CC Tetramer	SCOC 78-159 N125L/N132V	
pMSCV puro SCOC CC Tetramer SLP65-ΔN-M2,3	SCOC 78-159 N125L/N132V, SLP65-ΔN, C-terminal Citrine	
pMSCV puro SCOC CC Trimer SLP65-ΔN-M2,3	SCOC 78-159 E93V/K97L, SLP65-ΔN-M2,3, C-terminal Citrine	
pMSCV puro SCOC CC Trimer	SCOC 78-159 E93V/K97L	
pMSCV puro SCOC CC	SCOC 78-159	

Name	Description	Source
pMSCV puro SLP65-ΔN CCit	SLP65-ΔN, C-terminal Citrine tag	
pMSCV puro SLP65-ΔN-M2,3 CCit	SLP65-ΔN-M2,3, C-terminal Citrine tag	
pMSCV puro slp65-M2,3 CCit	SLP65-M2,3, C-terminal Citrine tag	
pMSCV puro SLP65-wt CCit	SLP65-wt, C-terminal Citrine tag	
pMSCV puro Syk tSH2	Syk tSH2 domains	Dr. M. Engelke
pMSCV puro SyktSH2 ΔN CCit	Syk tSH2 domains, SLP65-ΔN, C-terminal Citrine tag	
pMSCV puro SyktSH2-M2,3 CCit	Syk tSH2 domains, SLP65-ΔN-M2,3, C-terminal Citrine tag	
pMSCV puro VN	Venus 1-173	Dr. M. Engelke
pMSCV puro VN SLP65-ΔN RL	Venus 1-173, SLP65-ΔN R372L	
pMSCV puro VN SLP65-ΔN	Venus 1-173, SLP65-ΔN	
pMSCV puro VN SLP65-ΔN-M2,3	Venus 1-173, SLP65-ΔN-M2,3	

3.1.11 Bacteria

Tab. 3.12: Bacterial strains used in this study

Strain	Manufacturer
One Shot TOP10F' chemo-competent *E. coli*	Life technologies
One Shot BL21 (DE3) chemo-competent *E. coli*	Life technologies

3.1.12 Eukaryotic cell lines

DT40 (ATCC CRL-2111)

DT40 is a chicken B cell line which derived from an avian leucosis virus-induced bursal lymphoma [6]. This cell line displays IgM on the cell surface and shows a high ratio of targeted to random DNA integration. This facilitates genetic modification via homologous recombination [194].

Ramos (DSMZ: ACC 603)

The Ramos B cell line is established from the ascitic fluid of a 3-year-old boy with Burkitt lymphoma in 1972 [86]. The cell line displays IgM paired with a λ light chain on its surface. It is Epstein-Barr virus-negative.

Platinum-E

Platinum-E is a HEK 293T-derived retroviral packaging cell line [114]. It expresses the structural genes *gag*, *pol* and *env* of the moloney murine leukemia virus. This allows packaging of transfected DNA into retroviral particles.

3.2 Methods

3.2.1 Genetic methods

Molecular cloning techniques were performed according to established standard protocols as described in Sambrook and Russell [152] if not indicated otherwise.

3.2.1.1 Polymerase chain reaction (PCR)

PCR, originally described in Mullis *et al.* [115], was used to amplify DNA fragments for following cloning procedures. The enzyme Phusion High-Fidelity polymerase (NEB) was used to catalyze the PCR. The reaction mixture was composed according to the instructions given in the manufacturer's manual. A 20 µl reaction mixture contained 4 µl Phusion HF reaction buffer, dNTPs (0.2 mM), DNA oligonucleotides as primers (1 µM of each primer), 25-100 ng DNA template and 0.4 U Phusion High-Fidelity DNA polymerase. The indicated standard temperature protocol was used (Table 3.13). For GC-rich templates, the annealing temperature was increased to 60-65 ℃.

Tab. 3.13: Temperature gradient used for PCR

Step	Temperature [℃]	Time	Number of cycles
Initial denaturation	98	2 min	1
Denaturation	98	15 s	30-32
Annealing	55	30 s	30-32
Elongation	72	20 s/kB	30-32
Final elongation	72	10 min	1

3.2.1.2 Overlap extension PCR

Overlap extension PCR, a PCR variant to fuse two DNA fragments [68], was used to create DNA constructs encoding for chimeric or tagged proteins. First, two fragments were amplified by PCR as

described above. The primers for these two PCRs were designed to create an overlap between the fragments. After their isolation by agarose gel electrophoresis and following DNA purification, the two fragments were mixed and served as primers for each other in a following PCR of 15 cycles. Subsequently, primers corresponding to beginning and end of the final product were added at a concentration of 1 µM and a PCR of 20 cycles was launched. The annealing temperature of this final PCR was set to 60 °C to increase the specificity.

3.2.1.3 Site directed mutagenesis

The plasmid pCR2.1, which is optimized for cloning procedures, was used for mutagenesis reactions. The protocol was based on the QuikChange method (Stratagene) with modifications according to Edelheit *et al.* [36]. Two standard PCRs were carried out, one with a forward primer carrying the desired mutation, the other with the complementary reverse primer. The elongation time was chosen to allow a complete amplification of the plasmid. In the end, both reaction mixtures were combined and de- and re-natured according to the indicated temperature protocol (Table 3.14). The reaction mixture was digested with DpnI and transformed into the *E. coli* strain Top10F' (see 3.2.1.8)

Tab. 3.14: Temperature gradient for plasmid de- and re-naturation after mutagenesis PCR

Temperature [°C]	**Time**
95	5 min
90	1 min
80	1 min
70	30 s
60	30 s
50	30 s
40	30 s
37	5 min

3.2.1.4 Enzymatic digest of DNA

For following cloning procedures, DNA originating from PCRs or Plasmids was digested using type II restriction enzymes (NEB). Therefore, approx. 1 µg DNA was mixed with 0.5 µl of each restriction enzyme, the NEB buffer and BSA (final concentration 0.1 µg/µL). Water was added to a final reaction volume of 25 µL. The digest was performed for 2-16 h.

3.2.1.5 Agarose gel electrophoresis

To separate DNA fragments according to their size, agarose gel electrophoresis was used. 1% or 2% agarose gels were prepared in TAE buffer, 1 µg/mL ethidium bromide was added. The DNA containing samples were mixed with DNA loading buffer and loaded on the agarose gel. To estimate the DNA frag-

ment size, the DNA marker GeneRuler 1kb (Fermentas) was loaded on a lane next to the samples. The electrophoresis was performed at 100 V for 30-40 min (15 min for DNA fragments smaller than 300 bp) in TAE buffer. The DNA was visualized on an UV-illuminator.

3.2.1.6 Purification of DNA from agarose gels or PCR reactions

The purification of DNA fragments from PCR or agarose gels was performed using the Wizard SV Gel and PCR Clean-Up-Kit (Promega), following the manufacturer's instructions.

3.2.1.7 Ligation of DNA fragments

For the ligation of DNA fragments cut with restriction enzymes, 6.5 µl of the insert were mixed with 2 µl of the vector (cut plasmid), 1 µl T4 DNA ligase buffer (NEB) and 0.5 µl T4 DNA ligase (NEB). The reaction was incubated for 1 h at room temperature or overnight at 16 ℃. Undigested PCR products were ligated in the vector pCR2.1 by "TA"-cloning. A-overhangs were generated by incubating the PCR product with Taq PCR master mix at 72 ℃ for 20 min. Subsequently, 2 µl of the PCR product (containing A-overhangs) were mixed with 1 µl of linear pCR2.1 vector, 0.5 µl T4 DNA ligase and 1 µl T4 DNA ligase buffer and 4.5 µl H_2O. The ligation was incubated for 1 h at room temperature.

3.2.1.8 Transformation

2-5 µl of the ligation reaction were added to 50 µl chemocompetent E. coli Top10F'. After 30 min incubation on ice, the bacteria were incubated at 42 ℃ for 42 s, put on ice for 2 min and incubated at 37 ℃ for 30 min. Afterwards, they were plated of LB-agar dishes containing either Ampicillin (for pCR2.1, pMSCV, pABES and pET16b plasmids) or Kanamycin (for pCitN1 and pHCMV plasmids) and incubated at 37 ℃ for 12-16 h.

3.2.1.9 Preparation of plasmid DNA

Mini Preparation

The preparation of plasmid DNA in small scale was performed using the Invisorb Spin Plasmid Mini Two-kit (Invitek) according to the manufacturer's instructions. Shortly, the 4 ml bacterial cultures were grown overnight, the bacteria were pelleted and lysed by SDS/NaOH. The plasmid DNA was bound to a spin column and washed with buffer containing ethanol. The DNA was eluted with 50 µl nuclease-free water, the DNA concentration was spectrometrically determined using the Nanodrop system.

Midi Preparation

The preparation of plasmid DNA in medium scale was performed using the PureYield Plasmid Midiprep-kit (Promega) according to the manufacturer's instructions. 50 ml bacterial cultures were grown overnight, the remaining procedure resembled the *Mini* preparation procedure. The DNA was eluted with 400 µl

nuclease-free water.

3.2.2 Cell biological methods

3.2.2.1 Culturing of eukaryotic cells

The B cell lines DT40 and Ramos were cultured in RPMI-1640 medium, supplied with 10% FCS and Penicillin/Streptomycin. For the culturing of the DT40 cells, 5% chicken serum were additionally added. The cells were cultured at 37 °C and a CO_2 concentration of 5%. The retroviral packaging cell line Platinum-E was cultured in DMEM, supplied with 10% FCS and Penicillin/Streptomycin.

3.2.2.2 Freezing and thawing of eukaryotic cells

To freeze DT40, Ramos or Platinum-E cells, $5 \cdot 10^6$-$2 \cdot 10^7$ cells were pelleted (300 g, 4 min), resuspended in 1 ml freezing medium (FCS + 10% DMSO), and frozen at -140 °C. To thaw DT40, Ramos or Platinum-E cells, the frozen cells were thawed at 37 °C for 3 min and transferred into 10 ml cell culture medium. To reduce the DMSO concentration, the cells were pelleted (300 g, 4 min) and resuspended in 10 ml culture medium before further culturing.

3.2.2.3 SILAC labeling

The introduction of heavy labeled amino acids in the B cell lines DT40 and Ramos was performed according to Oellerich *et al.*, 2009 [122]. The cells were cultured in SILAC RPMI-1640 medium containing 0.12 mM L-arginine ($^{13}C_6$) (+6) and 0.27 mM L-lysine (4,4,5,5-D_4) (+4), 10% dialyzed FCS and Penicillin/Streptomycin. To achieve a complete labeling, the cells were cultured in this medium for at least 7 days. The unlabeled control cells were cultured in RPMI-1640 medium supplied with 10% dialyzed FCS and Penicillin/Streptomycin.

3.2.2.4 Retroviral transduction

A retroviral transduction system, described in Stork *et al.* [169], was used to integrate plasmid DNA stably in the genomic DNA of the DT40 B cell line. Retroviral particles were generated using the Platinum-E cell line. For the transfection of Platinum-E cells, 250 µl RPMI-1640 medium (serum free) were mixed with 8 µl TransIT-293 transfection reagent (Mirus). After 15 min incubation at room temperature, 1.7 µg plasmid DNA, coding for the protein of interest, and 0.5 µg of the plasmid pHCMV-VSV-G, coding for the envelope glycoprotein of VSV, were added. The mixture was incubated at room temperature for 20 min. The medium of a dish with Platinum-E cells (70-80% confluent) was removed and substituted with 2.5 ml of RPMI-1640 medium (10% FCS); afterwards the transfection mixture was added slowly. On the next day, 1.5 ml RPMI-1640 medium were added. On the second day after transfection, $1 \cdot 10^6$ DT40 cells were resuspended in 2 ml fresh RPMI-1640 medium, the supernatant of the Platinum-E culture, containing the retroviral particles, was added. To increase the efficiency of the retroviral infection, polybrene was added to a final concentration of 3 µg/ml. The medium was changed the next day to remove the polybrene.

The selection of successfully transduced cells started one day later. For DT40 cell, 1 µg/ml puromycin for 3 days respectively 50 µg/ml bleomycin for 2 days were used.

3.2.2.5 Transfection of eukaryotic B cells by Electroporation

Electroporation was used to introduce DNA stably in the genome of the B cell lines DT40 and Ramos as described in Oellerich *et al.* [122]. $1{\cdot}10^7$ cells were pelleted (300 g, 4 min) and resuspended in 700 µl PBS. 25 µg of the linearized DNA (plasmid pABESpuro) were added. The mixture was transferred to an electroporation cuvette and incubated on ice for 10 min. The electroporation was performed at 270 V and 960 µF. After incubation on ice for 10 min, the cells were resuspended in culture medium and incubated for 24 h at 37 ℃. Afterwards, the culture medium was changed and successfully transfected cells were selected with puromycin at a concentration of 1 µg/ml (DT40) or 0.5 µg/ml (Ramos). To isolate single clones, the cells were plated on 96 well culture plates. After 10-14 days of antibiotic selection, clones were transferred in 60 mm cell culture dishes and screened by immunoblotting for production of the protein corresponding to the transfected DNA.

3.2.3 Biochemical methods

3.2.3.1 Preparation of cell lysates

Lysates of DT40 cells were prepared as described in Stork *et al.* [169]. DT40 cells were pelleted (300 g, 4 min), washed once with PBS, and counted. They were resuspended in 20 µl Lysis buffer (containing 0.5% NP40) per $1{\cdot}10^6$ cells and lysed on ice for 1 h. The nuclei were pelleted by centrifugation (16,000 g, 20 min, 4 ℃), the supernatant, constituting the lysate, was transferred to subsequent applications (e.g. affinity purification, immunoblot analysis).

3.2.3.2 Affinity purification

For SILAC-based mass spectrometric analyses, Strep-tagged Proteins were purified using the Step-tag-Streptactin interaction as described in Oellerich *et al.*, [121]. Cell lysates of $5{\cdot}10^7$-$2{\cdot}10^8$ cells were prepared as described above (see 3.2.3.1), the lysis buffer contained additionally 0.5% n-dodecyl β-D-maltoside. The following purification was carried out at 4 ℃ to avoid protein degradation. The cell lysate was transferred to a column containing 200 µl Strep-Tactin Superflow beads (equilibrated in lysis buffer) and incubated overnight. After the flowthrough was removed, the beads within the column were washed five times with 1 ml lysis buffer. The internal column volume was overcome by adding 100 µl Strep-tag elution buffer (1x). Afterwards, the column was closed and incubated for 30 min with 500 µl Strep-tag elution buffer (1x).The elution fraction was collected. 200 µl Strep-tag elution buffer (1x) were added to the column to collect remaining eluting proteins. The elution fraction was concentrated to 50 µl by a Vivaspin 500 column (cut-off 10 kDa). LDS sample buffer and reducing agent were added, the sample was incubated for 10 min at 70 ℃. To allow SILAC quantification, two samples, one unlabeled and one R+6, L+4 labeled,

were combined at 1:1 ratio. The samples were analyzed by mass spectrometry in Prof. H. Urlaub's group.

To assess the association of proteins to phosphatidic acid (PA), a precipitation assay based on PA-coated beads was used. 20 µl of PA-coated beads were added to 5 µg of recombinant protein in 1 ml LEW buffer, the mixture was incubated for 1 h at 4 ℃. The beads were precipitated (350 g, 4 min, 4 ℃), the supernatant was discarded. After three washing steps with 1 ml LEW buffer, the proteins attached to the PA-coated beads were eluted by addition of 50 µl Laemmli-buffer (1x) and incubation at 90 ℃for 10 min. The sample was analyzed by immunoblotting.

3.2.3.3 VAMP7$^+$ vesicle enrichment

VAMP7$^+$ vesicles were enriched using the µMACS GFP Tagged Protein Isolation kit (Miltenyi) according to the manufacturer's instructions. $2{\cdot}10^8$ DT40 cells expressing Cerulean-tagged VAMP7 were disrupted by passing a Balch homogenizer as described for subcellular fractionation (see 3.2.3.5). The PNS was mixed with 50 µl α-GFP MicroBeads and incubated for 30 min one ice. A µMACS column was placed in a static magnet field and equilibrated first with ethanol (70%), then with homogenization buffer. The PNS-bead mixture was applied on the column, the column was washed five times with 1 ml homogenization buffer. Subsequently, 20 µl pre-heated Laemmli or NuPAGE LDS sample buffer (95 ℃) were applied to overcome the internal column volume, the column was incubated for 5 min. To elute proteins attached to the magnetic beads, 50 µl pre-heated Laemmli or NuPAGE LDS sample buffer (95 ℃) were added, the elution fraction was analyzed by immunoblotting or mass spectrometry.

3.2.3.4 Co-immunoprecipitation

Cell lysates were prepared as described above (see 3.2.3.1). After pelleting the nuclei, the lysate was transferred into a new tube, 1.5 µl of α-GPF antibody (Roche) were added, and the sample was incubated overnight at 4 ℃. Afterwards, 15 µl protein A/G beads were added, the sample was incubated for 1 h at 4 ℃. The beads were pelleted (250 g, 3 min, 4 ℃) and washed three times with 1 ml lysis buffer. The proteins were eluted by adding 50 µl Laemmli-buffer (1x) and incubating the sample for 10 min at 90 ℃.

3.2.3.5 Subcellular fractionation by Balch homogenization

Ramos and DT40 cells were mechanically disrupted by shearing forces and subsequently fractionated on a sucrose gradient based on the protocol described in Bethani *et al.* [12]. $3{\cdot}10^8$ cells were pelleted (300 g, 6 min) and washed once with homogenization buffer. They were resuspended in 1 ml homogenization buffer and disrupted by being passed 30 times through a Balch homogenizer. The used Balch homogenizer consisted of a metal block that contained two connected openings. A very exactly fitting metal sphere was placed in the conneting conduit. The liquid containing the cells was slowly passed through the conduit by using two syringes connected to the openings. Passing the small space between the sphere and the conduit walls exerts strong shearing forces to the cells. After disruption, the nuclei were sedimented

(2000 g, 15 min, 4 ℃). The postnuclear supernatant (PNS) was adjusted to a volume of 3 ml and a sucrose concentration of 55% and overlaid with 2 ml of 45%, 3 ml of 35%, and 3 ml of 25% sucrose. Upon centrifugation for 5 hours at 217,000 g, fractions were collected and analyzed by immunoblotting.

3.2.3.6 Subcellular fractionation by cavitation

Ramos B cells were disrupted by nitrogen cavitation. The cytosolic and the membranous fraction were separated as described in Araujo *et al.*, [33]. $5{\cdot}10^7$ cells were pelleted (300 g, 6 min), washed once with homogenization buffer, and resuspended in 2 ml homogenization buffer. The liquid containing the cells was transferred into a cell disruption vessel which was connected to a nitrogen bottle. The pressure in the vessel was increased to 8 bar for 3 min. Afterwards, the pressure was abruptly released to disrupt the cells by cavitation. The sample was centrifuged to pellet the nuclei (2000 g, 15 min, 4 ℃) and the postnuclear supernatant (PNS) was subjected to ultracentrifugation (100,000 g, 1h, 4 ℃). The supernatant containing the cytosolic proteins was removed and subjected to another centrifugation (100,000 g, 1h, 4 ℃) to remove remaining membranous components. The supernatant of the second centrifugation was considered as cytosolic fraction. The membrane pellet of the first centrifugation was resuspended in PBS containing 0.3% Triton X-100 and regarded as membranous fraction. Cytosolic and membranous fraction were analyzed by immunoblotting.

3.2.3.7 SDS-PAGE

To separate proteins according to their size under denaturing conditions, SDS-polyacrylamide gel electrophoresis (PAGE) was used, based on a protocol originally described by U. Laemmli [98]. In this discontinuous gel system, the proteins were first concentrated in a stacking gel, followed by separation in a resolving gel. The acrylamide concentrations for stacking gel (5% acrylamide) and resolving gel (10% acrylamide) were chosen according to the size of the proteins of interest (as described in Chrambach and Rodbard [25]). The solutions were prepared as indicated above (see 3.1.5). Gel casting and electrophoresis were performed with the Mini PROTEAN system (Biorad) or with the electrophoresis system Hoefer SE600 (Amersham). Before application on the gel, all samples were mixed with Laemmli buffer (5x, final concentration 1x) and incubated at 90 ℃ for 5 min. Electrophoresis was performed in SDS-PAGE running buffer, at a current of 15 mA to 25 mA for Mini PROTEAN gels or 10 mA for Hoefer SE600 gels. To standardize the observed protein sizes, a prestained protein marker (NEB) was used. After electrophoresis, the gel was subjected either to immunoblotting or Coomassie staining.

3.2.3.8 Coomassie staining

Recombinantly expressed proteins were visualized in polyacrylamide gels by staining with the dye Coomassie Brilliant Blue R-250 following a procedure described in De St. Groth *et al.* [57]. For the detection of proteins, the acrylamide gel was incubated for 1 h in Coomassie staining solution on a shaker followed by overnight incubation in H_2O to destain the gel matrix.

3.2.3.9 Immunoblotting

For the specific detection of a protein species, the proteins separated on a acrylamide gel were transferred to a nitrocellulose membrane as originally described in Towbin *et al.* [182]. Subsequently, proteins were visualized via Horseradish peroxidase (HRP)-coupled antibodies. The transfer from gel to membrane occurred in a semi-dry blotting apparatus. Gel and membrane were placed between two layers of Whatman paper soaked in blotting buffer. For protein transfer, a current of 200 mA (Mini PROTEAN gel) or 240 mA (Hoefer SE600 gel) was applied for 1 h. Afterwards, the membrane was incubated in blocking solution for 1 h, followed by overnight incubation in primary antibody solution containing the antibody against the protein of interest (primary antibody). The primary antibody was diluted 1:1000 (α-Blnk, α-clathrin heavy chain, α-GFP, α-GM130, α-Grb2, α-LAMP1, ,α-Lyn α-α-tubulin, α-VAMP7), 1:2000 (α-Akt, α-HA), 1:750 (α-CIN85), or 1:500 (α-Rab5). After three times washing in TBS-T (20 min each), the membrane was incubated for 1 h in TBS-T containing an HRP-conjugated antibody against the primary antibody (secondary antibody, dilution 1:10,000 in TBS-T). The membrane was washed three to five times for 20 min in TBS-T, the HRP-signal was visualized by adding ECL solution and recording the emitted chemiluminescence using the Chemi Lux Gel Imager (Intas). To reprobe the membrane with another primary antibody, the HRP-signal was erased by incubation with sodium azide (0.1% in TBS-T) for 1 h. After 1 h wahing in TBS-T, the next primary antibody was applied. The following chemiluminescence detection process remained unaltered.

3.2.3.10 Recombinant protein production in *E. coli*

The production of N-terminally His_6-tagged recombinant proteins was performed as described in Engelke *et al.* [40]. The pET16b plasmid carrying the desired insert was transformed into *E. coli* BL21. A *E. coli* culture in 50 ml LB medium containing Ampicillin was grown to a optical density (600 nm) of 0.6 before the protein expression was induced by adding 1 mM IPTG. 4 h after induction the bacteria were pelleted (4000 g, 10 min). The pellet was resuspended in 1 ml LEW buffer and homogenized by three times 30 s sonification. Triton X-100 was added to a final concentration of 0.25% before 30 min lysis on ice. The lysate was cleared of debris by centrifugation (16,000 g, 20 min, 4 ℃) and loaded on a Protino Ni-IDA column (Macherey-Nagel), equilibrated in LEW Buffer. After four times washing with LEW buffer containing 20 mM Imidazol, the His_6-tagged proteins were eluted by application of 1 ml Elution buffer (1x) (Macherey-Nagel). For liposome flotation experiments, the sample was dialyzed overnight against LEW buffer to reduce the imidazole concentration.

3.2.4 Optical methods

3.2.4.1 Confocal microscopy

The subcellular localization of proteins tagged with GFP-variants was observed via confocal laser scanning microscopy as decribed in Lösing *et al.* [104]. For this procedure, $1{\cdot}10^6$ cells were pelleted by

centrifugation (400 g, 3 min), washed twice with 1 ml Krebs-Ringer solution (1 mM $CaCl_2$) and finally resuspended in 800 µl Krebs-Ringer solution (1 mM $CaCl_2$). Each well of the microscope chamber was filled with 400 µl of the sample. The image acquisition of images began after a resting time of 30 min to allow the cells to attach to the ground. The images were recorded with a confocal laser scanning microscope (Leica).

3.2.4.2 Flow Cytometry

Citrine expression test

The expression of transduced DNA was checked by the observing the presence of the Citrine tag harbored in the chimeric proteins. $2{\cdot}10^5$-$1{\cdot}10^6$ cells were pelleted (300 g, 4 min), washed once in PBS, and resuspended in 400 µl PBS for Flow cytometry. The Citrine fluorescence was recorded in the FITC channel (excitation 488 nm, filters 505 LP, 530/30) of the instrument.

Calcium ion influx measurement

Changes of the intracellular Ca^{2+} concentration upon B cell stimulation were quantified by flow cytometry as described in Stork *et al.* [169]. For this purpose, INDO-1, a Ca^{2+}-sensitive fluoresent dye was used. It displays a fluorescence emission maximum at 475 nm in its free from and at 400 nm in its Ca^{2+}-bound form. 1-1.5$\cdot 10^6$ DT40 cells were pelleted (300 g, 4 min) and resuspended in 700 µl RPMI-1640 medium (5% FCS). After addition of 2.1 µl pluronic F-127 (5%) and 0.7 µl INDO-1 AM (Life technologies), the cells were incubated at 30 ℃ for 25 min. 800 µl RPMI-1640 medium (10% FCS) were added, followed by an incubation of 10 min at 37 ℃. The cells were washed three times with Krebs-Ringer solution (1 mM $CaCl_2$) and finally resuspended in 600 µl Krebs-Ringer solution (1 mM $CaCl_2$). A following incubation for 20 min at 25 ℃ ensured the resting status of the cells and a stable baseline for the fluorescence signals. Afterwards, the fluorescence signals for INDO-1 violet (excitation 325-355 nm, filter 405/20) and blue (excitation 325-355 nm, filters 450 LP, 530/30) were recorded for 30 s. The ratio of these signals was taken as parameter for the intracellular Ca^{2+} concentration. After the baseline acquisition, the cells were stimulated with an α-IgM antibody (M4) and the fluorescence signal was recorded for 210 s. The analysis of the data was performed using the Software FlowJo (Tree Star Inc.).

4 Results

4.1 CIN85 reduces the threshold for BCR recruitment of SLP65.

Our group has previously shown that the interaction of SLP65 with the adaptor protein CIN85 is crucial for SLP65-plasma membrane recruitment as well as BCR-triggered downstream signaling events like Ca^{2+} influx. [121]. To confirm this observation, I transduced *slp65*$^{-/-}$ DT40 B cells with SLP65-wt and the CIN85 binding deficient variant SLP65-M2,3 (CIN85-binding Motifs 2 and 3 inactivated by R-to-A exchange, Figure 4.1 A). I analyzed the Ca^{2+} influx upon BCR stimulation by flow cytometry. As shown in Figure 4.1 B, the Ca^{2+} influx mediated by SLP65-M2,3 was markedly reduced compared to SLP65-wt. The magnitude of this effect was dependent on the concentration of α-IgM antibody used for stimulation. At high antibody concentrations (2 µg/ml, lower panel), the difference between SLP65-wt and the M2,3 variant was relatively minute, while it increased with decreasing antibody concentrations (0-2 µg/ml, upper panel). This suggests that the SLP65-CIN85 interaction reduces the threshold of a B cell to respond to BCR ligation. Additionally, the BCR-stimulation induced plasma membrane recruitment of SLP65-M2,3 was impaired compared to SLP65-wt. (Figure 4.1 C).

4.2 A fraction of CIN85 and SLP65 is membrane associated in resting B cells.

Having confirmed the influence of CIN85 on the BCR signaling pathway, I addressed the mechanism by which CIN85 binding supports SLP65 function. The SLP65-recruitment process to the BCR consists of distinct steps, namely SLP65-membrane association in resting cells, followed by SLP65-translocation to the plasma membrane and recruitment to the BCR upon activation. Like the SLP65-N-terminus, the CIN85-CC has been implicated to mediate membrane association of proteins [40, 200]. To test if CIN85 may serve as a membrane anchor for SLP65 in resting B cells, I performed subcellular fractionation experiments. To visualize the membrane-bound pool of CIN85 and SLP65, I established a detergent-free mechanical method to disrupt the B cells as schematically shown in Figure 4.2 A. The cells were mechanically disrupted by being passed through a Balch homogenizer, a device that homogenizes cells by shearing them between two metal surfaces. Subsequently, the postnuclear supernatant (PNS) was subjected to ultracentrifugation on a sucrose step gradient, separating membrane fractions including membrane-associated proteins from the soluble cytosolic fraction. I tested the success of the subcellular fractionation by the detection of marker proteins for different organelles and the cytosol.

I analyzed fractionated Ramos B cells by immunoblotting with the marker proteins shown in Figure 4.2 B. The kinase Akt and Grb2 served as cytosolic markers. They were not present in the membrane fractions (M1 and M2) but only in the bottommost fractions (M3 + Cyt, lanes 11-13) which contained the cytosol.

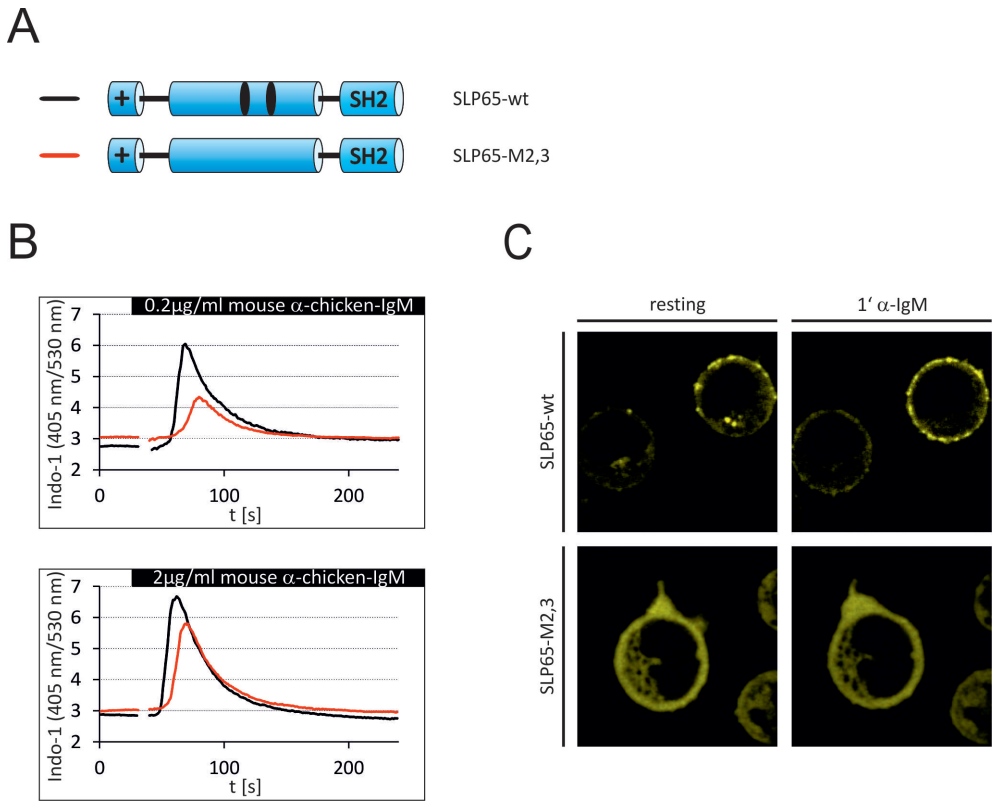

Fig. 4.1: CIN85 binding enhances BCR-induced Ca^{2+} influx and SLP65-membrane recruitment. *Slp65*$^{-/-}$ DT40 cells were transduced with Citrine-tagged SLP65-wt or SLP65-M2,3 (schematically shown in A). The Ca^{2+} influx in Citrine positive cells upon stimulation with 0.2 µg/ml or 2 µg/ml α-IgM was monitored by flow cytometry (B). The SLP65-membrane recruitment upon stimulation with 2 µg/ml α-IgM was observed by confocal microscopy (C).

A plasma membrane-associated protein, the Src-kinase Lyn, was present in all fractions with the exception of the cytosolic ones and was especially enriched in the membrane-containing fractions M1 (lanes 4 and 5) and M2 (lanes 8-9). GM130 as a maker for the low density Golgi-compartments was localized completely to the uppermost membrane fraction M1 (lanes 4 and 5), while the early endosome marker Rab5 was found in M1 (lanes 4 and 5), M2 (lanes 8 and 9) as well as in the cytosolic fractions (M11-13). SLP65 and CIN85 were present in M2 (lanes 8 and 9) and the cytosolic fractions (lanes 11-13). This indicated the existence of different pools of SLP65 and CIN85 in resting B cells, one membrane-bound and the other cytosolic.

I carried out further studies of the subcellular localization of SLP65 and CIN85 in DT40 B cells because *slp65*$^{-/-}$ DT40 cells could be reconstituted with different SLP65 variants without the background of endogenous SLP65. This allowed the assessment of the influence of SLP65-regions on the overall SLP65-localization. Like in Ramos cells, CIN85 and SLP65-wt were distributed between membrane (lanes 7 and 8) and cytosolic fractions (lanes 11-13) in DT40 cells (Figure 4.3 A, two upper panels). The majority of both proteins resided in the cytosolic fractions, confirming microscopic images that show a mostly

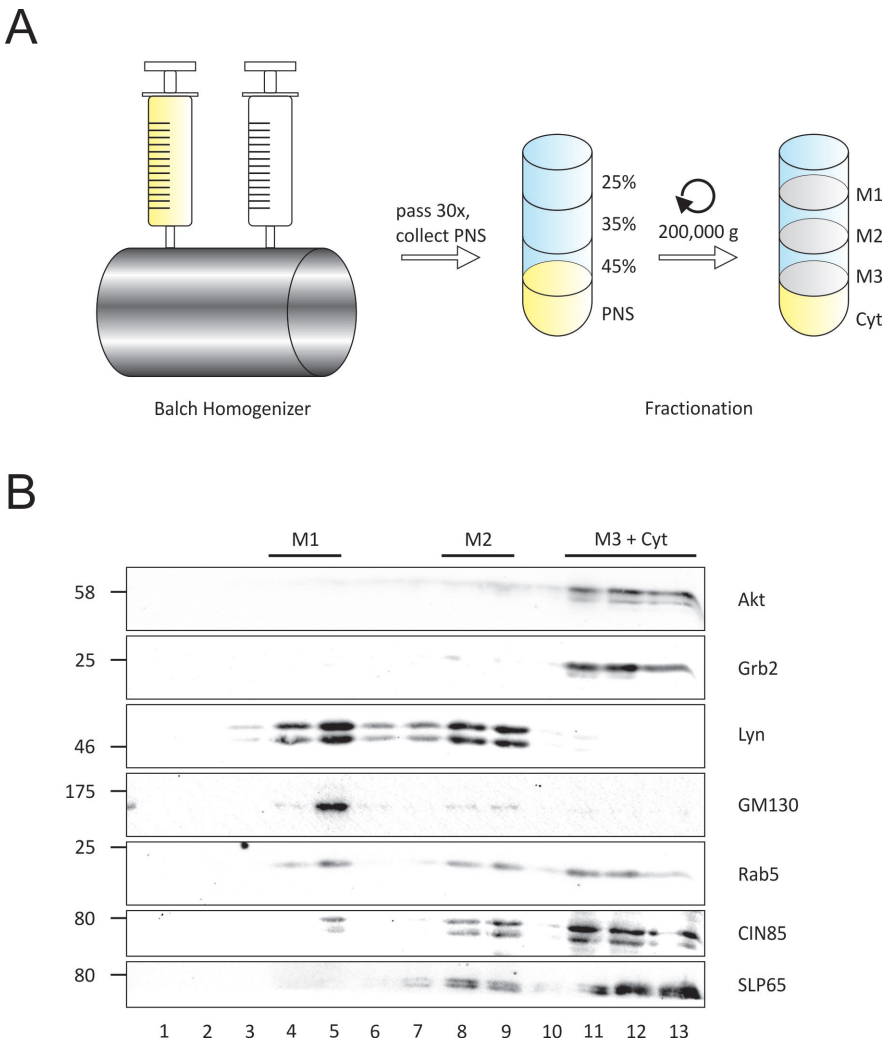

Fig. 4.2: SLP65 and CIN85 reside in cytosolic and membranous fractions. Ramos B cells were mechanically disrupted using a Balch homogenizer (see 3.2.3.5) and fractionated on a sucrose gradient (A). The fractions were collected from top (1) to bottom (13) and analyzed by immunoblotting for Akt, Grb2, Lyn, GM130, Rab5, CIN85, and SLP65 (B).

cytosolic localization of SLP65 [40]. Next, DT40 cells expressing the SLP65-ΔN variant, which is devoid of the SLP65 N-terminus, were analyzed. These cells lacked the membrane-bound pool of SLP65 (Figure 4.3, third panel), consistent with the observation that the SLP65 N-terminus is *per se* a membrane anchor [40]. The localization of CIN85 remained unaltered in these cells (Figure 4.3, forth panel). The SLP65-M2,3 variant, which does not bind to CIN85, showed a reduced membrane-bound pool compared to SLP65-wt (Figure 4.3 B, third panel). This suggested that CIN85 supports or enhances the SLP65 N-terminus-mediated membrane association. I determined the presence of SLP65-wt in the membrane fractions (Figure 4.3, first panel, lanes 7 and 8) and Akt exclusively in the cytosolic fractions (Figure 4.3 B, first panel, lanes 11-13) to control the success of the subcellular fractionation.

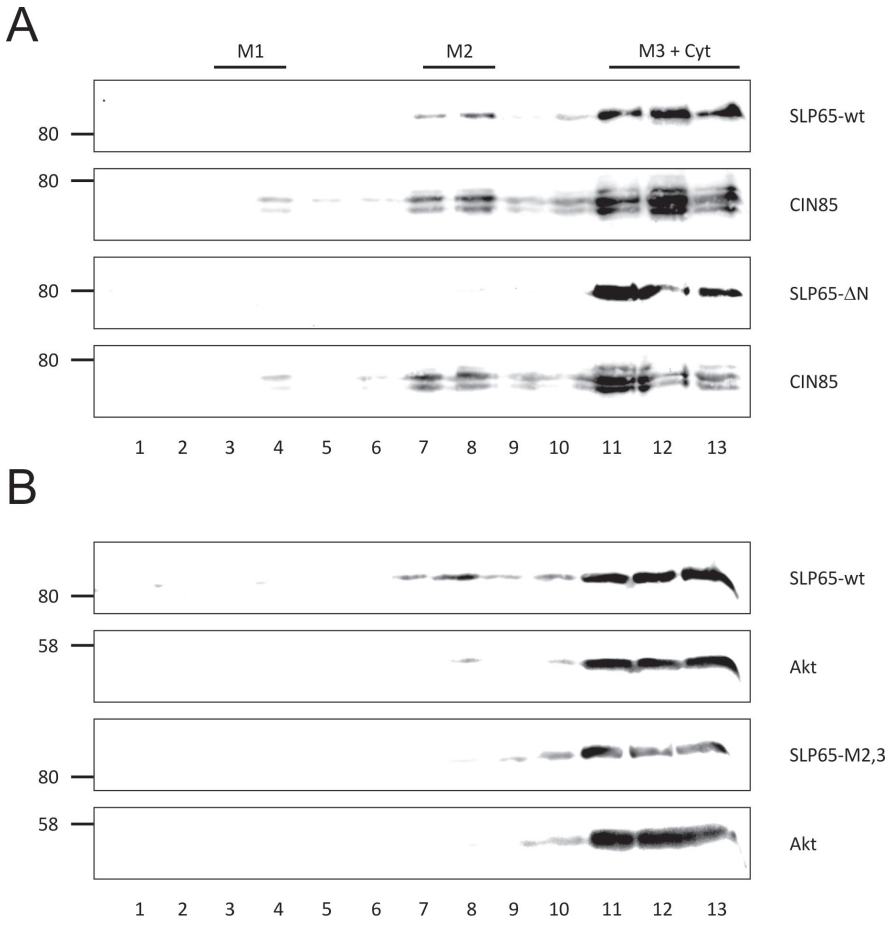

Fig. 4.3: The SLP65 variants ΔN and M2,3 show reduced membrane association compared to SLP65-wt. *Slp65*$^{-/-}$ DT40 cells reconstituted with SLP65-wt or SLP65-ΔN were mechanically disrupted using a Balch homogenizer (see 3.2.3.5) and fractionated on a sucrose gradient. The fractions were collected from top (1) to bottom (13) and analyzed by immunoblotting for SLP65 and CIN85 (A). *Slp65*$^{-/-}$ DT40 cells reconstituted with SLP65-wt or SLP65-M2,3 were mechanically disrupted using a Balch homogenizer (see 3.2.3.5) and fractionated on a sucrose gradient. The fractions were collected from top (1) to bottom (13) and analyzed by immunoblotting for SLP65 and Akt (B).

To assess a possible influence of the mechanical disruption method on these results, I also performed disruption by nitrogen cavitation as schematically shown in Figure 4.4 A. The cells were filled with nitrogen at a pressure of 10 bar. By abrupt decompression, resulting in very fast extension of the gas within the cells, the plasma membrane and potentially also the organelles were disrupted. The nucleus should stay intact to avoid a high DNA concentration in the PNS which complicates sample handling. The PNS was separated into two fractions by ultracentrifugation - the pellet containing membrane proteins and the supernatant containing cytosolic proteins. I analyzed the distribution of SLP65 and CIN85, as well as membrane and cytosolic markers between the two fractions (Figure 4.4 B). As expected, the integral membrane protein LAMP1 was only present in the membrane fraction, while the cytosolic proteins Akt and α-tubulin were concentrated in the cytosolic fraction. For SLP65 and CIN85, the signals in cytosolic and membrane fraction had a similar intensity. This confirmed the existence of a membrane-bound and a cytosolic pool of these two proteins in resting B cells.

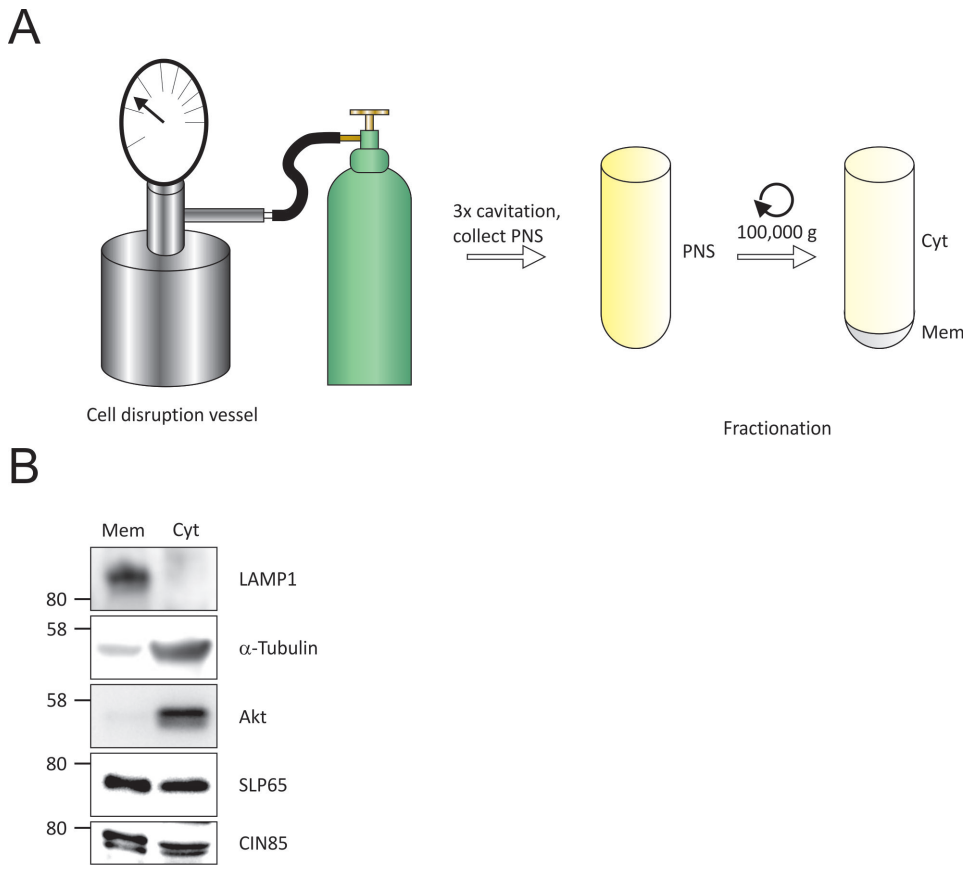

Fig. 4.4: SLP65 and CIN85 reside in the cytosolic and the membranous fraction. Ramos B cells were mechanically disrupted by cavitation in a cell disruption vessel (see 3.2.3.6) (A). Cytosol and membranes were separated by ultracentrifugation. The two fractions were analyzed by immunoblotting for LAMP1, α-tubulin, Akt, SLP65, and CIN85 (B).

4.3 VAMP7$^+$ vesicles display lysosomal characteristics but no detectable association with CIN85 and SLP65.

The existence of a membrane-bound pool of SLP65 has also been shown in a recent publication of our group. We demonstrated that SLP65 associates to specific intracellular vesicles positive for the Soluble NSF attachment protein receptor (SNARE) VAMP7 and for ATP [40]. To get more insight into the general composition of these vesicles and especially the role that CIN85 might play for targeting or anchoring SLP65 to vesicular membranes, I attempted to purify these vesicles. I disrupted DT40 cells expressing Cerulean-tagged VAMP7 mechanically and isolated VAMP7$^+$ vesicles by magnetic α-GFP-beads as depicted in Figure 4.5 A. Compared to cells expressing eGFP, the eluate from Cerulean-VAMP7 cells contained large amounts of VAMP7 (Figure 4.5 B, upper panel), and showed an enrichment for the vesicular coat protein clathrin (middle panel) and CIN85 (lower panel). The whole proteome of the isolated vesicles was determined by SILAC-based mass spectrometry, yielding a list of 358 enriched proteins in VAMP7$^+$ vesicles (Appendix 7.1). The majority of the identified proteins are known to exhibit Golgi apparatus (46 proteins), endosomal (45 proteins), lysosomal (63 proteins) or plasma membrane (82 proteins) localization or are implicated in vesicular transport (34 proteins). This is consistent with the previously described lysosomal and endosomal localization of VAMP7 (reviewed in [23]). However, SLP65 and CIN85 were not present in this vesicular proteome, suggesting either a weak association or a low abundance of SLP65 in the entire pool of VAMP7$^+$ vesicles. To analyze the VAMP7$^+$ SLP65$^+$ vesicles in detail, it will be necessary to identify further markers specific for these compartments.

4.4 Plasma membrane anchoring of SLP65 cannot substitute for the interaction with CIN85

If CIN85 served as a membrane anchor for SLP65, it should be possible to bypass the SLP65-CIN85 interaction by equipping SLP65 with a plasma membrane binding domain. To test this hypothesis, I created chimeric proteins, consisting of a membrane-targeting domain and SLP65, and tested their dependence on CIN85 binding. One chimeric protein contained the PLC-δ PH domain, a general plasma membrane-anchoring domain. The other chimeric protein encompassed the tandem SH2 (tSH2) domains of Syk, a specific BCR targeting device. It has been shown before that both domains, the Syk tSH2 domains and a plasma membrane-anchoring domain, can replace the SLP65-N-terminus [67]. For this reason, I deleted the SLP65 N-terminus (aa 1-45) in the chimeric proteins. This ensured that the membrane association of the chimeric proteins depended only on the non-SLP65 domain because it abolished the possibly interfering membrane targeting function of the SLP65-N-terminus. The SLP65 N-terminus might otherwise confer some specificity as its membrane binding capacity depends on membrane curvature [136].
On its own, the SLP65 variant lacking the N-terminus (SLP65-ΔN) shows neither specific intracellular

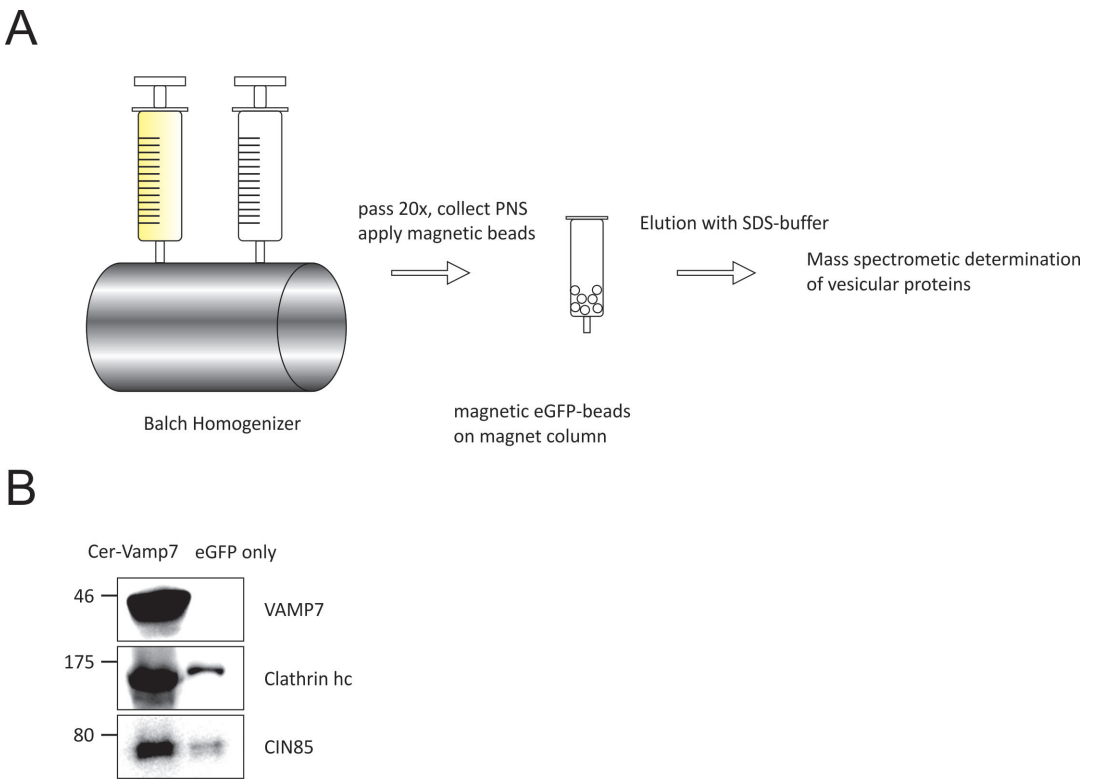

Fig. 4.5: VAMP7^{+} vesicles show an enrichment of the vesicular coat protein clathrin and CIN85. DT40 cells expressing either Cerulean-tagged VAMP7 or soluble eGFP were mechanically disrupted using a Balch homogenizer (see 3.2.3.5). Cerulean- or eGFP-containing components were enriched using affinity purification with an α-GFP antibody coupled to magnetic beads (A). The eluates derived from cells expressing Cerulean-tagged VAMP7 (left) or soluble eGFP (right) were analyzed by immunoblotting for VAMP7, the clathrin heavy chain (hc) and CIN85 (B).

localization in resting B cells nor plasma membrane recruitment or Ca^{2+} influx upon BCR stimulation ([87, 40], and Figure 4.6).

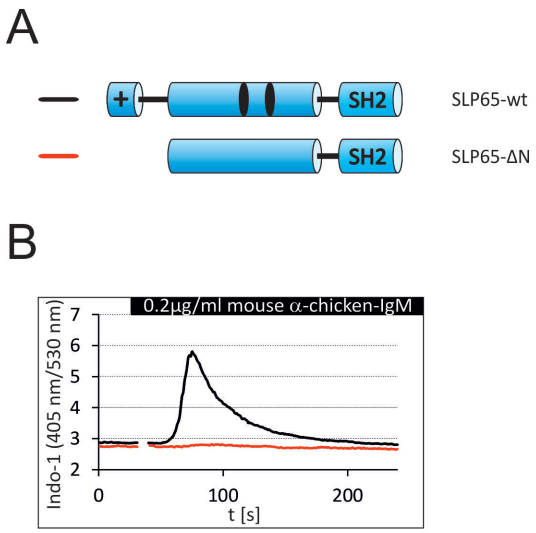

Fig. 4.6: The SLP65 N-terminus is crucial for BCR-induced Ca^{2+} influx. *Slp65*$^{-/-}$ DT40 cells were transduced with Citrine-tagged SLP65-wt or SLP65-ΔN (46-456) (schematically shown in A). The Ca^{2+} influx in Citrine positive cells upon stimulation with 0.2 µg/ml α-IgM was monitored by flow cytometry (B).

Slp65$^{-/-}$ DT40 cells were transduced with chimeric constructs that harbored SLP65 either capable (SLP65-ΔN) or incapable (SLP65-ΔN-M2,3) of CIN85 binding (shown schematically in Figure 4.7 A). I confirmed the plasma membrane targeting function of the PLC-δ PH domain by confocal microscopy in resting cells (Figure 4.7 C) and analyzed the Ca^{2+} influx upon BCR stimulation (Figure 4.7 B). For the PLC-δ-PH-SLP65 construct, CIN85 binding had an influence on Ca^{2+} signaling because the SLP65-M2,3 variant showed a strongly diminished Ca^{2+} influx (Figure 4.7 B). In contrast, there was no difference in Ca^{2+} influx between SLP65-ΔN and SLP65-ΔN-M2,3 for the Syk-tSH2-SLP65 construct. This suggests that CIN85 binding is dispensable for a SLP65-construct that is directly targeted to the BCR while it is still needed for a construct residing unspecifically at the plasma membrane. These results implicate that CIN85 is involved in the process of BCR targeting of SLP65.

4.5 The CIN85-CC supports SLP65 function.

Knowing from the last experiment that the function of CIN85 is not, or not exclusively, unspecific membrane anchoring of SLP65, I wanted to determine which domain of CIN85 contributes to BCR targeting

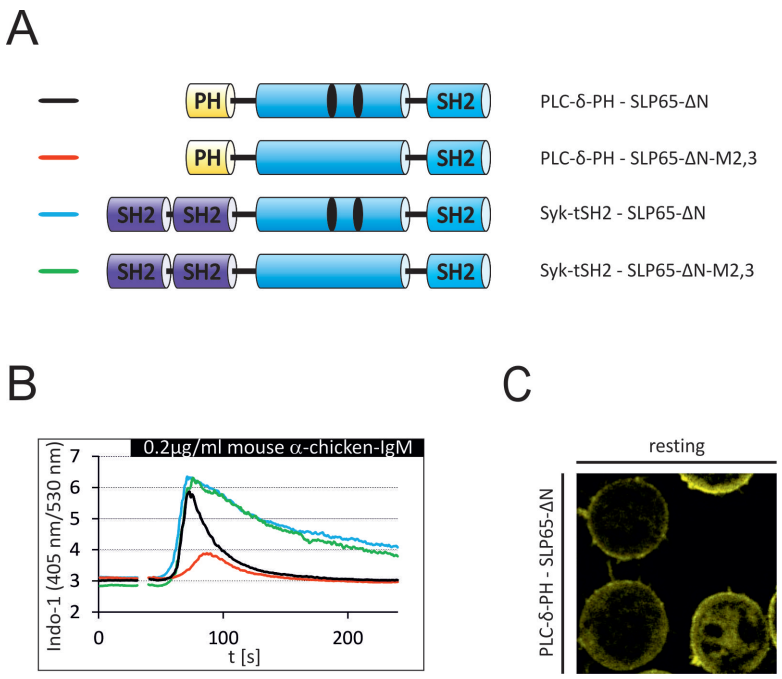

Fig. 4.7: SLP65 equipped with a plasma membrane anchor is still dependent on CIN85 binding. *Slp65*$^{-/-}$ DT40 cells were transduced with the Citrine-tagged chimeric proteins depicted in (A). The shown SLP65-ΔN variants were fused either to the PH domain of PLC-δ (black and red line) or to the tSH2 domains of Syk (blue and green line). The Ca^{2+} influx in transduced Citrine positive cells upon stimulation with 0.2 µg/ml α-IgM was monitored by flow cytometry (B). The intracellular localization of the chimeric PLC-δ-PH-SLP65-ΔN protein in resting cells was observed by confocal microscopy (C).

of SLP65. The SLP65-CIN85 interaction is mediated by the CIN85 SH3 domains [189, 121]. The effector function could reside in the SH3 domains, in the proceeding proline rich region (PRR), or in the C-terminal CC of CIN85. So I replaced the SLP65 N-terminus with the different CIN85 domains to investigate if the CIN85 domains can substitute the function of the SLP65 N-terminus for BCR recruitment. Furthermore, I used SLP65 variants either capable (SLP65-ΔN) or incapable (SLP65-ΔN-M2,3) of CIN85 binding to see if the chimeric proteins still depend on binding of full-length CIN85.

Slp65$^{-/-}$ DT40 cells were reconstituted with the CIN85-SLP65 chimeric protein depicted in Figure 4.8 A. The construct where the CIN85 SH3 domains (aa 1-328) substituted for the SLP65 N-terminus showed unspecific cytosolic localization in resting cells, no plasma membrane recruitment upon BCR stimulation (Figure 4.8 C, upper panel) and could not induce Ca^{2+} influx (Figure 4.8 B). In contrast, the construct where the C-terminal half of CIN85 (PRR and CC, aa 329-665) substituted for the SLP65 N-terminus resided in dot-like structures in resting cells (Figure 4.8 C, middle panel), comparable to the localization we have previously described for SLP65-wt [40]. The chimeric protein was recruited to the plasma membrane after BCR stimulation and enabled Ca^{2+} influx to the same extent as SLP65-wt (Figure 4.8 B). Abolishing CIN85 binding by introduction of the SLP65-M2,3 variant into this chimeric protein did not alter its localization (Figure 4.8 C, third panel) or diminish its signaling capacity.

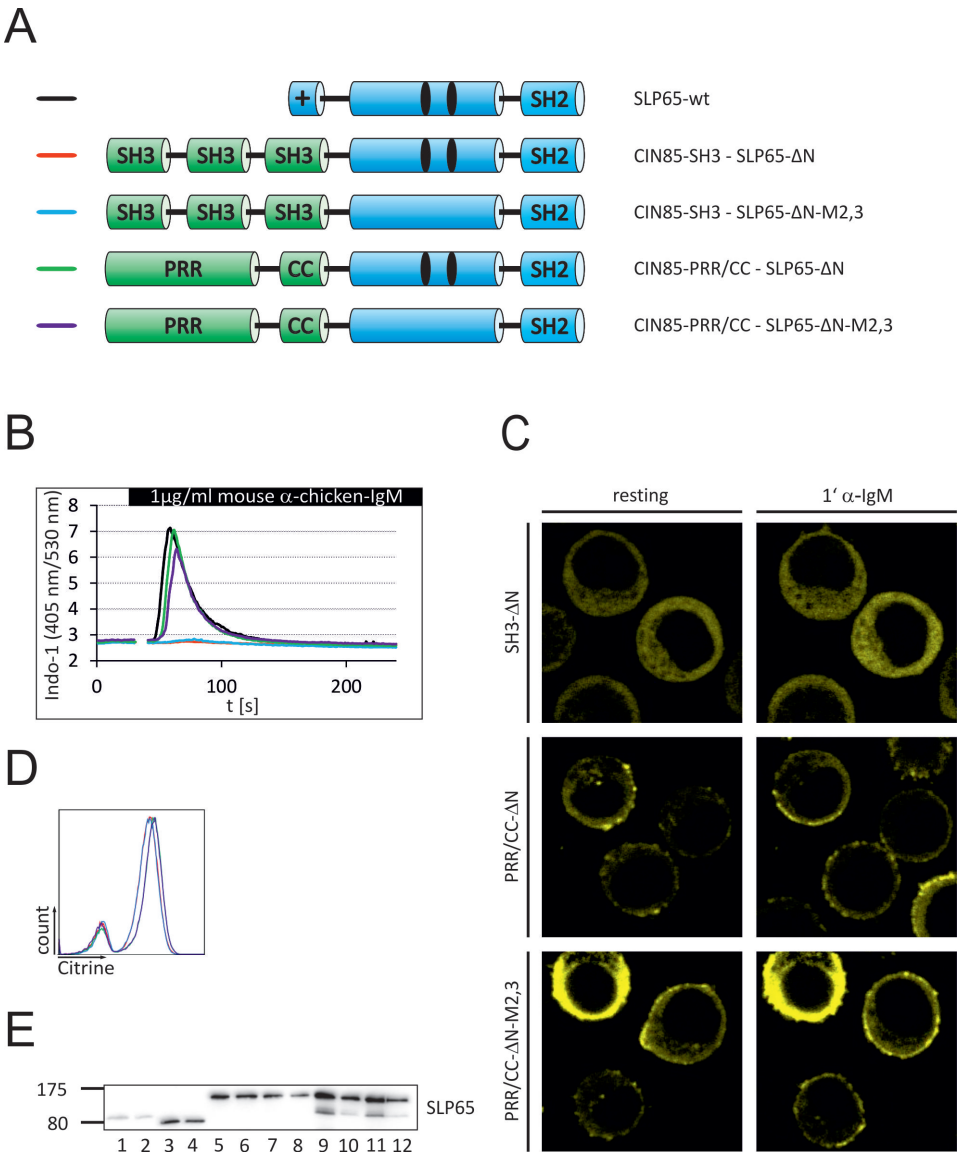

Fig. 4.8: The C-terminal part of CIN85 substitutes the SLP65 N-terminus. *Slp65*$^{-/-}$ DT40 cells were transduced with SLP65-wt or the Citrine-tagged chimeric proteins depicted in (A). The shown SLP65-ΔN variants were fused either to the SH3 domains of CIN85 (red and blue line) or to the PRR and CC of CIN85 (green and violet line). The Ca^{2+} influx in transduced Citrine positive cells upon stimulation with 1 µg/ml α-IgM was monitored by flow cytometry (B). Intracellular localization and membrane recruitment of the chimeric proteins 1 min after BCR stimulation (2 µg/ml α-IgM) were observed by confocal microscopy (C). The expression levels of the chimeric proteins were compared by detection of the Citrine fluorescence signal by flow cytometry (D). Cell lysates of cells producing SLP65-wt (lanes 1 and 2), SLP65-ΔN (lanes 3 and 4), CIN85-SH3-SLP65-ΔN (lanes 5-8), or CIN85-PRR/CC-SLP65-ΔN (lanes 9-12) were subjected to immunoblot analysis for SLP65 (E).

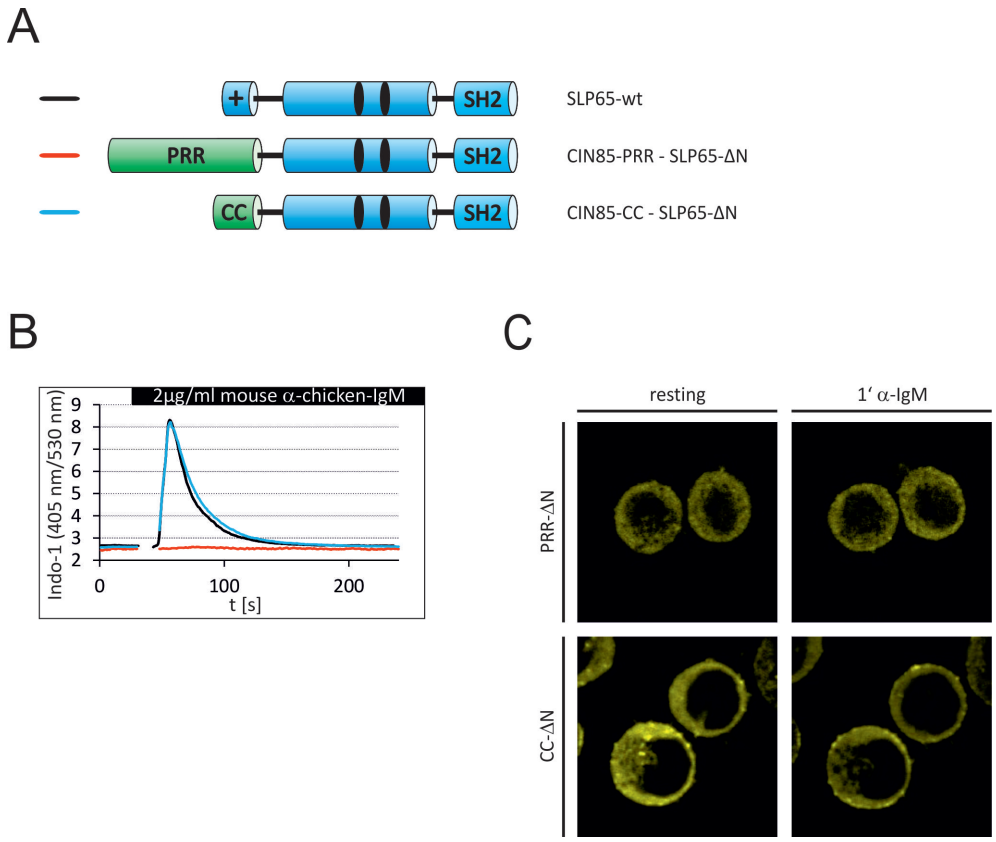

Fig. 4.9: The CIN85-CC substitutes the SLP65 N-terminus. *Slp65*$^{-/-}$ DT40 cells were transduced with SLP65-wt or the Citrine-tagged chimeric proteins depicted in (A). SLP65-ΔN was fused either to the PRR of CIN85 (red line) or to the CC of CIN85 (blue line). The Ca^{2+} influx in transduced Citrine positive cells upon stimulation with 2 µg/ml α-IgM was monitored by flow cytometry (B). Intracellular localization and membrane recruitment of the chimeric proteins 1 min after BCR stimulation (2 µg/ml α-IgM) were observed by confocal microscopy (C).

To specify the effector region of CIN85, I divided the C-terminal half of CIN85 into its two regions, creating the chimeric proteins shown in Figure 4.9 A. These constructs were expressed in *slp65*$^{-/-}$ DT40 cells. The construct where the the CIN85-PRR (aa 329-599) substituted for the SLP65 N-terminus was not capable of exhibiting any of the SLP65-wt functions (Figure 4.9 B and C). In contrast, the construct where the CIN85-CC (aa 594-665) substituted the SLP65 N-terminus was functional with regard to plasma membrane recruitment and Ca^{2+} mobilization. This chimeric protein was present in dot-like-structures in resting cells and exhibited plasma membrane recruitment and Ca^{2+} influx upon BCR stimulation (Figure 4.8 B and Figure 4.9 C, lower panel), comparable to SLP65-wt. By these experiments, I allocated the effector function of CIN85 to the CC, namely the last 72 amino acids of the protein. Abolishing CIN85 binding by introduction of the SLP65-M2,3 variant in the CIN85-PRR-SLP65-

ΔN and CIN85-CC-SLP65-ΔN constructs (Figure 4.10 A), led to no change regarding Ca^{2+} signaling, localization and membrane recruitment (Figure 4.10 B and C). This indicates that a covalent link to the CIN85-CC supports the function of SLP65 making the SLP65 N-terminus and CIN85 binding dispensable.

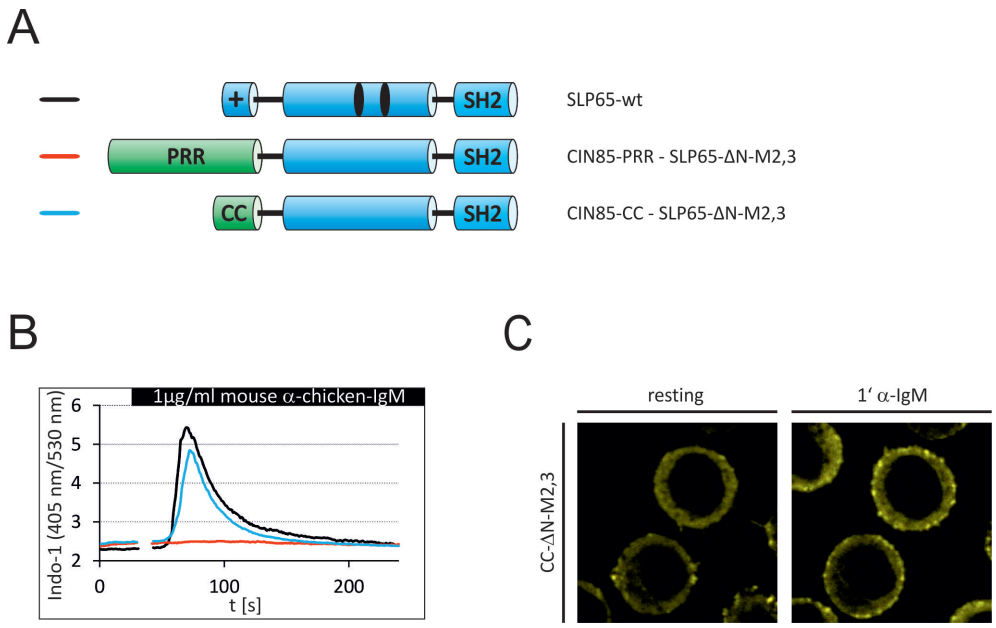

Fig. 4.10: The CIN85-CC substitutes the SLP65 N-terminus and CIN85 binding. *Slp65*$^{-/-}$ DT40 cells were transduced with SLP65-wt or the Citrine-tagged chimeric proteins depicted in (A). The SLP65-ΔN-M2,3 variant was fused either to the PRR of CIN85 (red line) or to the CC of CIN85 (blue line). The Ca^{2+} influx in transduced Citrine positive cells upon stimulation with 1 µg/ml α-IgM was monitored by flow cytometry (B). Intracellular localization and membrane recruitment of the chimeric CIN85-CC-SLP65-ΔN-M2,3 protein 1 min after stimulation (2 µg/ml α-IgM) were observed by confocal microscopy (C).

4.6 The CIN85-CC is an autonomous domain and can be assembled from its two halves.

To investigate if a specific spatial arrangement of the CIN85-CC with regard to SLP65 is needed for the CC function, I created chimeric proteins harboring the CC at different intramolecular positions. The chimeric proteins shown above (Figure 4.9 and Figure 4.10) had the CC arranged N-terminally of SLP65-ΔN, so I created chimeric proteins with C-terminal CC (Figure 4.11 A) and monitored the Ca^{2+} influx of *slp65*$^{-/-}$ DT40 cells reconstituted with these constructs (Figure 4.11 B). Like the constructs with N-terminal CC, the constructs with C-terminal CC showed Ca^{2+} mobilization comparable to SLP65-wt. This led to the conclusion that the CC most likely acts as an independent module, providing its function

independently of its position within the entire chimeric protein.

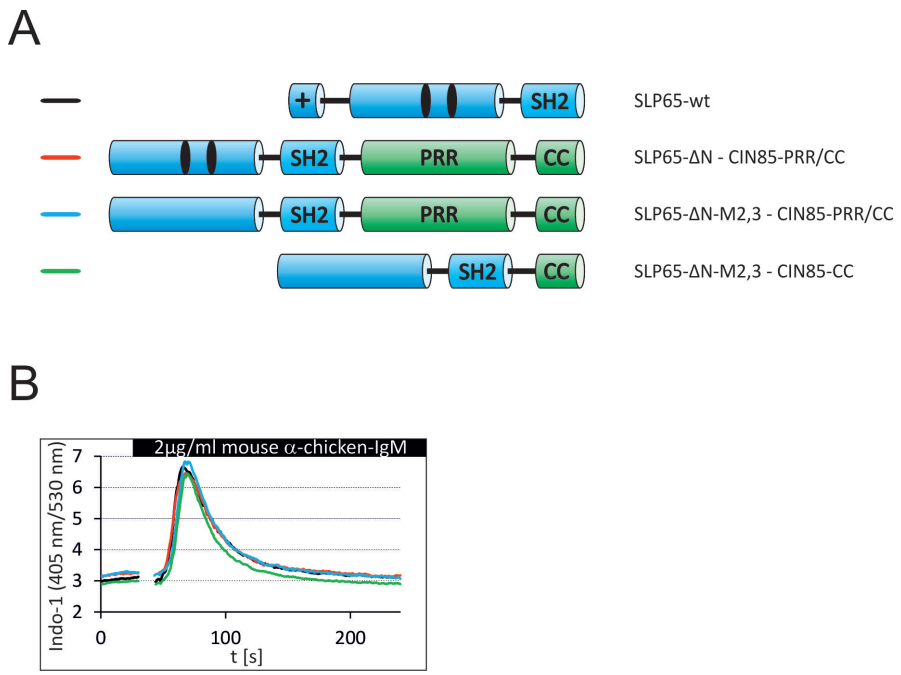

Fig. 4.11: C-terminal as well as N-terminal fusion of CIN85-CC to SLP65 substitutes the SLP65 N-terminus and CIN85 binding. *Slp65*$^{-/-}$ DT40 cells were transduced with SLP65-wt or the Citrine-tagged chimeric proteins depicted in (A). The shown SLP65-ΔN variants were N-terminally fused either to PRR and CC of CIN85 (red and blue line) or only to the CC of CIN85 (green line). The Ca^{2+} influx in transduced Citrine positive cells upon stimulation with 2 µg/ml α-IgM was monitored by flow cytometry (B).

In the following step, I created chimeric proteins containing only parts of the CC to identify a minimal amino acid sequence that contributed to SLP65 localization and function. I analyzed constructs harboring either the N-terminal (C_N, aa 594-631) or the C-terminal half (C_C, aa 632-665) of the CIN85-CC. These constructs were not functional, regardless if the half CC was arranged N-terminally (Figure 4.12 A) or C-terminally (Figure 4.12 B) of SLP65-ΔN. This led to the conclusion that the CIN85-CC has to act as a whole entity.

To determine possible complementation of the two CC halves, I created a construct that contained one half of the CC at the N-terminus, the other half at the C-terminus of SLP65-ΔN-M2,3 (Figure 4.13 A). In one orientation, C_C at the N-terminus and C_N at the C-terminus of SLP65, the protein was totally functional with regard to Ca^{2+} mobilization and membrane recruitment (Figure 4.13 B and C), substituting SLP65-wt completely. In the other orientation, C_N at the N-terminus and C_C at the C-terminus

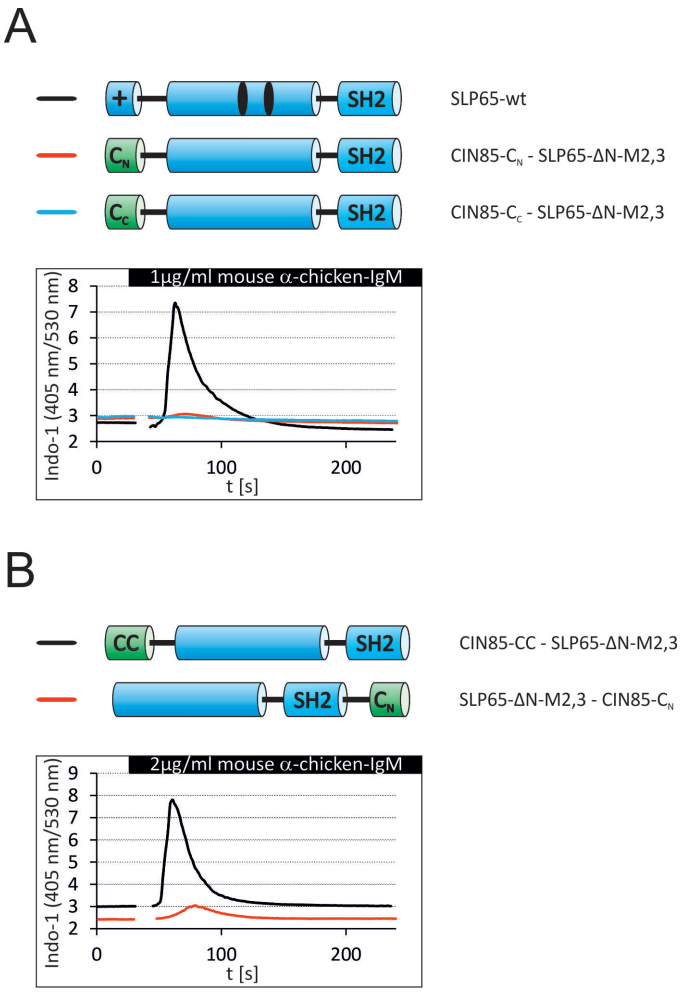

Fig. 4.12: Only the entire CIN85-CC can substitute the SLP65 N-terminus. *Slp65*$^{-/-}$ DT40 cells were transduced with SLP65-wt or the Citrine-tagged chimeric proteins depicted in (A) and (B). The SLP65-ΔN-M2,3 variant was fused either to the N-terminal (C_N, aa 594-631, red line) or to the C-terminal half of CIN85-CC (C_C, aa 632-665), blue line). The partial CIN85-CC was placed N-terminally (A) or C-terminally (B) of SLP65. The Ca^{2+} influx in transduced Citrine positive cells upon stimulation with 1 or 2 µg/ml α-IgM was monitored by flow cytometry (A and B).

of SLP65, the protein was not functional. This indicated that not only the presence of the two CC halves but also their spatial orientation in respect to each other is crucial. The functional orientation would enable the reconstitution of the CC, on the condition that the SLP65 part of the protein has the ability to form a loop-like structure. This reconstitution would be impossible in the other orientation because the order of the two CC halves would be wrong. The reconstitution of the CC seems to occur only intramolecularly. When two chimeric CIN85-SLP65 proteins, each bearing one half of the CC, were expressed simultaneously in *slp65*$^{-/-}$ DT40 cells, this did not enable Ca^{2+} mobilization (Figure 4.13 D). These results suggest that the entire CC is needed to support SLP65 functionally, but its position within the chimeric protein has no influence on its function.

4.7 The CIN85-CC and the SLP65 SH2 domain have distinct functions.

Fusion with the CIN85-CC could substitute for the SLP65 N-terminus as well as for CIN85 binding. The third functionality of SLP65 that mediates BCR recruitment is its SH2 domain (see 2.4). To see if the CIN85-SLP65 chimeric protein still needs a functional SLP65 SH2 domain, I introduced the amino acid exchange R372L in the SH2 domain. This exchange has been reported to lead to loss of function of SLP65 [2]. I transduced a variant of CIN85-CC-SLP65-ΔN containing the R372L exchange (Figure 4.14 A) in *slp65*$^{-/-}$ DT40 cells. This construct did not induce Ca^{2+} influx upon BCR stimulation (Figure 4.14 B), despite membrane recruitment could be observed to a certain extent (Figure 4.14 C). That implies that the CIN85-CC cannot replace the function of the SLP65 SH2 domain.

4.8 The interactome of CIN85 is diverse, but the number of interaction partners of the CIN85-CC is diminutive.

To find possible protein ligands of the CIN85-CC, I performed interactome studies based on mass spectrometry including SILAC. This labeling procedure by heavy amino acid isotopes allows a reduction of the background by the simultaneous analysis of a heavy labeled sample and a light labeled control (see 3.2.3.2). The identified ligands of CIN85 in the human B cell line Ramos, stimulated for 5 min with α-IgM-F(ab')$_2$, are listed in Table 4.1. The majority of the proteins in the CIN85 interactome have been previously described to interact with CIN85. I confirmed the well-established interactions with SLP65, CD2AP, c-Cbl and Cbl-b. I also found the known CIN85 interacting adaptor proteins Crk, SH3BP1 and STAP1. Furthermore, I identified the Crk-related protein Crk-like as a CIN85 interactor for the first time. The interactome contained seven subunits of the cell cycle regulating ubiquitin ligase Anaphase

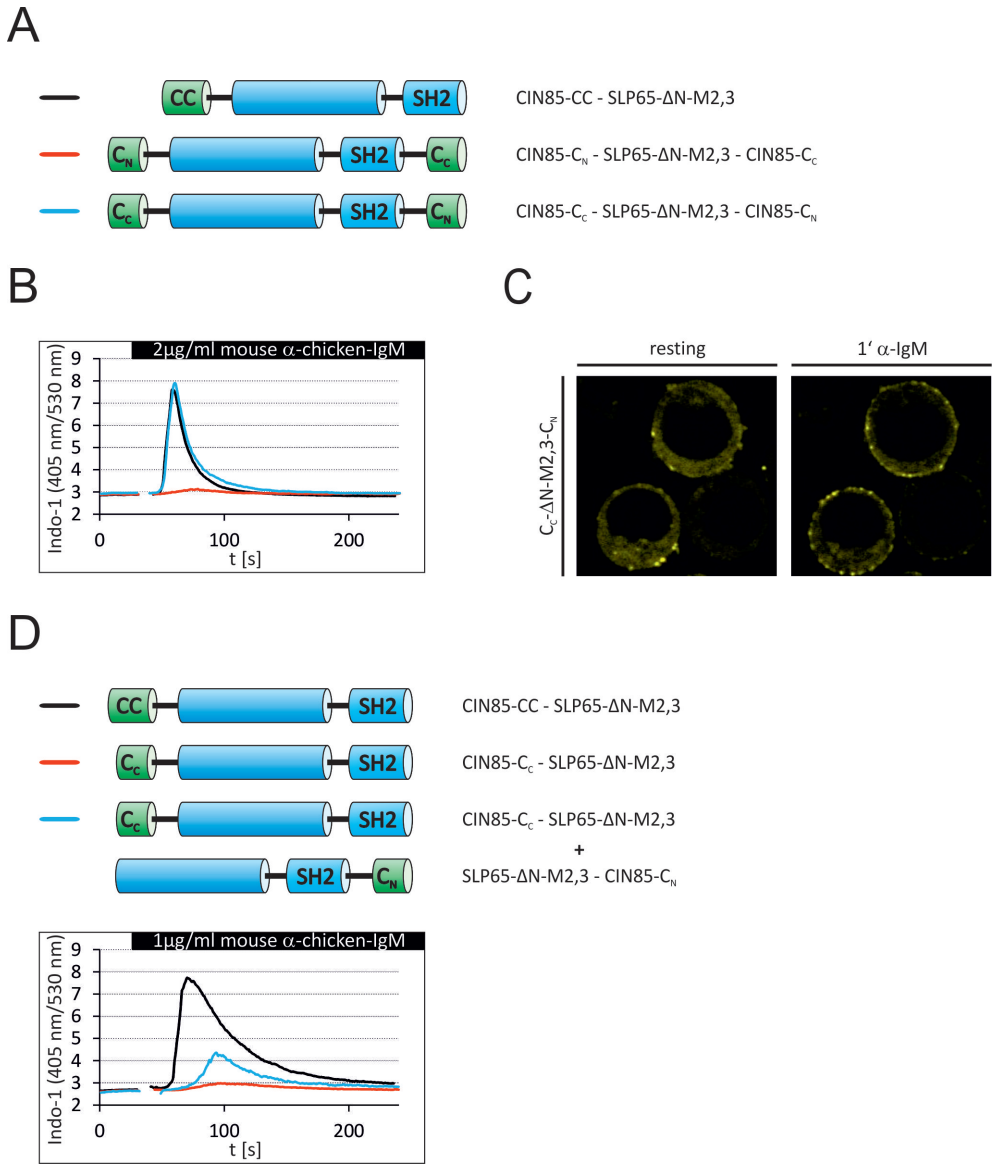

Fig. 4.13: The CIN85-CC is complemented by its two halves in *cis*. *Slp65*$^{-/-}$ DT40 cells were transduced with SLP65-wt or the Citrine-tagged chimeric proteins depicted in (A). For the first construct (red line), SLP65-ΔN-M2,3 was C-terminally fused to the first half of CIN85-CC (C1, aa 594-631) and N-terminally fused to the second half of CIN85-CC (C2, aa 632-665). For the second construct (blue line), SLP65-ΔN-M2,3 was C-terminally fused to the second half of CIN85-CC (C2, aa 632-665) and N-terminally fused to the first half of CIN85-CC (C1, aa 594-631). The Ca^{2+} influx in transduced Citrine positive cells upon stimulation with 2 µg/ml α-IgM was monitored by flow cytometry (B). Intracellular localization and membrane recruitment of the chimeric proteins 1 min after BCR stimulation (2 µg/ml α-IgM) were observed by confocal microscopy (C). *Slp65*$^{-/-}$ DT40 cells were transduced with the Citrine-tagged chimeric proteins depicted in D. The SLP65-ΔN-M2,3 variant was fused to the whole CIN85-CC (black line) or to the second half of CIN85-CC (C2, aa 632-665), red line). Cells transduced with the later construct were subsequently transduced with another Citrine-tagged chimeric protein, harboring SLP65-ΔN-M2,3 N-terminally fused to the first half of CIN85-CC (C1, aa 594-631). This resulted in cells co-producing two chimeric proteins, each carrying half a CIN85-CC (blue line). The Ca^{2+} influx in transduced Citrine positive cells upon stimulation with 1 µg/ml α-IgM was monitored by flow cytometry (D).

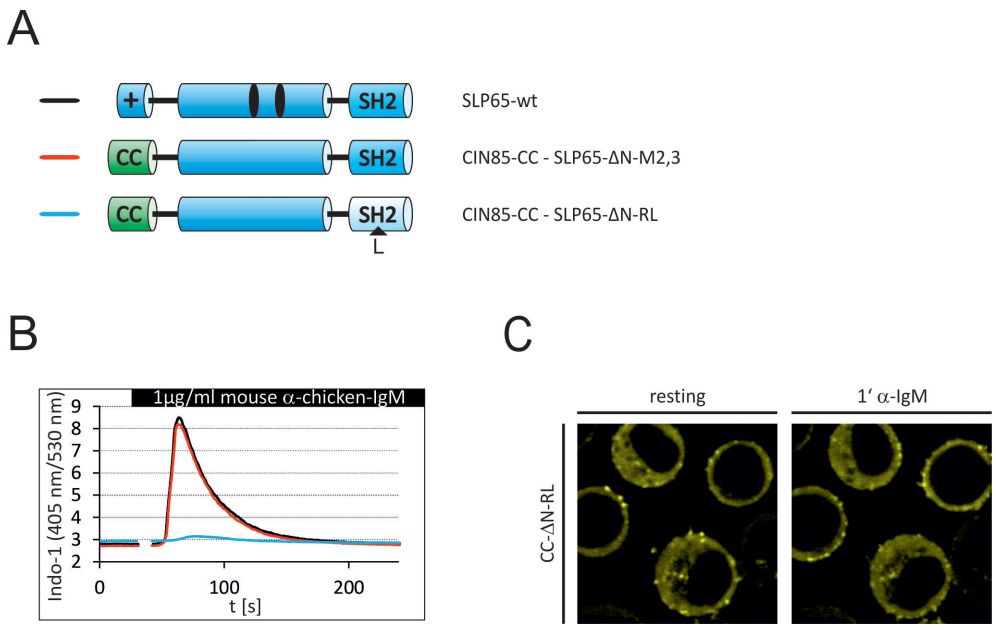

Fig. 4.14: CIN85-CC cannot substitute the function of the SLP65 SH2 domain. *Slp65*$^{-/-}$ DT40 cells were transduced with SLP65-wt or the Citrine-tagged chimeric proteins depicted in (A). CIN85-CC was fused to SLP65-ΔN-M2,3 (red line) or SLP65-ΔN harboring the additional amino acid exchange L372R (RL, blue line). The Ca^{2+} influx in transduced Citrine positive cells upon stimulation with 1 µg/ml α-IgM was monitored by flow cytometry (B). Intracellular localization and membrane recruitment of the chimeric protein CIN85-CC-SLP65-ΔN L372R 1 min after BCR stimulation (2 µg/ml α-IgM) were observed by confocal microscopy (C).

promoting complex (APC/C), four of which are known CIN85 interaction partners. It contained additionally the cell cycle regulator CDC21 homolog for which no CIN85 interaction has been described yet. The remaining identified proteins were Cytoskeleton regulators (CapZ proteins, Anillin), GTPase-activating proteins (ARHGAP17, ARAP1, ASAP1, ADAP2), PI3 kinases or phosphatases (p85, p110, SHIP1), the membrane trafficking regulator MIRab13 and the motor protein myosin ID. Three proteins of unknown function were identified as CIN85 interactors in this interactome, SHKBP1, CCDC88B and rhotekin 2. Via literature research, I was able to assign the CIN85 binding domains for most interaction partners. 17 of the identified 27 interaction partners are known to bind to the CIN85 SH3 domains. They are therefore most likely not relevant in the context of the SLP65-CIN85 interaction because the CIN85-SH3-SLP65 construct was not functional (Figure 4.8). The same is true for four other interactions partners known to bind to the CIN85-PRR as the CIN85-PRR-SLP65 construct was also not functional (Figure 4.9). The remaining six proteins are CD2AP, Crk-like protein, CDC21 homolog, ADAP2, myosin ID and CCDC88B.

Crk-like protein is very likely to bind to CIN85-PRR due to its homology to Crk. CD2AP is known to bind to CIN85-CC, but its knockout has no effect on Ca^{2+} influx in DT40 cells [18]. So it does not play a crucial role in BCR signaling. For the four remaining proteins, ADAP2, CDC21 homolog, myosin ID and CCDC88B, there is no evidence or indication for a membrane-anchoring or BCR targeting function, even though this cannot be formally ruled out. I also determined the interactome of CIN85 in resting

Ramos B cells which gave a list of interaction partners that did not differ from Table 4.1. The set of interaction partners in resting and activated Ramos cells is almost identical, indicating that the interactions of CIN85 are mediated by constitutive SH3-PRR and CC interactions which are not influenced by the phosphorylation processes occurring after BCR stimulation.

Tab. 4.1: The interactome of CIN85 in the human B cell line Ramos. A plasmid coding for strep-tagged CIN85 was introduced in Ramos cells by electroporation. Three clones were selected, mixed to avoid clonal effects, and labeled by growing them in SILAC medium containing the heavy isotope labeled amino acids lysine+4 and arginine+6. As control, wt Ramos cells were grown in medium with light amino acids. The differently labeled cells were stimulated for 5 min with α-IgM-F(ab')$_2$ and subjected to affinity purification by streptavidin-coated beads. The light and heavy labeled samples were pooled in 1:1 ratio and subsequently analyzed by mass spectrometry. The experiment was repeated 4 times. Proteins appearing at least 2 times at a heavy-to-light ratio of 3 or higher were regarded as definitive interaction partners of CIN85. The forth column of the table indicates the CIN85 region that has been described to interact with this ligand in the literature. This can be either the SH3 domains (SH3), the proline rich region (PRR) or the coiled coil (CC).

Protein	**Uniprot**	**Function**	**CIN85 domain**
SLP65	Q8WV28	Adaptor protein	[20, 189, 130, 119, 121], SH3
CD2AP	Q9Y5K6	Adaptor protein	20, [48, 72], CC
Crk	P46108	Adaptor protein	[55, 189], PR
Crk-like protein	P46109	Adaptor protein	
SH3BP1	Q9Y3L3	Adaptor protein	[20], SH3
STAP1	Q9ULZ2	Adaptor protein	[20, 91], SH3
c-Cbl	P22681	Adaptor protein, ubiquitin E3 ligase	[20, 65, 16, 189, 130, 200, 166], SH3
Cbl-b	Q13191	Adaptor protein, ubiquitin E3 ligase	[20, 65, 16, 174, 59] SH3
APC/C subunits 1, 3, 4, 5, 6, 8, 10	Q9H1A4, P30260, Q9UJX5, Q9UJX4, Q13042, Q9UJX2, Q9UM13	Cell cycle regulator	For APC/C 4,5,6,8: [65], SH3
CDC21 homolog	P33991	Cell cycle regulator	
Anillin	Q9NQW6	Cytoskeleton regulator	[65], SH3
CapZ α-1	P52907	Cytoskeleton regulator	[71, 72], PR
CapZ α-2	P47755	Cytoskeleton regulator	[71], PR
CapZ β	P47756	Cytoskeleton regulator	[71], PR
ARHGAP17	Q68EM7	GTPase-activating protein	[20, 65, 190], SH3

Protein	Uniprot	Function	CIN85 domain
ARAP1	Q96P48	GTPase-activating protein	[20, 65, 199], SH3
ASAP1	Q9ULH1	GTPase-activating protein	[20, 65, 125, 117, 91], SH3
ADAP2	Q9NPF8	GTPase-activating protein	
MIRab13	Q8N3F8	Membrane trafficking regulator	[20, 65], SH3
PI3K p110 α	P42336	PI3 kinase	[55]
PI3K p110 δ	O00329	PI3 kinase	[20], SH3
PI3K p85 α	P27986	PI3 kinase	[55, 17, 20], SH3+PR
SHIP1	Q92835	PI3 phosphatase	[20, 91], SH3
Myosin ID	O94832	Motor protein	
SHKBP1	Q8TBC3	unknown	[20, 65, 43, 16], SH3
CCDC88B	A6NC98	unknown	
Rhotekin 2	Q8IZC4	unknown	[20], SH3

To investigate the extent of conservation of CIN85 interactions between species, I determined the interactome in chicken DT40 cells (Table 4.2). There were interaction partners common between human and chicken cells, namely SLP65, CD2AP, Crk, SH3BP1, c-Cbl, Cbl-b, CapZ proteins, ASAP1, MIRab13, p110, p85 and rhotekin 2. All of them have been shown before to interact with CIN85 SH3 domains or PRR (with the exception of CD2AP, mentioned above). This means that no conserved interactor of the CIN85-CC that could play a role in BCR signaling was identified.

Furthermore, the chicken CIN85 interactome contained the proteins Endophilin A2, FBXO28, G2 and S phase-expressed protein 1, Katanin p60 ATPase-containing subunit A1, SH3 domain-containing protein 19, RASAL2, ASAP2, TBC1 domain family member 10A, SIPA1, three Carboxy-terminal kinesin proteins and CLEC17a. The only membrane protein amongst these is CLEC17a. For this protein, a knock-out in DT40 cells shows no effect on BCR signaling (Master thesis S. Pirkuliyeva).

Tab. 4.2: The interactome of CIN85 in the chicken B cell line DT40. A plasmid coding for strep-tagged CIN85 was introduced in DT40 cells by electroporation. Three clones were selected, mixed to avoid clonal effects, and labeled by growing them in SILAC medium containing the heavy isotope labeled amino acids lysine+4 and arginine+6. As control, wt DT40 cells were grown in medium with light amino acids. The differently labeled cells were stimulated for 5 min with α-IgM (M4) and subjected to affinity purification by streptavidin-coated beads. The light and heavy labeled samples were pooled in 1:1 ratio and subsequently analyzed by mass spectrometry. The experiment was repeated 2 times. Proteins appearing 2 times at a heavy-to-light ratio of 3 or higher were regarded as definitive interaction partners of CIN85. The forth column of the table indicates the CIN85 region that has been described to interact with this ligand in the literature. This can be either the SH3 domains (SH3), the proline rich region (PRR) or the coiled coil (CC).

Protein	**Uniprot**	**Function**	**CIN85 domain**
SLP65	Q9YGC1	Adaptor protein	[20, 189, 130, 119, 121], SH3
CD2AP	E1BW77	Adaptor protein	[48, 72], CC
Crk	Q04929	Adaptor protein	[55, 189], PR
Endophilin A2	Q8AXV0	Adaptor protein	[131], PR
SH3BP1	F1NDY2	Adaptor protein	[20], SH3
c-Cbl	F1NXW5	Adaptor protein, ubiquitin E3 ligase	[20, 65, 16, 189, 130, 200, 166], SH3
Cbl-b	F1NL77	Adaptor protein, ubiquitin E3 ligase	[20, 65, 16, 174, 59] SH3
FBXO28	F1P2Q9	Part of ubiquitin E3 ligase complex	
G2 and S phase-expressed protein 1	F1NIS1	Cell cycle regulator	[20, 65], SH3
CapZ α-1	P13127	Cytoskeleton regulator	[71, 72], PR
CapZ α-2	P28497	Cytoskeleton regulator	[71], PR
CapZ β	P14315	Cytoskeleton regulator	[71], PR
Katanin p60 ATPase-containing subunit A1	Q1HGK7	Cytoskeleton regulator	[65], SH3
SH3 domain-containing protein 19	F1N8H5	Cytoskeleton regulator	[65], SH3
ARHGAP-17	E1C8J2	GTPase-activating protein	[20, 65, 190], SH3
RASAL2	F1NW82	GTPase-activating protein	[65], SH3
ASAP1	E1BTH6	GTPase-activating protein	[20, 65, 125, 117, 91], SH3
ASAP2	F1NKX8	GTPase-activating protein	[125], SH3

Protein	Uniprot	Function	CIN85 domain
TBC1 domain family member 10A	F1NSI7	GTPase-activating protein	
SIPA1	R4GHA6	GTPase-activating protein	
MIRab13	F1N8S7	Membrane trafficking regulator	[20, 65], SH3
Kinesin-like protein KIF23	Q5ZI55	Motor protein	[65], SH3
Kinesin-like protein	F1NBH9	Motor protein	
Kinesin-like protein	R4GGT8	Motor protein	
PI3K p110 α	O42391	PI3 kinase	[55]
PI3K p85 β	E1C2C5	PI3 kinase	
CLEC17a	H9L2G9	Transmembrane lectin	
Rhotekin 2	F1NAV3	unknown	[20], SH3

To address the question of CIN85-CC interaction partners more specifically I elucidated the interactome of a strep-tagged CIN85-CC-SLP65-ΔN chimeric protein in *slp65*$^{-/-}$ DT40 cells. The list of interaction partners of CIN85-CC-SLP65-ΔN in resting DT40 cells (Table 4.3) contains CIN85, CD2AP, Grb2 and CapZ which are also found to interact with SLP65-wt in resting DT40 cells [121]. Of the remaining four identified proteins, only FBXO28 is also found in the CIN85 interactome, indicating that this is an interactor of the CIN85-CC and not of SLP65-ΔN. As a part of a soluble E3 ubiquitin ligase complex, there is no hint that FBXO28 contributes to membrane anchoring or BCR targeting.

Taken together, the interactome analyses did not indicate that CIN85-CC exhibits its effector function for SLP65 through interaction with a protein ligand.

Tab. 4.3: The interactome of the chimeric protein CIN85 CC-SLP65-ΔN in the chicken B cell line DT40. A plasmid coding for strep-tagged CIN85-CC-SLP65-ΔN was introduced in *slp65*$^{-/-}$ DT40 cells by electroporation. Three clones were selected, mixed to avoid clonal effects, and labeled by growing them in SILAC medium containing the heavy isotope labeled amino acids lysine+4 and arginine+6. As control, wt DT40 cells were grown in medium with light amino acids. The differently labeled cells were subjected to affinity purification by streptavidin-coated beads. The light and heavy labeled samples were pooled in 1:1 ratio and subsequently analyzed by mass spectrometry. The experiment was repeated 3 times. Proteins appearing at least 2 times at a heavy-to-light ratio of 3 or higher were regarded as definitive interaction partners of the chimeric protein. The forth column of the table indicates if this interaction has been described before for SLP65.

Protein	**Uniprot**	**Function**	**Reference**
SLP65	Q9YGC1	Adaptor protein	[121]
CD2AP	E1BW77	Adaptor protein	[121]
CIN85	F1NKX7	Adaptor protein	[121]
Grb2	Q07883	Adaptor protein	[121]
CapZ α-1	P13127	Cytoskeleton regulator	[121]
CapZ β	P14315	Cytoskeleton regulator	[121]
FBXO28	F1P2Q9	Part of ubiquitin E3 ligase complex	
TRIM62	E1BX13	Part of ubiquitin E3 ligase complex	
HUS1	E1C8I4	Cell cycle regulator	
Acyl-CoA thioesterase 8	E1BVK8	Metabolic regulator	

4.9 The CC mediates PA association, but this is not sufficient to support SLP65 function.

Because no protein ligand for the CIN85-CC with an obvious link to BCR signaling could be identified, I studied direct lipid binding of the CC. There are two reports stating that CIN85 binds to the intracellular membrane lipid phosphatidic acid (PA) by its CC [200, 201]. This binding depends on the presence of the basic amino acid residues K645, K646, R648 and R650 of CIN85 [201]. To confirm the PA binding capacity of the CIN85-CC within the chimeric CIN85-SLP65 protein, I performed an affinity purification with PA coated beads (Figure 4.15 A). While recombinant SLP65-wt and SLP65-ΔN showed little or no affinity to the beads, recombinant CIN85-CC-SLP65-ΔN associated to them.

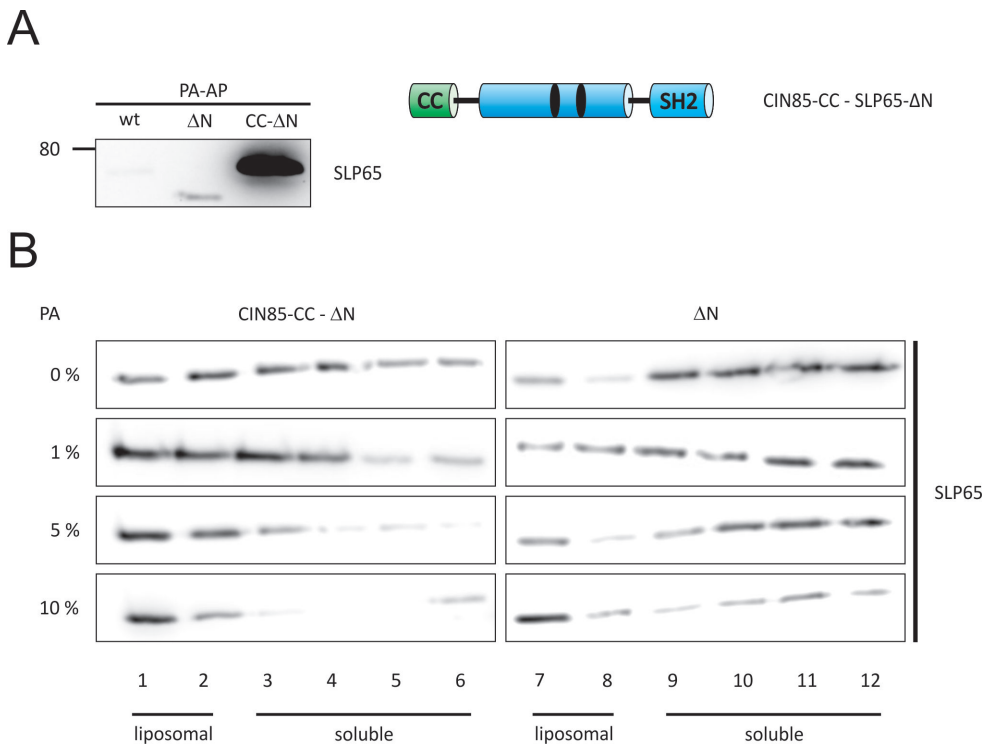

Fig. 4.15: The CIN85-CC associates with PA containing membranes. His_6-tagged recombinant proteins of SLP65-wt (wt), SLP65-ΔN (dN) and the chimeric protein CIN85-CC-SLP65-ΔN (CC-ΔN, schematically shown in A) were produced. The association of these proteins to PA coated beads was tested by affinity purification (A). The binding of CIN85-CC-SLP65-ΔN and SLP65-ΔN to liposomes containing different PA concentration was determined by a liposome flotation experiment (B). The recombinant proteins were mixed with liposomes, followed by separation of liposomes and soluble fraction by ultracentrifugation. Liposomal fractions (1 and 2 for CC-ΔN, 7 and 8 for-ΔN) and soluble fractions (3-6 for CC-ΔN, 9-12 for-ΔN) were collected and analyzed by immunoblotting for SLP65. The liposome flotation experiment was carried out by Sona Pirkuliyeva (see [136] for experimental details).

To address the lipid anchoring mode of the CIN85-CC in system more comparable to intracellular structures, I conducted liposome-protein interaction studies together with Sona Pirkuliyeva. We investigated the binding of a recombinantly produced CIN85-CC-SLP65-ΔN chimeric protein to liposomes containing different concentrations of PA by a liposome flotation assay. Fractions containing liposomes (lanes 1-2, and 7-8) and soluble proteins (lanes 3-6 and 9-12) were analyzed by immunoblotting (Figure 4.15 B). The chimeric protein did not bind to liposomes lacking PA (upper panel). With increasing PA concentration, the amount of liposome-bound protein increased. A concentration of 10% PA (lowest panel) was sufficient to associate virtually the complete amount of protein to the liposomes. SLP65-ΔN without the CIN85-CC did not bind to liposomes (Figure 4.15 B, right part), independent of the PA concentration. Only at a PA concentration of 10% there seems to be a weak association to the liposomes, probably dependent on the positively charged His-tag of the recombinant protein. The lack of PA binding of SLP65-ΔN suggests that the observed PA binding is a function inherent to the CIN85-CC. To assess the effect of PA binding in regard to SLP65 function *in vivo*, I transduced a SLP65-ΔN construct containing the PA binding motif of Raf1 (Figure 4.16 A) in *slp65*$^{-/-}$ DT40 cells. The PA binding motif of Raf1 has been shwon to direct other proteins to PA-containing cellular compartments [81]. The chimeric Raf1-SLP65 protein was not able to restore Ca^{2+} influx (Figure 4.16 B), indicating that PA binding is not sufficient to support SLP65 function.

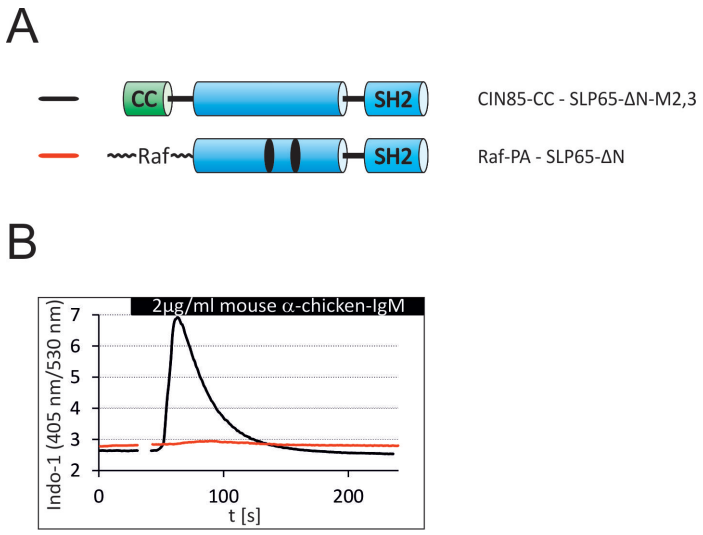

Fig. 4.16: The PA binding motif of Raf is insufficient to substitute the SLP65 N-terminus. *Slp65*$^{-/-}$ DT40 cells were transduced with the Citrine-tagged chimeric proteins depicted in (A). The shown SLP65-ΔN variants were fused either to the CIN85-CC (black line) or to the PA binding motif of Raf (aa 391-426, red line). The Ca^{2+} influx in transduced Citrine positive cells upon stimulation with 2 µg/ml α-IgM was monitored by flow cytometry (B).

4.10 The CIN85-CC forms a stable parallel trimer.

Due to the fact that the search for protein and lipid interaction partners of the CIN85-CC gave no hint on a mechanism for SLP65 support, we investigated the structure of the CC. Multiangle laser light scattering (Figure 4.17 A) and mass spectrometry (Figure 4.17 B) analyses with the recombinant CIN85-CC were performed by Dr. Leo Wong and Dr. Stefan Becker in Prof. Griesinger's department. From the results, it was evident that the CIN85-CC forms a trimer. NMR spectroscopy studies by Dr. Leo Wong resulted in the parallel trimer structure of the CC shown in Figure 4.18 A. This structure demonstrated that the CIN85 region between amino acid 609 and 662 forms an continuous CC. The CIN85-CC trimer displayed a high stability as denaturation occurred only at 85 °C(Figure 4.18 B).

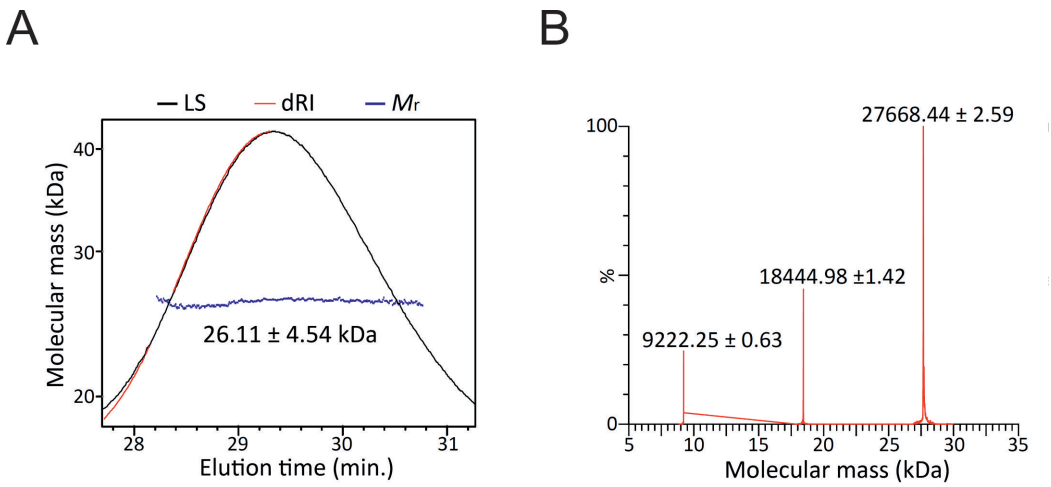

Fig. 4.17: The CIN85-CC forms a trimer. A His_6-tagged recombinant protein of the CIN85-CC was produced and isolated by affinity purification. After cleavage of the His_6-tag, the protein was analyzed by light scattering (A) and mass spectrometry (B). For the light scattering analysis, the protein was subjected to size exclusion chromatography. The chromatogram displayed a single peak which corresponded to a molecular mass of 26.11 kDa according to multiangle laser light scattering (MALLS) analysis. This corresponds to a CIN85-CC trimer (calculated weight of 26.2 kDa). The CIN85-CC was also subjeted to ESI mass spectrometry. The spectrum displayed three peaks, corresponding to CIN85-CC monomer, dimer and trimer. The trimer peak showed the highest intensity. The slightly higher molecular weight of the trimer (27.67 kDa) compared to MALLS analysis resulted from isotope labeling of the CC for subsequent NMR analysis (calculated isotope labeled weight of 27.7 kDa). The experiments were performed and analyzed by Dr. Leo Wong and Dr. Stefan Becker.

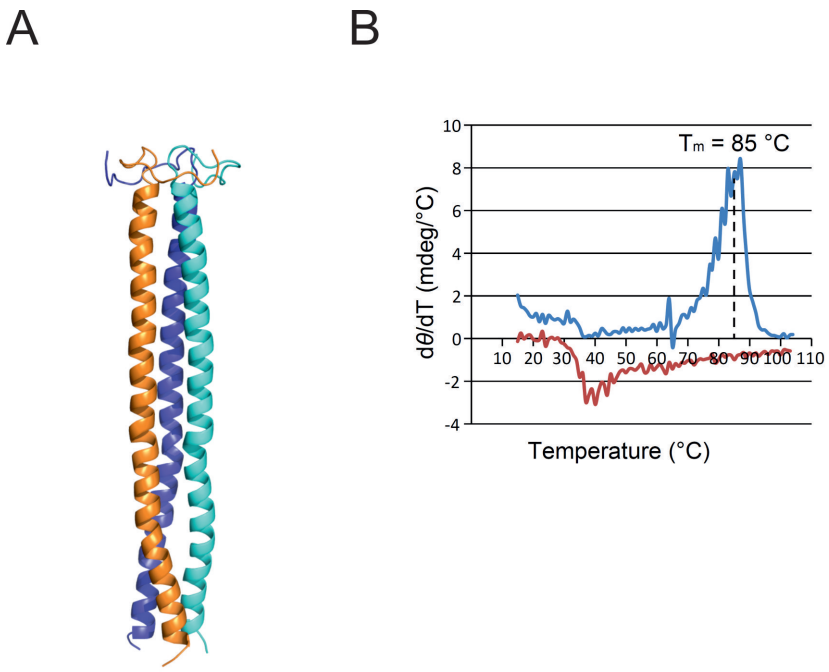

Fig. 4.18: The CIN85-CC trimer displays a high stability. The preliminary structure of the CIN85-CC was calculated on the base of data obtained in several NMR spectroscopy experiments (A). The CIN85-CC was found to form a parallel trimer consisting of three molecules with continuous α-helical structure between amino acid 609 and 662. The stability of the CIN85-CC against heat-induced denaturation was determined by circular dichroism spectroscopy (B). The trimer denaturated at a temperature of 85 °C. The experiments were performed and analyzed by Dr. Leo Wong.

4.11 An amino acid exchange in the hydrophobic interface of the CC disrupts its oligomerization and function.

Based on these observations, I wondered if oligomerization is *per se* the crucial function that the CIN85-CC provides to SLP65. To abolish oligomerization of the CIN85-CC, I introduced an amino acid exchange in the hydrophobic interface of the CC, exchanging leucine 619 for lysine. Leucine 619 is involved in the formation of the CIN85-CC trimer (Figure 4.19 A), thus I suspected that its exchange might lead to loss of oligomerization. Indeed, exclusively the monomeric form of CIN85-CC L619K could be observed by mass spectrometry (Figure 4.19 B). I obtained an identical result by co-immunoprecipitation of differently tagged forms of the chimeric CIN85-SLP65 protein (Figure 4.19 C). When I co-transfected cells with HA-tagged CIN85-CC-wt SLP65-ΔN and Citrine-tagged CIN85-CC-wt SLP65-ΔN, it was possible to co-precipitate the HA-tagged form with the Citrine-tagged form (lane 3), indicating oligomerization. If one of the transfected proteins harbored the L619K exchange in the CC (lane 4), this co-precipitation was not possible, suggesting a loss of oligomerization.

I fused the CIN85-CC L619K variant to SLP65-ΔN-M2,3 (Figure 4.20 A), transduced the construct in *slp65*$^{-/-}$ DT40 cells, and analyzed the Ca^{2+} influx in these cells upon α-IgM stimulation (Figure 4.20 B). The Ca^{2+} influx mediated by the chimeric protein with L619K exchange was severely impaired compared

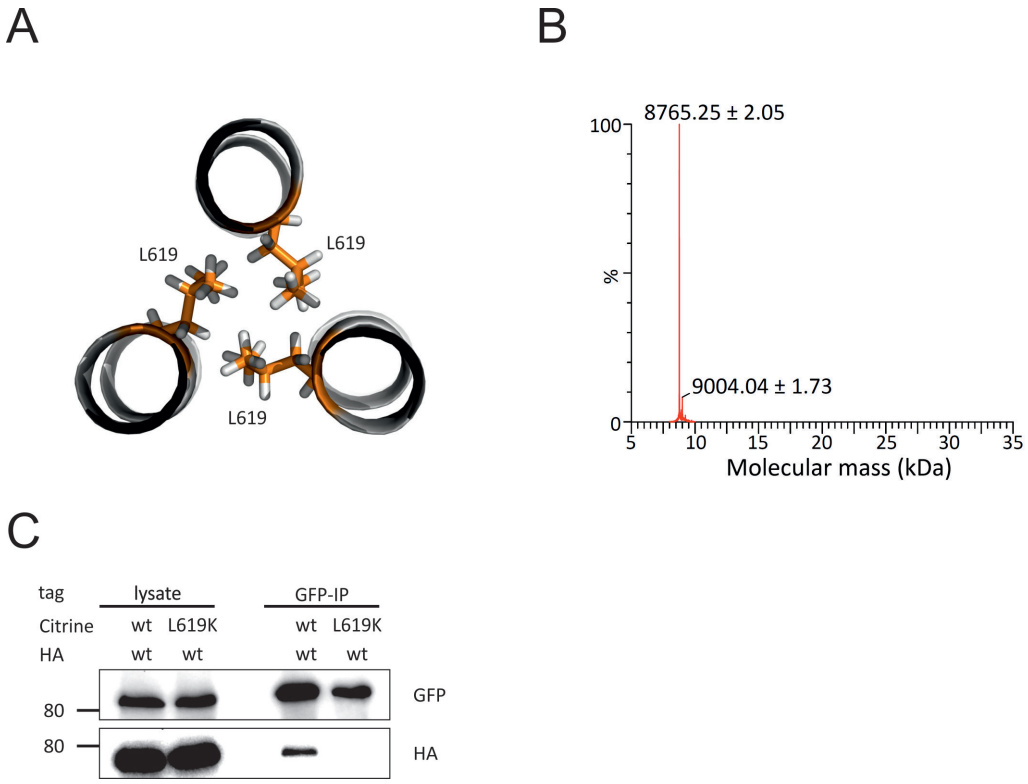

Fig. 4.19: The exchange of leucine 619 for lysine prevents the oligomerization of the CIN85-CC. As seen from the CIN85-CC structure, leucine 619 is involved in the formation of the hydrophobic interface of the CC trimer (A). A His_6-tagged recombinant protein of the CIN85-CC harboring L619K was produced and analyzed by ESI mass spectrometry (B). The only identified species corresponds to a monomer of CIN85-CC. The experiments were carried out by Dr. Leo Wong and Dr. Stefan Becker. *Slp65*$^{-/-}$ DT40 cells were co-transduced with HA- and Citrine-tagged chimeric proteins of CIN85-CC and SLP65-ΔN-M2,3. The CIN85-CC of the Citrine-tagged proteins consisted either of CC-wt or CC L619K. The Citrine-tagged proteins were immunoprecipitated using α-GFP antibody. Cell lysates (left part) and immunoprecipitated fractions (right part) were analyzed by immunoblotting for GFP and HA (C).

to the construct harboring the CIN85-CC-wt. Also its membrane recruitment was strongly impaired (Figure 4.20 C). This implicated that the CIN85-CC L619K variant provided hardly any support for the SLP65 function. In contrast, a CIN85-CC variant with the exchange of leucine 619 for alanine which preserved the integrity of the hydrophobic interface showed only a slight decrease in Ca^{2+} signaling compared to CIN85-CC-wt (Figure 4.20 B).

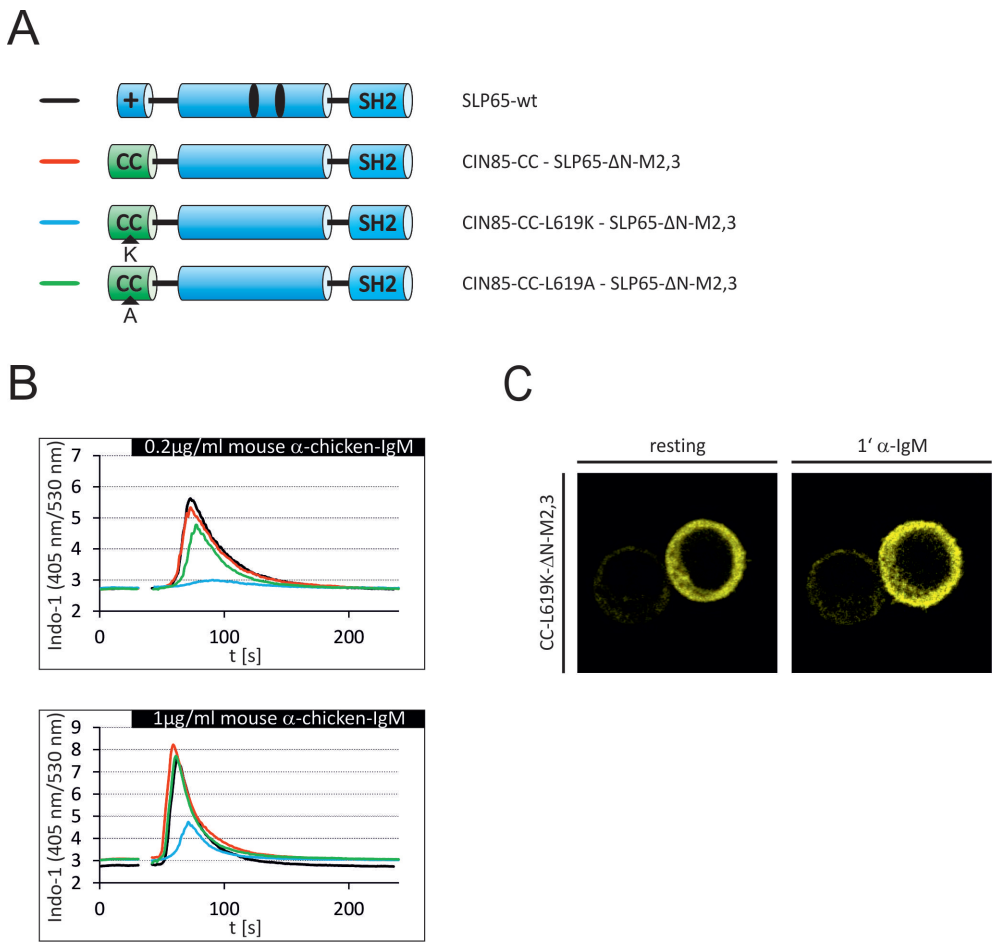

Fig. 4.20: Preventing CIN85-CC oligomerization abolishes its supporting function for SLP65. *Slp65*$^{-/-}$ DT40 cells were transduced with SLP65-wt or the Citrine-tagged chimeric proteins depicted in (A). The SLP65-ΔN-M2,3 variant was fused to CIN85-CC, either CC-wt (red line), CC L619K (blue line) or CC L619A (green line). The Ca^{2+} influx in transduced Citrine positive cells upon stimulation with 0.2 or 1 µg/ml α-IgM was monitored by flow cytometry (B). Intracellular localization and membrane recruitment of the chimeric CIN85-CC L619K SLP65-ΔN-M2,3 protein 1 min after BCR stimulation (2 µg/ml α-IgM) were observed by confocal microscopy (C).

I tested the PA binding ability of CIN85-CC L619K by a liposome flotation assay (Figure 4.21). The CIN85-CC-L619K-SLP65-ΔN protein (lanes 7-12) behaved in this assay like CIN85-CC-wt-SLP65-ΔN

protein (lanes 1-6), indicating that the L619K exchange does not abolish PA binding of the CIN85-CC. So the loss of oligomerization, but not of the PA binding ability, correlated with a loss of function.

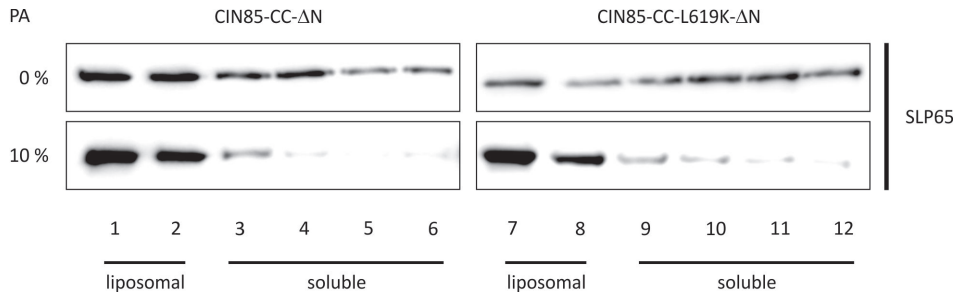

Fig. 4.21: CIN85-CC L619K associates with PA containing membranes. His_6-tagged recombinant CIN85-CC-wt-SLP65-ΔN and CIN85-CC-L619K-SLP65-ΔN proteins were produced. The binding of these proteins to liposomes containing different PA concentration was determined by a liposome flotation experiment. The recombinant proteins were mixed with liposomes, followed by separation of liposomes and soluble fraction by ultracentrifugation. Liposomal fractions (1 and 2 for CC-wt, 7 and 8 for CC L619K) and soluble fractions (3-6 for CC-wt, 9-12 for CC L619K) were collected and analyzed by immunoblotting for SLP65. The liposome flotation experiment was carried out by Sona Pirkuliyeva (see [136] for experimental details).

4.12 Other CC domains can replace the CIN85-CC to support SLP65.

If oligomerization was the main or exclusive mechanism of the CIN85-CC to support SLP65 function, it should be possible to substitute the SLP65 N-terminus and CIN85 binding by fusion to other oligomerization domains. First, I fused SLP65-ΔN to the CC of the CIN85 homolog CD2AP (CD2AP aa 568-639, Figure 4.22 A). The CIN85-CC and the CD2AP-CC display a high degree of similarity, harboring 38% identical and another 32% similar amino acid residues. I transduced the CD2AP-CC-SLP65-ΔN construct in *slp65*$^{-/-}$ DT40 cells, the Ca^{2+} influx upon α-IgM stimulation was monitored. The construct enabled a Ca^{2+} influx comparable to SLP65-wt (Figure 4.22 B). The deletion of the CIN85 binding sites in the CD2AP-CC-SLP65-ΔN construct, resulting in CD2AP-CC-SLP65-ΔN-M2,3, impaired the Ca^{2+} influx only slightly, indicating that CIN85 binding is dispensable for CD2AP-CC-SLP65-ΔN. The chimeric CD2AP-SLP65 protein was recruited to the plasma membrane upon BCR stimulation (Figure 4.22 C).

To investigate if there may be binding partners which could recruit the CD2AP-CC to the BCR, I studied the CD2AP interactome in the human B cell line Ramos by SILAC-based mass spectrometry. This experiment resulted in the list of interaction partners given in Table 4.4. The interactome of CD2AP was

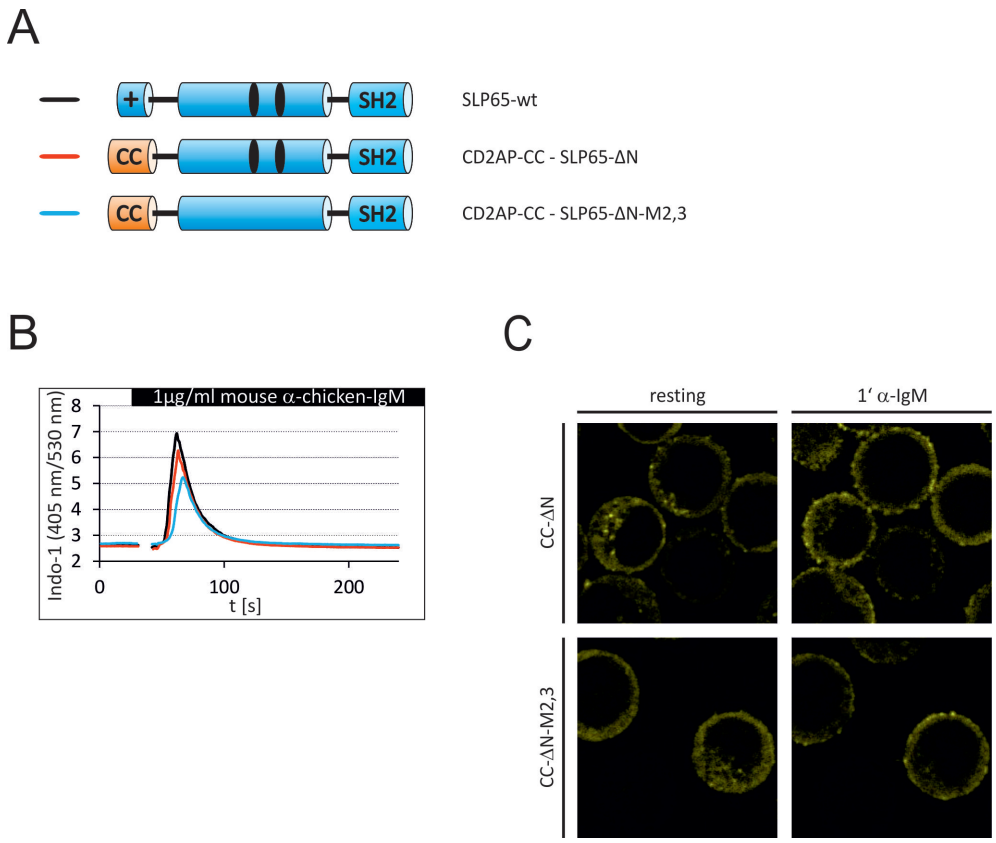

Fig. 4.22: The CD2AP-CC substitutes the SLP65 N-terminus. *Slp65*$^{-/-}$ DT40 cells were transduced with SLP65-wt or the Citrine-tagged chimeric proteins depicted in (A). The shown SLP65-ΔN variants were fused to the CD2AP-CC (red line and blue line). The Ca^{2+} influx in transduced Citrine positive cells upon stimulation with 1 µg/ml α-IgM was monitored by flow cytometry (B). Intracellular localization and membrane recruitment of the chimeric proteins 1 min after BCR stimulation (2 µg/ml α-IgM) were observed by confocal microscopy (C).

partially identical to the interactome of CIN85. Additionally, the heavy chain of the IgD-BCR, but not the one of the IgM-BCR, was found to interact with CD2AP. There were no obvious candidate molecules mediating membrane anchoring or IgM-BCR recruitment of the CD2AP-CC.

Tab. 4.4: The interactome of CD2AP in the human B cell line Ramos. A plasmid coding for strep-tagged CD2AP was introduced in Ramos cells by electroporation. Three clones were selected, mixed to avoid clonal effects, and labeled by growing them in SILAC medium containing the heavy isotope labeled amino acids lysine+4 and arginine+6. As control, wt Ramos cells were grown in medium with light amino acids. The differently labeled cells were stimulated for 5 min by α-IgM-F(ab')$_2$ and subjected to affinity purification by streptavidin-coated beads. The samples of strep-tagged CD2AP expressing and control cells were pooled in 1:1 ratio and subsequently analyzed by mass spectrometry. The experiment was repeated 3 times. Proteins appearing at least 2 times at a heavy-to-light ratio of 3 or higher were regarded as definitive interaction partners of CD2AP. The forth column of the table indicates if this interaction has been described before for CD2AP.

Protein	**Uniprot**	**Function**	**Reference**
SLP65	Q8WV28	Adaptor protein	[121]
CIN85	Q96B97	Adaptor protein	[48, 181, 73]
SH3BP1	Q9Y3L3	Adaptor protein	
STAP1	Q9ULZ2	Adaptor protein	[73]
ALKBH2	Q6NS38	DNA repair protein	
CapZ α-1	P52907	Cytoskeleton regulator	[71, 180, 8]
CapZ α-2	P47755	Cytoskeleton regulator	[180, 73]
CapZ β	P47756	Cytoskeleton regulator	[180, 8]
ARHGAP17	Q68EM7	GTPase-activating protein	[190]
ARAP1	Q96P48	GTPase-activating protein	[72]
MIRab13	Q8N3F8	Membrane trafficking regulator	
Ig δ chain C region	P01880	Immunoglobulin chain	
Rhotekin 2	Q8IZC4	unknown	[72]

As for CIN85-CC, I considered direct lipid binding of the CD2AP-CC. In contrast to the basic CIN85-CC (pI 9.06), the CD2AP-CC is rather acidic (pI 5.50, as calculated with ExPASy.org) which could influence the electrostatic interactions with membrane lipids to a large extent. I studied the PA binding of CD2AP-CC in vitro by affinity purification. In contrast to CIN85-CC-SLP65-ΔN, CD2AP-CC-SLP65-ΔN could not be precipitated with PA coated beads (Figure 4.23). This indicated that the PA binding ability of the CC domains might be mainly driven by electrostatic interactions. As CIN85-CC and CD2AP-CC can support SLP65 to a similar extent, the PA interaction seems to be dispensable for the function that

is exhibited by the CC domains towards SLP65.

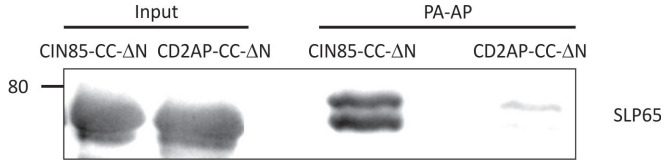

Fig. 4.23: CIN85-CC, but not CD2AP-CC, associates with PA. His6-tagged recombinant CIN85-CC-SLP65-ΔN and CD2AP-CC-SLP65-ΔN proteins were produced. The association of these proteins to PA coated beads was tested by affinity purification. The protein input (left side) and the affinity-purified protein amount (PA-AP, right side) were analyzed by immunoblotting for SLP65.

In the next step, I employed CC domains with different oligomerization states to see if the formation of differently sized SLP65 complexes influenced SLP65 function. The CC of the Small Coiled Coil protein (SCOC) normally forms a dimer, but it can be converted to a trimer or tetramer by the exchange of two amino acids [10]. I fused the SCOC-CC-wt (aa 78-159) to SLP65-ΔN (Figure 4.24 A), transduced the construct in *slp65*$^{-/-}$ DT40 cells, and monitored the Ca^{2+} influx upon α-IgM stimulation. The SCOC-CC enabled Ca^{2+} influx, although the level was slightly decreased compared to the CIN85-CC (Figure 4.24 B). The introduction of the M2,3 variant in the SCOC-CC-SLP65 construct enhanced this difference (Figure 4.24 B). Also compared to CD2AP-CC, the SCOC-CC enabled Ca^{2+} influx to a lesser extent (Figure 4.25). Nevertheless, the SCOC-CC-SLP65-ΔN construct was recruited to the plasma membrane upon BCR stimulation (Figure 4.24 C).

In the following experiment, I fused variants of the SCOC-CC with different oligomerization states to SLP65-ΔN-M2,3 (Figure 4.26 A), transduced the constructs in *slp65*$^{-/-}$ DT40 cells, and monitored the Ca^{2+} influx upon α-IgM stimulation. A higher oligomerization state of the SCOC-CC-SLP65-ΔN-M2,3 fusion proteins resulted in stronger Ca^{2+} influx (Figure 4.26 B and C). This effect was specially pronounced at stimulation with low α-IgM concentrations (Figure 4.26 B). These results indicate again that the oligomerization state of CC-SLP65-ΔN chimeric proteins has a crucial influence on their functionality.

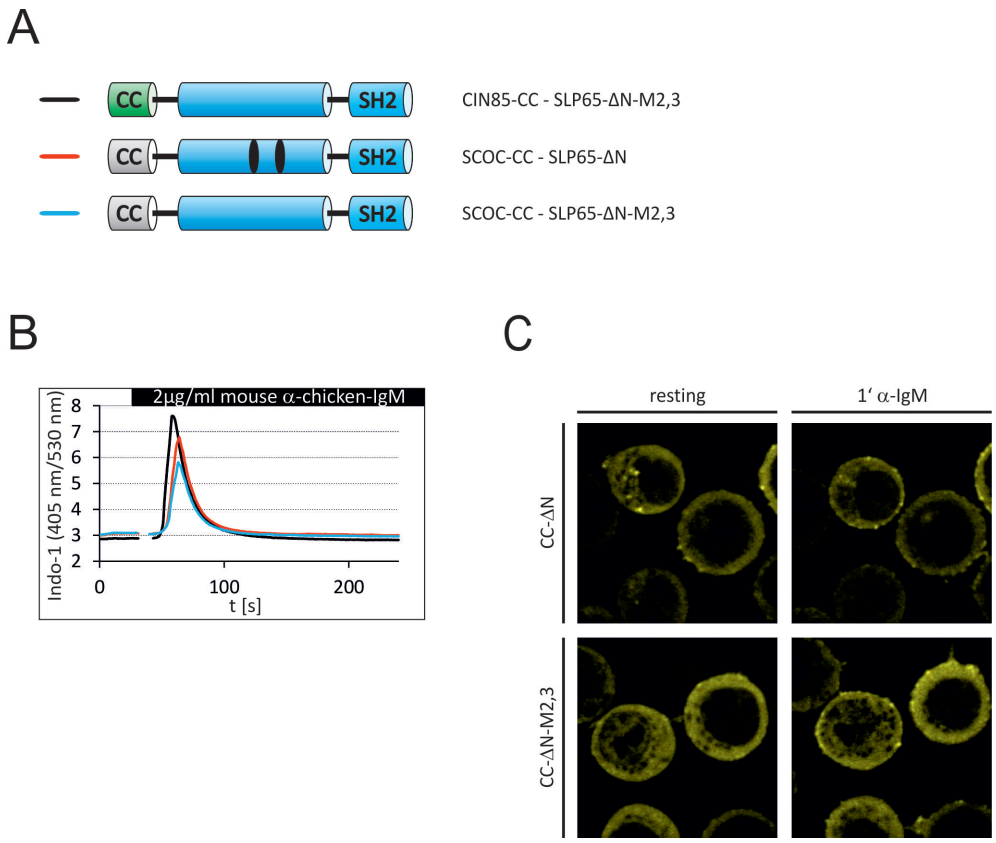

Fig. 4.24: The SCOC-CC substitutes the SLP65 N-terminus. *Slp65*$^{-/-}$ DT40 cells were transduced with the Citrine-tagged chimeric proteins depicted in (A). The shown SLP65-ΔN variants were fused to CIN85-CC (black line) or to SCOC-CC (red line and blue line). The Ca^{2+} influx in transduced Citrine positive cells upon stimulation with 2 µg/ml α-IgM was monitored by flow cytometry (B). Intracellular localization and membrane recruitment of the chimeric proteins 1 min after BCR stimulation (2 µg/ml α-IgM) were observed by confocal microscopy (C).

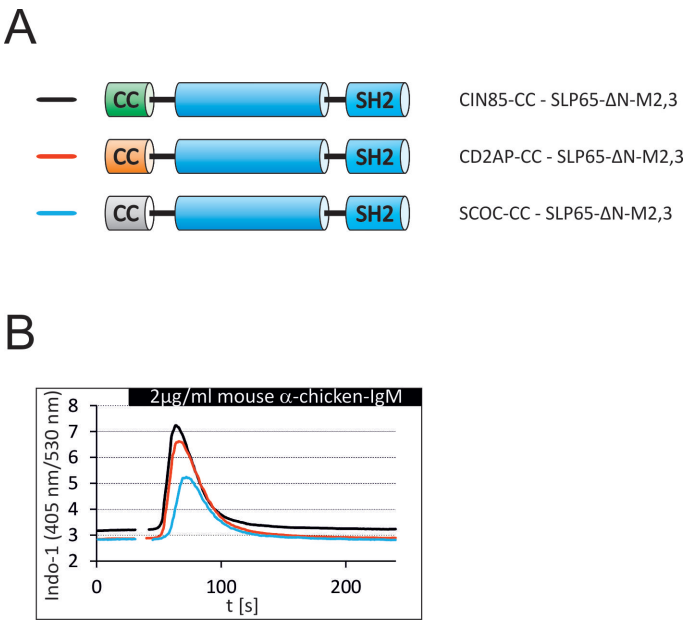

Fig. 4.25: CIN85, CD2AP and SCOC-CC support the SLP65 function to a different extent. *Slp65*$^{-/-}$ DT40 cells were transduced with the Citrine-tagged chimeric proteins depicted in (A). SLP65-ΔN-M2,3 was fused to CIN85-CC (black line), CD2AP-CC (red line) or SCOC-CC (blue line). The Ca^{2+} influx in transduced Citrine positive cells upon stimulation with 2 µg/ml α-IgM was monitored by flow cytometry (B).

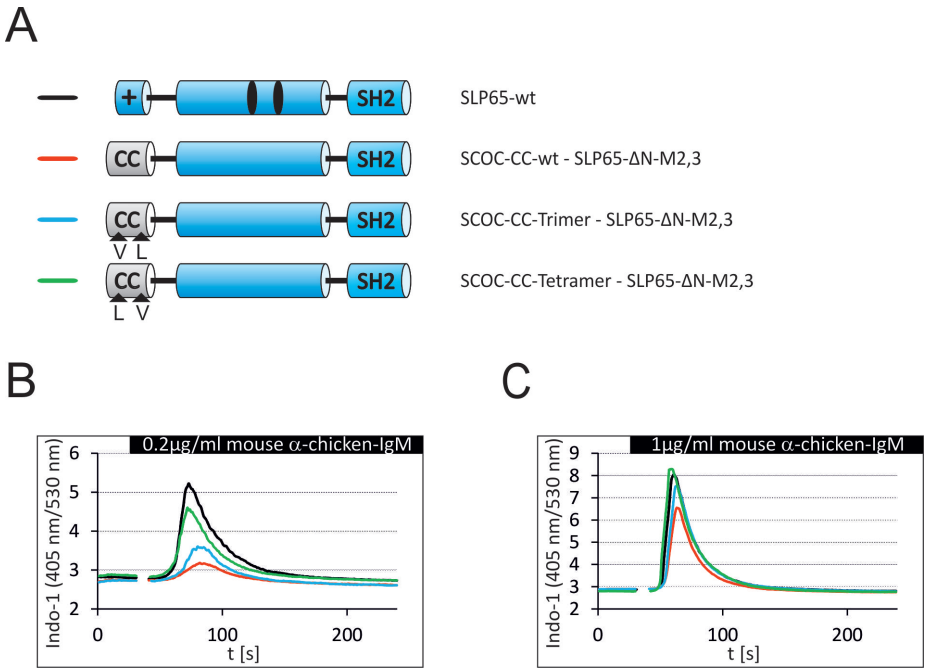

Fig. 4.26: Higher oligomerization states of SCOC-CC enhance its supporting function for SLP65. The oligomerization state of SCOC-CC was changed by the introduction of amino acid exchanges (according to [10]). *Slp65*$^{-/-}$ DT40 cells were transduced with SLP65-wt or the Citrine-tagged chimeric proteins depicted in (A). The SLP65-ΔN-M2,3 variant was fused to SCOC-CC, either CC-wt (dimeric, red line), CC E93V/K97L (trimeric, blue line), or CC N125L/N132V (tetrameric, green line). The Ca^{2+} influx in transduced Citrine positive cells upon stimulation with 0.2 or 1 µg/ml α-IgM was monitored by flow cytometry (B and C).

4.13 Oligomerization enables SLP76 to take part in the BCR signaling cascade.

To see if the concept of oligomerization of adaptor proteins could be generalized, I performed experiments with SLP76, the SLP65-homolog in T cells. *Slp65*$^{-/-}$ DT40 B cells reconstituted with SLP76-wt show virtually no Ca^{2+} influx or SLP76-membrane recruitment upon BCR stimulation, so SLP76-wt is not capable to substitute SLP65 in BCR signaling [196]. This might be due to the lack of oligomerization of SLP76, as the protein does not contain CIN85 binding sites. When CIN85 binding sites are introduced to SLP76, this modified SLP76 protein mediates Ca^{2+} influx in B cells [121], indicating that increased oligomerization could enable SLP76 to function in B cells. To test the oligomerization hypothesis, I equipped SLP76 which the CIN85-CC (Figure 4.27 A). The construct was transduced in *slp65*$^{-/-}$ DT40 cells, the Ca^{2+} influx upon BCR-stimulation was comparable to CIN85-CC-SLP65-ΔN-M2,3 (Figure 4.27 B). A fraction of the chimeric CIN85-SLP76 protein was plasma membrane associated in unstimulated cells. This plasma membrane localization seemed to be slightly enhanced upon BCR stimulation (Figure 4.27 C). To ensure that this gain of function is really induced by the oligomerization function of the CIN85-CC, I used also the monomeric CC variant L619K. When fused to SLP76, CIN85-CC L619K failed to enable Ca^{2+} influx (Figure 4.27 B). So oligomerization is a prerequisite for SLP76 to participate in BCR signaling.

4.14 Oligomerization of SLP65 is sufficient to enable BCR recruitment and Ca^{2+} signaling.

To test oligomerization devices other than CC domains, I fused SLP65-ΔN to the two parts of the split Venus protein. Split Venus is used for Bimolecular fluorescence complementation (BiFC) studies because its two halves VN and VC link covalently when they are spatially close to each other. This occurs for example when they are fused to two interacting proteins (Figure 4.28 A). I transduced the constructs VN-SLP65-ΔN and VC-SLP65-ΔN (Figure 4.28 B) either individually or simultaneously in *slp65*$^{-/-}$ DT40 cells. The successful fusion of the Venus parts VN and VC in simultaneously transduced cells was confirmed by their Venus fluorescence (Figure 4.28 C). This indicated the formation of a covalent SLP65 dimer.

I monitored the α-IgM-induced Ca^{2+} influx in the co-transduced cells. This revealed that a VN-SLP65-ΔN-VC-SLP65-ΔN dimer enabled Ca^{2+} influx and plasma membrane recruitment comparable to SLP65-wt (Figure 4.29). The functionality of the protein was not impaired by the introduction of the M2,3 variant in both of the SLP65 parts (Figure 4.30). On the other hand, the function of the SH2 domain in the SLP65 parts was still important because the inactivating amino acid exchange R372L in both SLP65

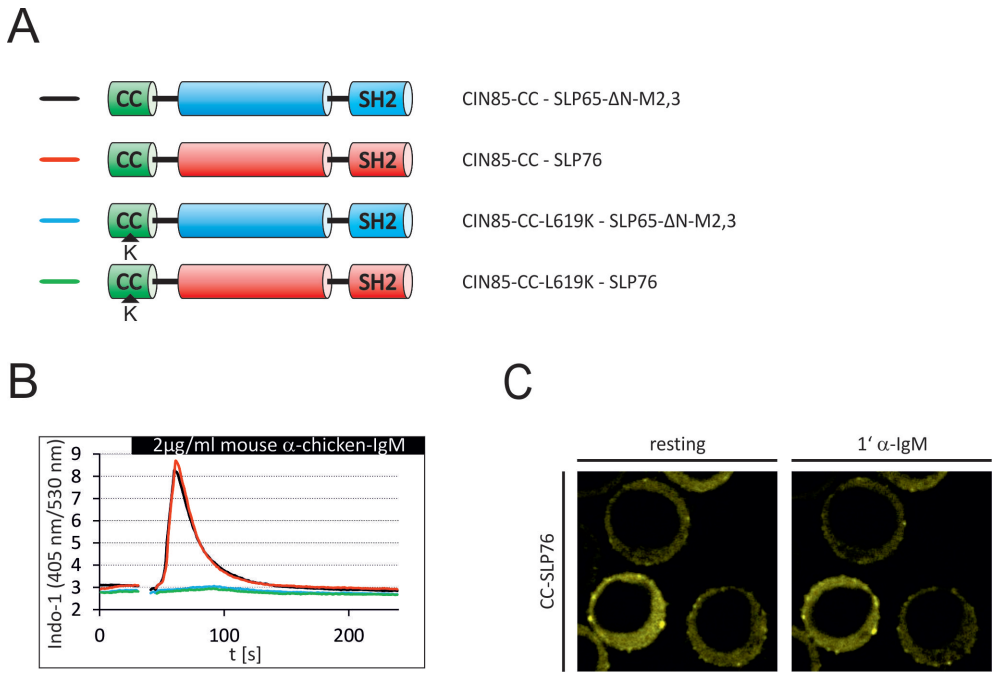

Fig. 4.27: The CIN85-CC enables SLP76 to mediate BCR-induced Ca^{2+} influx. *Slp65*$^{-/-}$ DT40 cells were transduced with the Citrine-tagged chimeric proteins depicted in (A). SLP65-ΔN-M2,3 was fused to CIN85-CC-wt (black line) or to CIN85-CC L619K (blue line). SLP76 was fused to CIN85-CC-wt (red line) or to CIN85-CC L619K (green line).The Ca^{2+} influx in transduced Citrine positive cells upon stimulation with 2 µg/ml α-IgM was monitored by flow cytometry (B). Intracellular localization and membrane recruitment of the chimeric protein CIN85-CC-wt-SLP76 1 min after BCR stimulation (2 µg/ml α-IgM) were observed by confocal microscopy (C).

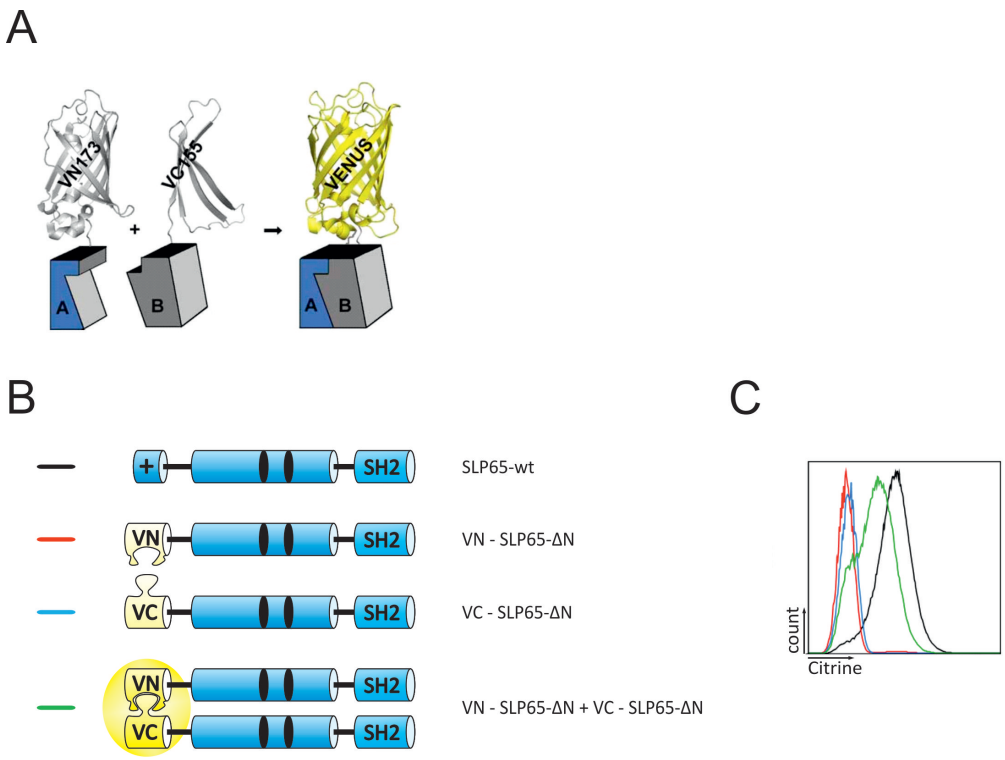

Fig. 4.28: A covalently linked SLP65-ΔN dimer is obtained by fusion of a split Venus protein. The yellow fluorescent protein (YFP) variant Venus can be reconstituted by its two parts VN (aa 1-173) and VC (aa 156-239). This fusion is enabled by spatial proximity of proteins linked to VN and VC (schematic in A, graphic from Shyu *et al.* [165]). *Slp65*$^{-/-}$ DT40 cells were transduced with Citrine-tagged SLP65-wt or SLP65-ΔN fused to a part of Venus chimeric proteins, as depicted in (B). SLP65-ΔN was fused to VN (red line) or VC (blue line). Moreover, *slp65*$^{-/-}$ DT40 cells were co-transduced with VN-SLP65-ΔN and VC-SLP65-ΔN (green line). The fluorescence of the transduced cells was monitored by flow cytometry in the FITC channel (C).

parts totally abolished the functionality of the SLP65-dimer (Figure 4.30). This result indicated that SLP65 oligomerization can fully substitute the functions of SLP65 N-terminus and CIN85 binding. It further suggested that the function of CIN85 in the BCR signaling pathway is the stabilization of large SLP65 oligmers, presumably in cooperation with the membrane binding ability of the SLP65 N-terminus.

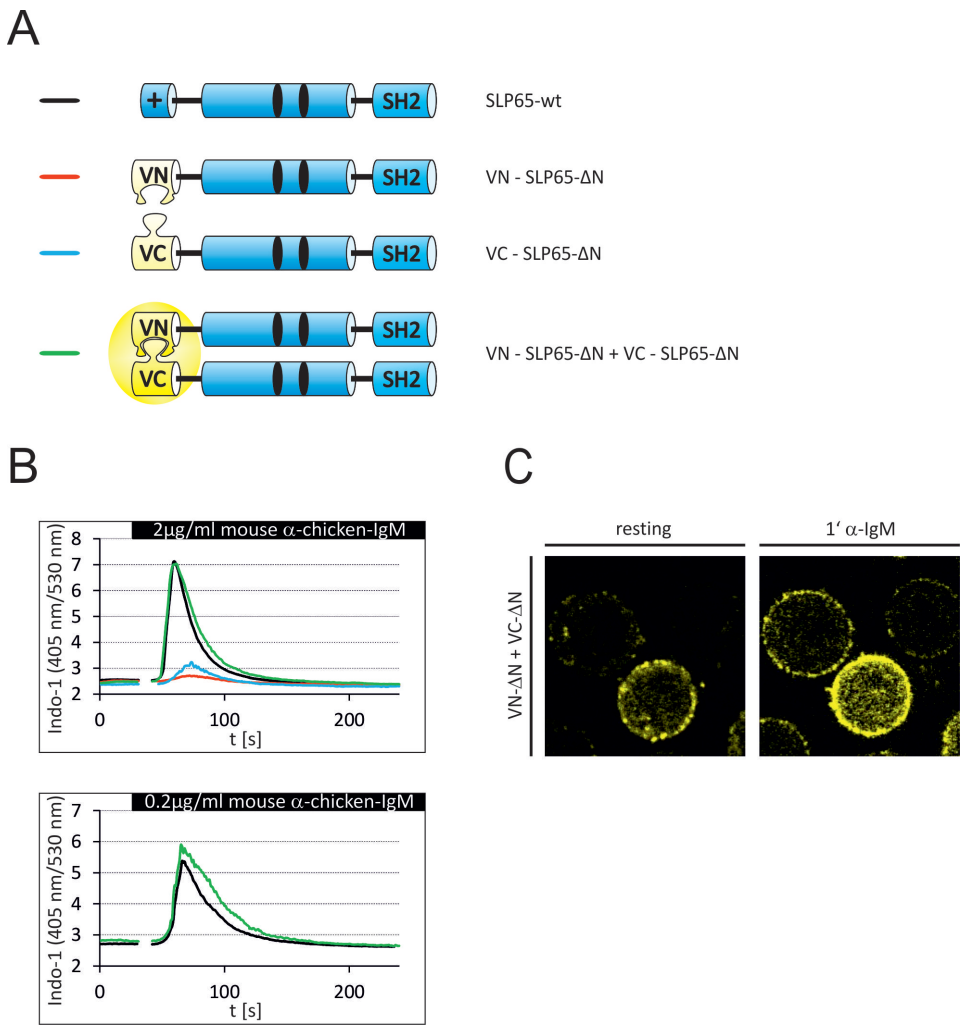

Fig. 4.29: Covalent linkage of two SLP65 molecules substitutes the SLP65 N-terminus. *Slp65*$^{-/-}$ DT40 cells were transduced with Citrine-tagged SLP65-wt or SLP65-ΔN fused to a part of Venus chimeric proteins, as depicted in (A). VN SLP65-ΔN and VC SLP65-ΔN were transduced individually (red and blue line) or simultaneously (green line). The Ca^{2+} influx in transduced cells upon stimulation with 0.2 or 2 µg/ml α-IgM was monitored by flow cytometry (B). For cells expressing VN-SLP65-ΔN and VC-SLP65-ΔN simultaneously, intracellular localization and membrane recruitment 1 min after BCR stimulation (2 µg/ml α-IgM) were observed by confocal microscopy (C).

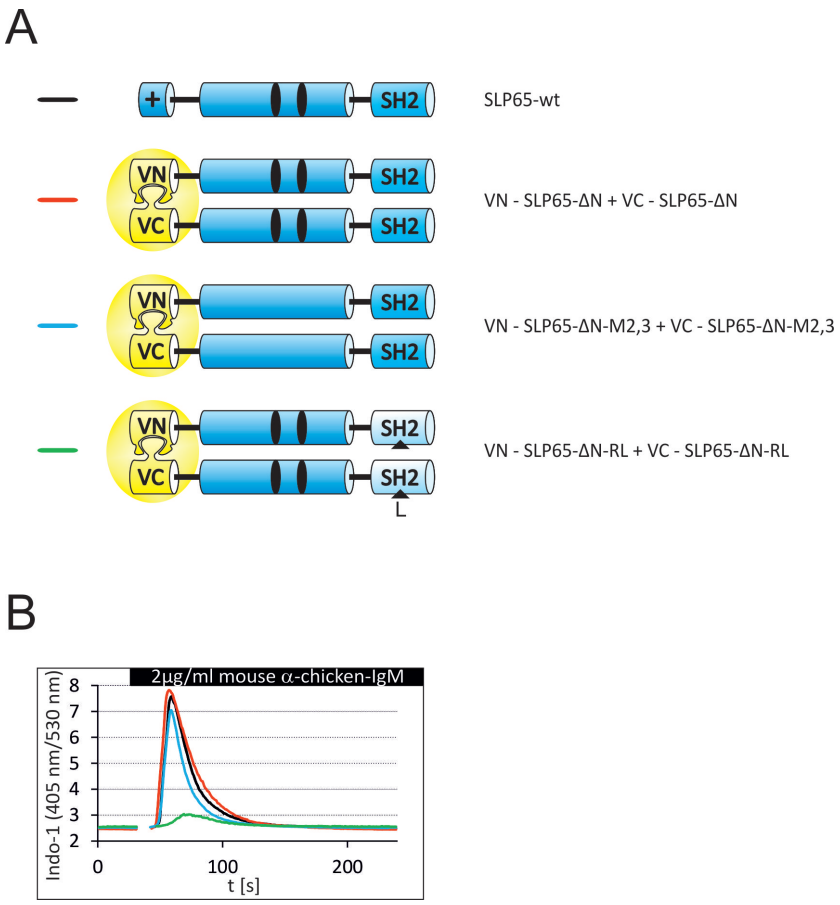

Fig. 4.30: CIN85 binding is dispensable for the covalently linked SLP65-ΔN dimer. *Slp65*$^{-/-}$ DT40 cells were transduced with Citrine-tagged SLP65-wt or with one VN-SLP65-ΔN and one VC-SLP65-ΔN construct simultaneously. Both SLP65-ΔN parts of the proteins harbored either the wt form (red line), the M2,3 variant (blue line) or the R372L variant (green line). The Ca^{2+} influx in transduced cells upon stimulation with 2 µg/ml α-IgM was monitored by flow cytometry (B).

5 Discussion

5.1 CIN85-mediated oligomerization of SLP65

In this doctoral thesis, I investigated the influence of the adaptor protein CIN85 on BCR signaling. I focussed on the interaction of CIN85 with the adaptor protein SLP65. This interaction is important for efficient SLP65-membrane recruitment and Ca^{2+} signaling in DT40 cells (Figure 4.1 and [121]). To elucidate the mechanism by which CIN85 supports SLP65 function, I constructed chimeric proteins of SLP65 and membrane-anchoring domains and investigated if CIN85 binding is required for the function of these chimeric proteins. The SLP65-CIN85 interaction could not be substituted by the PLC-δ PH domain, a general plasma membrane anchor (Figure 4.7). Other chimeric proteins of SLP65 and membrane-anchoring domains have been investigated on their need for CIN85 binding. SLP65-ΔN was fused to the plasma membrane-anchoring domain of TIRAP [18], to the Golgi apparatus-anchoring OSBP1 PH domain [121] and to the vesicle anchoring amphiphysin N-BAR domain [136]. In consistence with my results, it was found that all these domains can substitute for the SLP65 N-terminus, but all constructs were still dependent on CIN85 binding for Ca^{2+} signaling. Thus, CIN85 seems to exhibit its function on SLP65 regardless of the SLP65 localization which is determined by the extrinsic membrane-anchoring domains or, for SLP65-wt, by the SLP65 N-terminus [40]. Because the extrinsic membrane-anchoring domains confer specific and strong membrane anchoring, it is unlikely that CIN85 is important for the association of SLP65 with membranes. On the other hand, I could show that CIN85 binding is dispensable for chimeric SLP65 proteins containing the BCR-anchoring Syk tandem SH2 domains (Figure 4.7). This indicates that CIN85 is important for the recruitment process of membrane associated SLP65 to the BCR rather than for subsequent anchoring of SLP65 to the activated BCR.
A similar phenomenon has been found for the adaptor function that SLP65 itself provides for PLC-γ2. The PLC-γ2 recruitment to the BCR is dependent on its binding to SLP65. This need cannot be bypassed by targeting PLC-γ2 unspecifically to the plasma membrane by fusion with the PLC-δ PH domain [149]. However, targeting PLC-γ2 specifically to lipid rafts and thus in proximity of the BCR via a 9-amino acid membrane anchor of Lyn is sufficient to enable PLC-γ2 function without SLP65 binding. [149]. It is likely that the attachment of the membrane anchor of Lyn to SLP65 would make CIN85 binding dispensable.

By the creation of CIN85-SLP65 chimeric proteins, I could attribute the supporting function of CIN85 to its CC domain (Figure 4.8, Figure 4.9 and Figure 4.10) because chimeric proteins of SLP65-ΔN and the CIN85-CC were not dependent on additional CIN85 binding (Figure 4.10). The CIN85-CC could be located N- or C-terminally of SLP65 with the same outcome (Figure 4.11). It could even be reconstituted from its two halves placed on the two ends of the chimeric protein (Figure 4.13). These observations indicate that the CIN85-CC is an independent functional domain that supports SLP65 function regardless

of its position and thereby probably without interactions with other parts of the fusion protein.
However, a protein ligand of the CIN85-CC that is known to influence BCR signaling could not be identified by mass spectrometry (Table 4.1 Table 4.2 and Table 4.3). The CIN85 interactome of human Ramos B cells and chicken DT40 B cells overlapped to a large extent with the interactome that Büchse and colleagues prepared from the mouse B cell line WEHI 231. [20]. Also their interactome gives no hint of an interaction partner that could direct the CIN85-CC in proximity of the BCR. The direct interaction of the CIN85-CC with PA, reported by Zhang and colleagues [200], could be confirmed by our experiments (Figure 4.15) but seemed dispensable for the functional support of SLP65 (Figure 4.16, Figure 4.21, and Figure 4.23).
The need of SLP65 oligomerization for its function could be demonstrated by the creation of chimeric proteins with different oligomerization domains. The CN85-CC and the CD2AP-CC could substitute for the SLP65 N-terminus and for CIN85 binding. However, this left the possibility that these two closely related domains might bind to a ligand responsible for BCR recruitment, even though no such ligand could be identified in my studies. The N-terminus of SLP65 could also be substituted by the SCOC-CC which is not related to the CIN85-CC and the CD2AP-CC. By modifying the oligomerization state of the SCOC-CC due to introduction of amino acid exchanges, I could observe that SLP65 functions the better the higher it is oligomerized (Figure 4.26). As the SCOC-CC shows no relation to the CIN85-CC, it can be presumed that their only common function is oligomerization.
The gradual differences in the ability of the CC domains to support SLP65 function (Figure 4.25) can be explained by their different oligomerization states and their affinity for oligomerization. In cooperation with C. Griesinger's group, I could show that the CIN85-CC forms a very stable trimer. This trimer formation seemed to be slightly impaired by the exchange of leucine 619 for alanine, resulting in a slight decrease in Ca^{2+} influx (Figure 4.20). The exchange of leucine 619 for lysine abolished the trimer formation completely (Figure 4.19) and led to almost complete inhibition of Ca^{2+} signaling mediated by chimeric CIN85-SLP65 proteins (Figure 4.20). The CD2AP-CC forms presumably an oligomer very similar to the CIN85-CC, due to their large degree of homology, resulting in a similar ability to support SLP65 function (Figure 4.25). Also hetero-trimerization of CD2AP-CC and CIN85-CC is possible. In contrast, the SCOC-CC-wt forms a dimer that might be less stable than the CIN85-CC and CD2AP-CC oligomers. To support SLP65 function as efficiently as these two CC domains, it is necessary to introduce amino acid exchanges in the SCOC-CC that result in a higher oligomerization state (trimer or tetramer).
The covalent dimerization of SLP65 by chimeric proteins with split Venus could substitute for the SLP65-N terminus and for CIN85 binding (Figure 4.30). Two Venus molecules have been shown to associate with low affinity [144, 116], so that also a SLP65 tetramer could be formed. This can explain why the fusion to split Venus can support the SLP65 function to the same extent as fusion to the CC domains. Taken together, the results suggest that SLP65 membrane recruitment crucially requires oligomerization. Furthermore, they indicate that the SLP65 N-terminus and CIN85 might cooperate in the oligomerization

of SLP65 because oligomerized chimeric SLP65 proteins were not dependent on both of them.

5.2 The formation of the SLP65-CIN85 complex

In the physiological situation, the oligomerization of SLP65 will occur by its interaction with CIN85. The CIN85-CC forms a trimer, resulting in a CIN85 protein complex with nine SH3 domains which means nine potential binding sites for SLP65 molecules. The CIN85 trimer could be very potent in forming large protein complexes as it binds to several SLP65 molecules at the same time. However, native PAGE experiments reveals exclusively the existence of a SLP65-containing 180 kDa complex [173]. This might be a hint that the large complexes are very labile or require the presence of intact membranes. Their existence might also mainly depend on the local concentration of the two interacting proteins. The equilibrium of complex formation will always be shifted towards the loss of oligomerization by conventional purification methods. The physiological size of the SLP65-CIN85 complexes remains to be elucidated. Nevertheless, the physiological relevance of the SLP65-CIN85 interaction *in vivo* is proven by co-localization experiments in living cells and the fact that the CIN85 binding deficient SLP65 variant M2,3 shows reduced plasma membrane recruitment and Ca^{2+} signaling upon BCR stimulation [121].
The CIN85-mediated SLP65 oligomerization seems to require pre-concentration of SLP65 to be efficient. The exclusively cytosolic SLP65 variant ΔN, which is still capable of CIN85 binding *in vitro*, is not functional in regard to membrane recruitment and Ca^{2+} mobilization [40] and Figure 4.6). This indicates that SLP65 oligomerization by CIN85 SH3 domain binding is not sufficient to enable the formation of large SLP65-ΔN complexes as it can be achieved by direct fusion of SLP65-ΔN to the mentioned oligomerization domains. The pre-concentration of SLP65 might have a major influence on the equilibrium of the SLP65-CIN85 interaction. Interactions between SH3 domains and proline motifs have typically a modest affinity in the low micromolar range [100, 82]. So a functional interaction might require high avidity by high local concentrations of both binding partners. Low-affinity interactions that are largely influenced by concentrations might provide a possibility to modify the composition of protein complexes very rapidly, a feature especially important in signal transduction. Kowanetz and colleagues proposed a rapid exchange of CIN85 interaction partners dependent on varying local concentrations at different time points of EGFR internalization [91].

A high local concentration of SLP65, provided by N-terminus-mediated membrane association of SLP65 molecules, might be necessary to outcompete the various other binding partners of the CIN85 SH3 domains. This promiscuity of CIN85 interactions is outlined by the CIN85 interactome (Table 4.1). The competition of different proteins for CIN85 SH3 domain binding and its functional consequences have already been described for c-Cbl. Ubiquitination and internalization of the EGFR are dependent on CIN85-mediated c-Cbl-clustering [92]. The proteins Alix, Sprouty, Dab2 and SHKBP1 can compete with

c-Cbl for CIN85 SH3 domain binding. Their expression reduces the effective clustering of c-Cbl by CIN85, thereby inhibiting the internalization of the EGFR [159, 58, 93, 43].
The oligomerization state of CIN85 itself plays also a role for its interactions. A CIN85 variant lacking the CC domains, which abolishes CIN85 trimerization, is not recruited to the plasma membrane after BCR stimulation [18]. This indicates that its affinity to SLP65, c-Cbl and other BCR-recruited protein is too low to allow an stable interaction. Zhang and colleagues showed this effect for the CIN85-c-Cbl interaction by co-immunoprecipitation. The CIN85-c-Cbl interaction was strongly reduced for a CIN85 variant lacking the CC in comparison to CIN85-wt [200].

Besides the concentration of the interaction partners, a further layer of control might be added by their post-translational modifications. It has been reported that the affinity of CIN85 to its ligands can be modulated by their modification. Different influences of phosphorylation have been described. The interaction of CIN85 with c-Cbl has been reported to increase after BCR stimulation, correlating with enhanced c-Cbl phosphorylation. [20]. The tyrosine phosphorylation of the ESCRT-I complex subunit MVB12A facilitates its interaction with CIN85 [89]. In contrast, threonine phosphorylation of endophilin A1, serine phosphorylation of Dab1 and tyrosine phosphorylation of Alix reduce their affinity to CIN85 [80, 153, 158]. Because SLP65 is heavily phosphorylated at tyrosine, serine and threonine residues during its activation upon BCR stimulation [122], this might affect its affinity to CIN85. Once SLP65 has reached its destination, the BCR, and is phosphorylated by Syk, further SLP65 clustering by CIN85 might be dispensable. The dissolution of the SLP65-CIN85 complex at the BCR could be useful because it might increase the steric accessibility of phosphorylated SLP65 for the new interaction partners. On the other hand, it is possible that the SLP65-CIN85 clusters remain constant to stabilize the emerging microsignalosomes. It has been shown that CIN85 can interact with unphosphorylated and phosphorylated SLP65 [189, 121]. However, an exact determination of the affinities to both forms is still missing.
Also CIN85 itself can be modified to modulate its interactions. It has been shown that tyrosine phosphorylation of CIN85 can occur by Src [160]. This phosphorylation affects the tyrosine residues Y10, Y109, Y271 and Y278 which are located in the SH3 domains and might thus influence the SH3 domain-mediated interaction of CIN85. Possible modifications of CIN85 after BCR stimulation have not been studied yet.

5.3 Inhibiton of complex formation by intramolecular CIN85 interactions

Another layer of regulation of CIN85 complex formation might be the autoinhibitory capability of CIN85. The first and second SH3 domain of CIN85 have been shown to bind intramolecularly to a PPKKPR motif in the PRR of CIN85 [17, 92, 179]. This means that the CIN85 SH3 domains would be no longer available to mediate interactions with other proteins resulting in loss of CIN85 clustering function. The autoinhibition might be even enhanced by CIN85 oligomerization, as proposed by Havrylov and col-

leagues who speculated that in a CIN85 oligomer, the SH3 domains of one CIN85 molecule would bind to the PPKKPR motif of another [64]. Deletion of the CIN85 region containing this motif leads to more efficient binding of CIN85 to c-Cbl [179]. Besides the competition with other interaction partners, the intramolecular interaction of CIN85 might provide a hurdle to cluster CIN85 interaction partners that are not locally pre-concentrated, like SLP65-ΔN. For effective complex formation, the autoinhibiton of CIN85 has to be overcome by offering a high concentration of binding sites for CIN85.

Interestingly, it seems also possible to overcome the intramolecular binding of CIN85 by expression of CIN85 at very high levels. In cells heavily overexpressing fluorescently tagged CIN85, there are large aggregate-like dots of the tagged CIN85 protein ([189, 199] and own unpublished observation). At high intracellular CIN85 concentrations, the intermolecular CIN85 binding might be favored. The binding of the SH3 domains of one CIN85 molecule to the PRR of another would result in the formation of very large CIN85 clusters. These aggregates are not translocated to the plasma membrane upon either BCR or latrunculin stimulation (own unpublished observations) or influenced by EGF stimulation [199]. This suggests that they are non-functional and do not take part in signaling processes.

The influence of the autoinhibitory function of CIN85 might be assessed by comparison with its paralog CD2AP. CD2AP does not possess this intramolecular SH3 domain binding site due to an R to T exchange in the PPKKPR motif. Consistently, overexpression of CD2AP does not induce the formation of large aggregates that are observed for CIN85 [18]. In contrast to CIN85, CD2AP is partially pre-recruited to the plasma membrane in resting B cells [18]. These differences could be explained by the lack of autoinhibiton of CD2AP. This would allow the binding of other molecules to the CD2AP SH3 domains, even if the interaction partners are not pre-concentrated. Compared to CIN85, the lower specificity of CD2AP interactions might impair the capability of CD2AP to induce the formation of large complexes. This could explain the minute influence of CD2AP on BCR signaling despite its individual SH3 domains have an affinity to SLP65 that seems to be in the same range as the affinity of the CIN85 SH3 domains [121]. Another explanation for the differences between CIN85 and CD2AP localization could be the actin binding sites of CD2AP which are not present in CIN85 [83, 179, 48]. The binding to actin might sequester CD2AP from the sites of SLP65 pre-concentration. It would be interesting to see if a mutant of CIN85 without the intramolecular binding site would be still able to mediate efficiently the formation of SLP65 complexes.

5.4 The influence of SLP65 and CIN85-CC lipid binding

While the membrane association of SLP65 due to its N-terminus is crucial for the SLP65-CIN85 complex formation (see 5.2), the PA-association of the CIN85-CC seems to be dispensable. Zhang and colleagues showed that deletion of the CIN85-CC results in loss of PA binding and membrane association of CIN85 [200] and demonstrated in a follow-up work that deletion of the CC results also in loss of endosomal

localization of CIN85 [201]. Furthermore, they showed that the CIN85-CC-PA interaction depends on four basic amino acids in the CC [201]. The exchange of these amino acids for alanine abolished PA binding, but also oligomerization of CIN85 [201] which made it impossible to distinguish between these two mechanisms in their studies. In B cells, it would be possible that the CIN85-CC directs SLP65 to specific membranes within the Golgi apparatus due to its PA association. PA has been shown to be present in the Golgi apparatus complex where it is produced by phospholipase D2 [147]. However, there are arguments against the importance of CIN85-PA binding for SLP65 function. The PA binding is conserved in the monomeric CIN85-CC variant L619K which does not support SLP65-mediated Ca^{2+} influx (Figure 4.21). The CC of CD2AP, which does not bind to PA (Figure 4.23), supports SLP65-mediated Ca^{2+} influx as well as the CIN85-CC (Figure 4.22). SLP65 function can also be supported by the SCOC-CC and by the Venus protein both of which are not related to the CIN85-CC (Figure 4.23 and Figure 4.29). It is not known that the SCOC-CC exhibits the same PA binding function as CIN85 and it is hard to imagine that the YFP variant Venus binds to PA. Furthermore, the specific PA binding motif of Raf is not sufficient to substitute the CIN85-CC in chimeric proteins (Figure 4.16). All these results point in the direction that PA binding of the CIN85-CC is not required for its function on SLP65.

5.5 The chronological order of SLP65-CIN85 complex formation

Based on our results and the previous considerations, I developed the model of SLP65-CIN85 complex formation shown in Figure 5.1. In a first step, SLP65 molecules can associate to membranes due to the SLP65 N-terminus, as shown by our group [40]. Subsequently, the high local concentration of SLP65 will overcome the autoinhibition of CIN85 which allows binding of CIN85 to multiple SLP65 molecules (b). The bridging of several SLP65 molecules can additionally stabilize their membrane association. The lipid binding affinity of the SLP65 N-terminus might be relatively low. Oligomerization of SLP65 by CIN85 can enhance the membrane binding by the creation of larger SLP65 complexes with multiple membrane binding sites and thus high avidity. This could explain why not only the deletion of the SLP65 N-terminus but also the disruption of the SLP65-CIN85 interaction reduces SLP65 membrane association (Figure 4.3). Due to its multiple CIN85 binding motifs, each SLP65 molecule can recruit multiple CIN85 molecules to the emerging complex; free CIN85 SH3 domains can recruit additional SLP65 molecules (c). This results in the formation of large membrane-associated SLP65-CIN85 complexes (d). One assembly site of these complexes are ATP-containing, VAMP7-positive vesicles. The idea of a membrane associated pool of SLP65 which takes part in signaling was already proposed by Koretzky *et al.* in 2006, interpreting results by Koehler *et al.* [90]. My results support this theory, explaining additionally the important role of CIN85 in the assembly of membrane-associated SLP65 complexes.

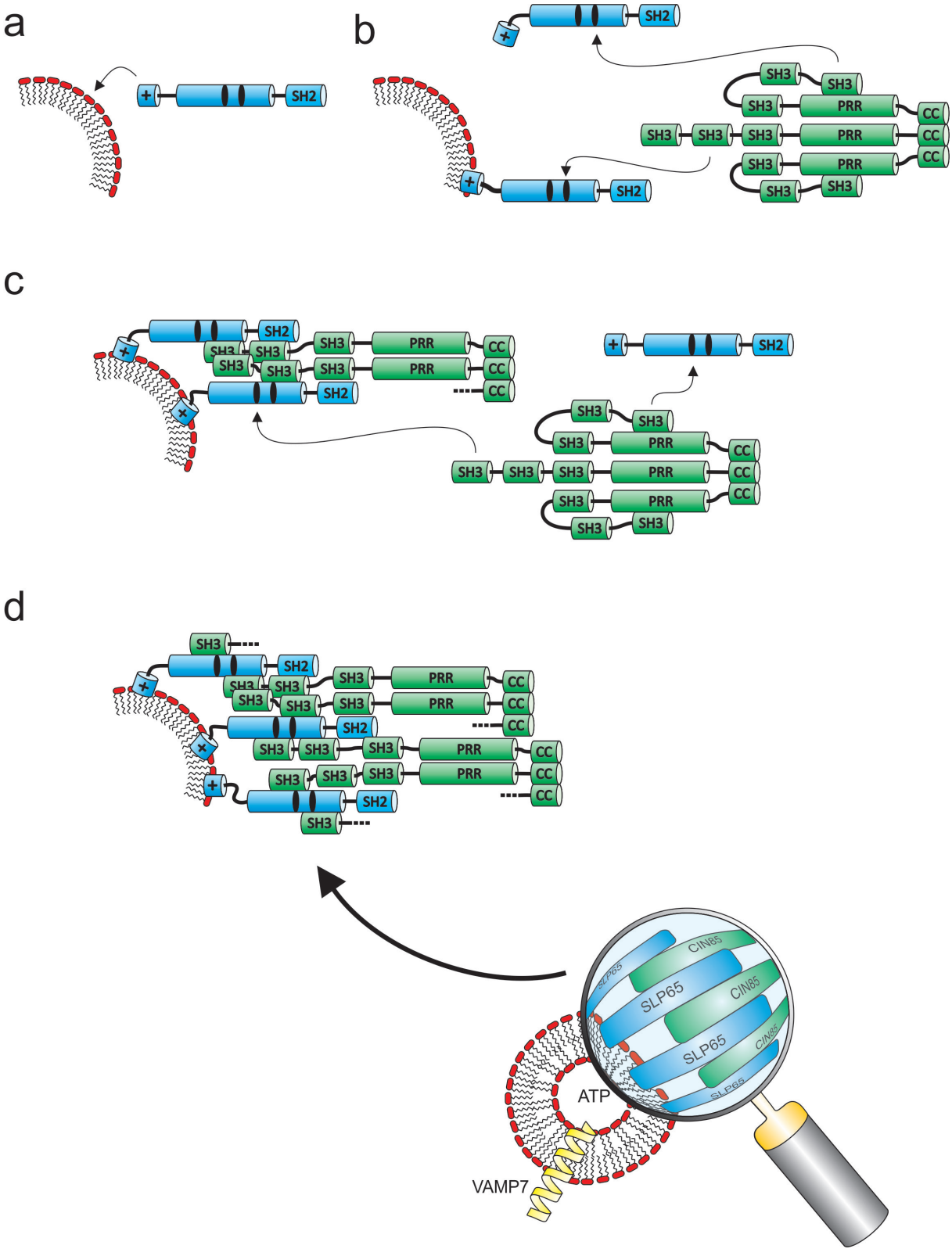

Fig. 5.1: Complex formation of SLP65 and CIN85 at vesicular membranes. The SLP65 N-terminus associates to lipids, recruiting SLP65 to intracellular membranes (a). The high local concentration of CIN85 binding sites (black ovals) allows binding of a CIN85 trimer to membrane associated SLP65 (b). For this process, it is necessary to overcome the autoinhibitory intramolecular CIN85 SH3 PRR interaction. Due to their multiple binding sites, CIN85 and SLP65 recruit additional CIN85 and SLP65 molecules to the growing complex (c). Large SLP65-CIN85 complexes are localized on VAMP$^+$ ATP-containing vesicles (d).

5.6 The regulation of oligomerization as a general feature in signaling pathways

The concept of adaptor protein-induced oligomerization might not be restricted to the SLP65-CIN85 interaction. I could show that the T-cell homolog of SLP65, SLP76, has to be oligomerized to function in BCR signaling. The mechanism of action of SLP76 seems to differ from the one of SLP65, it assembles the Ca^{2+} initiation complex not by SH2 domain-pY but by SH3 domain-PRR-mediated recruitment of PLC-γ (reviewed in [90]). Nevertheless, for its function in B cells it needed oligomerization, which could be artificially provided by interaction with CIN85 (introduction of CIN85 binding sites [121] or direct fusion to CIN85-CC (Figure 4.27)).

Because SLP76-wt harbors no CIN85 interaction sites, it would be interesting to see if it can undergo oligomerization by other means in physiological situations. Oligomerization, probably mainly dimerization, of SLP76 upon TCR stimulation has been described. The oligomerization is mediated by the N-terminal SLP76 SAM domain [102]. However, SAM domain-mediated dimerization could be not observed in B cells for chimeric SLP76-SAM-SLP65-ΔN proteins (S. Pirkuliyeva, unpublished data). The reason could be that SAM oligomerization depends on a TCR-triggered process like a post-translational modification of SLP76 that cannot be triggered by the BCR. It is also possible that the SAM-mediated oligomerization depends on interactions with additional proteins that are not expressed in B cells.

Coussens and collegues stated that adaptor protein-mediated oligomerization of SLP76 is needed for its physiological function in TCR signaling [30]. This oligomerization is mediated by the adhesion and degranulation-promoting adaptor protein (ADAP), also known as FYN-binding protein (FYB). The SLP76-ADAP interaction is required for efficient recruitment of SLP76 to microsignalosome, PLC-γ1 activation and Ca^{2+} mobilization [30]. ADAP contains three binding sites for the SLP76 SH2 domain and can potentially trimerize SLP76 [50, 14, 99]. It was shown that at least two binding sites are needed to support SLP76 function, indicating the requirement of simultaneous binding of two or three SLP76 molecules [30]. ADAP is expressed in T cells, but not in B cells [31], providing one possible explanation why SLP76 cannot substitute for SLP65.

Interestingly, ADAP contains one SH3 domain and one CC [31]. The CC might enable further ADAP oligomerization, though this has not been studied yet. ADAP has been shown to be crucial for the NfκB activation in TCR signaling [109, 167], like CIN85 in BCR signaling [88]. Furthermore, ADAP has also been shown to interact with c-Cbl [124]. Even though the proteins ADAP and CIN85 are not related, these fascinating parallels indicate that the two molecules have adapted similar roles in TCR respectively BCR signaling. In this homology model, a pre-concentration of SLP76 by the oligomerization of its SAM domain might substitute for the pre-concentration mediated by the SLP65 N-terminus. As already mentioned, SLP76 expressed in SLP65-deficient B cells needs additional adaptor protein

mediated-oligomerization to function in BCR signaling, either by the introduction of CIN85 binding sites [121] or by coexpression of LAT [196]. SLP65 expressed in SLP76-deficient T cells does not need the coexpression of additional adaptor proteins, probably because CIN85 is expressed in T cells. It requires only the expression of the kinase Syk [2], maybe because it cannot be efficiently phosphorylated by ZAP70, the T cell homolog of Syk. Table 5.1 gives an overview of similar and different properties of the two adaptors CIN85 and ADAP in BCR respectively TCR signaling.

Tab. 5.1: Comparison between CIN85 and ADAP in BCR respectively TCR signaling

Function	**CIN85**	**ADAP**
Interaction with SLP adaptor	SLP65	SLP76
Interaction mechanism with SLP adaptor	SH3-proline motif	SH2-phospho-tyrosine
Number of interaction sites present in CIN85/ADAP	3 (SH3 domains)	3 (phospho-tyrosines)
Number of interaction sites present in SLP65/SLP76	2 or 3 [1]	1 (SH2 domain)
c-Cbl binding	yes	yes
Involvement in NfκB signaling	yes, by unknown mechanism	yes, by recruitment of TAK1 to the CBM complex
Oligomerization by CC domain	yes	possible
Expression in B cells	yes	no
Expression in T cells	yes	yes

The importance of adaptor protein oligomerization has been described for other signaling pathways, in particular the NfκB pathway (reviewed in [66]). Oligomerization of the Inhibitor of κB kinase (IKK) is crucial for its activation which is thought to occur by *trans* auto-phosphorylation. The platform of IKK oligomerization is provided by oligomerized adaptor proteins [66]. The IKK binding protein NEMO can form trimers [3] or tetramers [178, 35] due to its CC domain. Constitutive oligomerization of NEMO or IKK components by fusion to FK506 binding protein domains is sufficient to activate IKK [74, 137]. The oligomerization of NEMO is controlled by different mechanisms, by the NEMO-intrinsic N-terminal dimerization domain, by the C-terminal CC domain and by its interaction with the kinase RIP1 [74, 106, 35]. This resembles the dually regulated oligomerization of SLP65 by its N-terminus and CIN85 binding that was found in this work.

[1] The binding of CIN85 to the first of the three PXXXPR motifs in SLP65 is weak *in vitro*. The disruption of this binding by amino acid exchange shows no physiological phenotype. Therefore, only the second and the third PXXXPR motif seem to be relevant.

The activation of NfκB upon BCR and TCR signaling depends on the formation of the CARD11-BCL10-MALT1 (CBM) complex that is required for the activation of IKK (reviewed in [186]). The formation of the functional CBM complex requires multiple oligomerization steps. CARD11 induces BCL10 oligomerization [138]. The oligomerization and subcellular localization of CARD11 itself are controlled by its CC domain [177]. Disruption of the CC-mediated oligomerization results in impaired CARD11 function. On the other hand, it was shown that homo-oligomerization of the CARD domains of CARD11 can impair their interaction with BCL10, thereby preventing the formation of a functional CBM complex [128]. This indicates again that the oligomerization state of adaptor proteins is crucial to control their function in signaling pathways. There can be multiple layers of oligomerization that control the formation of one complex, like CARD11 and BCL10 oligomerization for the CBM complex or CIN85 and SLP65 for the Ca^{2+} initiation complex.

Regulation of the oligomerization state has also been described for bacterial protein ClpC which is involved in proteolysis. Its function depends on its oligomerization by the adaptor protein MecA [84]. This shows that adaptor protein-mediated control of the oligomerization state is an evolutionary very ancient principle.

5.7 The transport of SLP65 and CIN85 to the plasma membrane

My data strongly suggests that SLP65 oligomerization mediated by CIN85 is required for SLP65 function. From the point of utility, SLP65 multimerization makes a lot of sense. Because SLP65 does not contain an enzymatic function, the activation of multiple SLP65 molecules at the same time is its only way for SLP65 to provide signal amplification. The pre-assembly of large SLP65-CIN85 complexes in resting cells enables the cell to react faster and more efficiently to BCR stimulation. However, it remains to be elucidated how multimerization of SLP65 facilitates recruitment of the SLP65 complexes to the plasma membrane and the BCR.

It is possible that the site of the complex assembly, a specific type of ATP-containing vesicles, positive for VAMP7 [40], is important for the following transport process to the plasma membrane and the BCR. The translocation of the SLP65-CIN85 complexes could occur by vesicular transport, triggered by BCR stimulation. This raises the question how the specificity of the SLP65-CIN85 complexes for these vesicles is obtained. Assuming that the function of CIN85 is only the multimerization of SLP65, the targeting function should be inherent to SLP65. It cannot be located in the N-terminus because highly oligomerized SLP65 variants are not dependent on the N-terminus for the formation of complexes, observed as dot-like structures by confocal microscopy (Figure 4.10, Figure 4.22 and Figure 4.29). Furthermore, the presence of SLP65 in dot-like structures did not require a functional SH2 domain (Figure 4.14). This leads to the conclusion that the vesicle-targeting feature of SLP65 resides in its central proline rich part (aa 46-345). This is consistent with the observation that the exchange of the central part for an unstructured glycine-serine linker resulted in the loss of dot-like location of the protein [136]. The central part of SLP65 has

been shown to be intrinsically disordered by NMR spectroscopy (unpublished data by L. Wong, L. Russo and [136]). So it does not contain a structured domain that could recruit SLP65 to vesicles, e.g. by lipid binding. The interactome of SLP65 has been studied by mass spectrometry [121]. SLP65 can interact with Unc119, a protein implicated in trafficking of myristoylated proteins to specific membrane compartments [26] and endosomal targeting of proteins in T cells [54]. Unc119 has been found to be important for TCR signaling [53], its role in B cells has not been studied yet. It could be a potential candidate molecule for the recruitment of SLP65 to specific vesicles. The VAMP7-positve vesicles might serve as a starting platform for plasma membrane recruitment by vesicular transport. The vesicle transport process might require cytoskeletal rearrangements like actin depolymerization that occurs upon BCR stimulation [60].

For the anchoring of SLP65 complexes to the BCR, the avidity of the SLP65 SH2 domains might play a major role. Covalent SLP65 oligomerization by chimeric proteins of SLP65 with split Venus could not substitute for the function of the SLP65 SH2 domain (Figure 4.30), indicating that the SH2 domain does not take part in SLP65 oligomerization but in a sequential process. The inactivation of the SLP65 SH2 domains preserved the dot-like localization of chimeric CIN85-CC-SLP65 proteins, but it abolished stable plasma membrane localization upon BCR stimulation and thus Ca^{2+} signaling (Figure 4.16). This suggests again that the SLP65 SH2 domain might be involved in anchoring SLP65 to the BCR, not the initiation of its translocation to the plasma membrane.
The SLP65 SH2 domain can bind to pY204 in Igα [42, 79]. This interaction could be crucially dependent on the avidity of the SLP65 SH2 domains and thus on the SLP65 oligomerization state. It is astonishing that the SLP65-CIN85 interaction is strongly required for SLP65 BCR recruitment and Ca^{2+} signaling upon stimulation with 0.2 µg/ml α-IgM, while its influence is not that pronounced upon stimulation with 2 µg/ml α-IgM (Figure 4.1). This could be explained by modification of the activation threshold by different extents of Igα phosphorylation. Upon stimulation with 0.2 µg/ml α-IgM, only a minor portion of Igα can be phosphorylated, large SLP65 complexes with high SH2 domain avidity would be required to enable a stable interaction and thereby effective BCR anchoring. Stimulation with 2 µg/ml α-IgM would result in higher Igα phosphorylation, also smaller SLP65 complexes with lower avidity might mediate efficient binding, BCR anchoring and thus signaling. This model fits to an effect I observed for chimeric SCOC-CC-SLP65 proteins of different oligomerization states (Figure 4.26). The difference in Ca^{2+} influx between dimeric, trimeric and tetrameric increased with decreasing α-IgM concentrations.
The requirement for high avidity of SH2 domain binding has been reported before. The two SH2 domains of Syk bind in tandem much more effective to ITAMs than individually [164]. Also other signaling proteins like ZAP70, PLC-γ, SHP2 and the PI3K subunit p85 possess tandem SH2 domains [126, 9], indicating a general need of bi- or multivalent interactions for SH2 domains. While single SH2 domains bind to pY-peptides with a micromolar affinity, tandem SH2 domains can bind to bi-pY-peptides with

nanomolar affinity [126]. This demonstrates the enormous power of affinity enhancement by avidity.

There might be also other additional mechanisms which could anchor SLP65 to the plasma membrane. Some membrane protein ligands linking SLP65 to the BCR have been proposed in the past, like the tetraspanning membrane protein CMTM7 [111]. However, we were not able to confirm the association of SLP65 with this or other membrane proteins ([121] and own unpublished data). If interactions of SLP65 with other membrane proteins than Igα are physiologically relevant, they could also be influenced by SLP65 multimerization and thus by CIN85. So the oligomerization of SLP65 by CIN85 serves at least two purposes: It mediates the association of SLP65 to specific vesicles by a hypothetic targeting device in the SLP65 central region and allows efficient BCR targeting of SLP65 complexes by amplifying the avidity of the SLP65 SH2 domains. A model of SLP65 recruitment to the BCR and the involvement of CIN85 is given in Figure 5.2.

5.8 The overall effect of CIN85 expression in B cells

Having shown the importance of CIN85 for the function of SLP65, it is intriguing that there are different reports on the influence of CIN85 on BCR signaling. Experiments of our group have shown that the knockdown of CIN85 in chicken DT40 B cells and the knockout of CIN85 in human Ramos B cells result in a modest reduction in Ca^{2+} signaling ([121, 18] and unpublished observations K. Schulz). This corresponds with the reduced efficiency of SLP65 BCR recruitment in these cells due to loss of SLP65 clustering. However, the effect of reduced CIN85 expression is weaker than the reduction of Ca^{2+} signaling that occurs in SLP65-deficient cells reconstituted with the CIN85 binding deficient SLP65 mutant M2,3 (Figure 4.1 and [121]). Niiro and colleagues reported that CIN85 knockdown in the human Burkitt lymphoma cell line BJAB even increases BCR signaling while overexpression of CIN85 decreases BCR-induced phosphorylation and expression level of Syk, phosphorylation of PLC-γ2 and Ca^{2+} influx [119]. We could not confirm these results in DT40 or Ramos B cells where CIN85 overexpression had no effect on BCR signaling (own unpublished observations). For human primary B cells, Niiro and colleagues reported that the knockdown of CIN85 enhances survival, growth and differentiation [119]. Recently, our group was able to identify a patient that carries a deletion in the CIN85 gene, resulting in the loss of CIN85 protein expression (unpublished observation). This patient showed a modestly reduced Ca^{2+} signaling and a severe block of BCR-induced NfκB activation upon BCR stimulation. This corresponds partially with results obtained from a mouse strain harboring a B cell specific CIN85 deficiency [88]. These mice show impaired NfκB activation and loss of B1a cells while the Ca^{2+} signaling in B2 cells is not affected.

These different observations concerning CIN85 deficiency in B cells could be explained by the promiscuity of CIN85 interactions. As a potent oligomerizer, CIN85 would enhance the functions of several

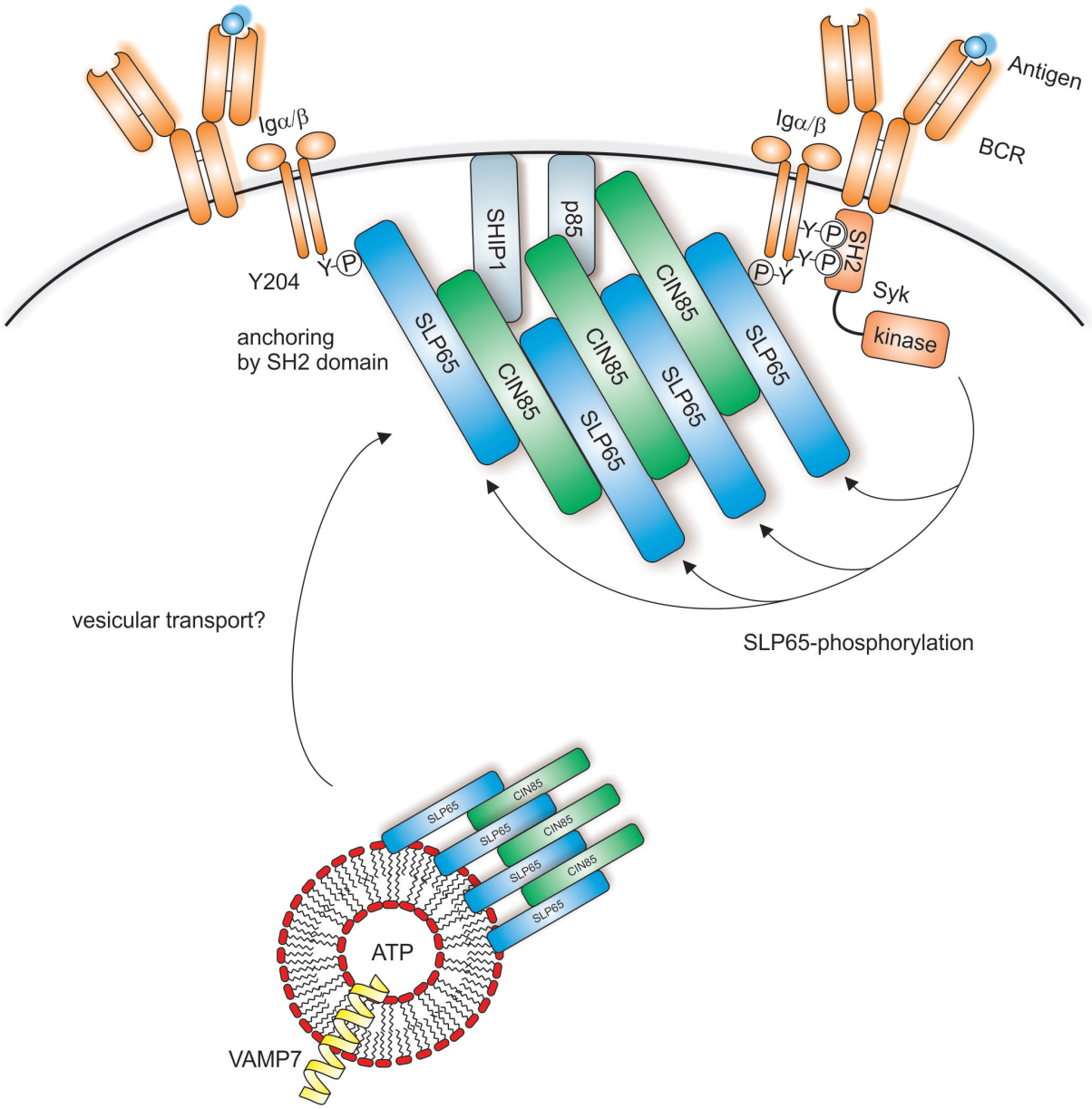

Fig. 5.2: Model for plasma membrane recruitment of SLP65 and CIN85. Large SLP65-CIN85 complexes are localized on VAMP$^+$ ATP-containing vesicles (Figure 5.2). Upon BCR stimulation, the vesicles are translocated to the membrane, were the SLP65 complexes can be anchored to the BCR by the interaction of the SH2 domains to pY204 in Igα. This anchoring allows multiple phosphorylations of the whole SLP65 complex by Syk. The phosphorylated complex provides an extended platform for the assembly of signal-transducing molecules like Btk and PLC-γ2. The CIN85 molecules in the complex can interact with other proteins in the proximity of the activated BCR, e.g. SHIP1 and p85. This might modulate the function of these CIN85 interactors. Additionally, these interactions could provide additional membrane anchoring for the SLP65-CIN85 complex and stabilize the emerging microsignalosomes.

interaction partners given that they are present in a concentration that enables a stable interaction. In many cases, CIN85 seems to be a general enhancer of the function of its ligands. CIN85 associates with the GTPase ARAP1, coexpression of these two proteins leads to localization of ARAP1 in dot-like structures. The knockdown of ARAP1 accelerates trafficking and degradation of the EGFR, the knockdown of CIN85 has the same effect [199]. CIN85 associates also with the GTPase dynamin 2, both proteins are localized in dot-like structures supposed to be endosomes [161]. Dynamin 2 influences trafficking of proteins in late endosomes, a knockdown of either dynamin 2 or CIN85 delays EGFR degradation [161]. CIN85 associates with the GTPase ASAP1 which is known to play a role in invasion of breast cancer cells [125]. Both proteins were found to colocalize in invadopodia of breast cancer cells [117]. The chemoinvasion activity of these cells is inhibited by knockdown of ASAP1 or CIN85 or by disruption of their interaction [117]. Beside these reports, which can be explained by mere functional enhancement by CIN85-mediated clustering, CIN85 has been shown to regulate protein activity by competition with other interaction partners. It reduces the association of c-Cbl with Sts1, a negative regulator of c-Cbl activity, by competitive binding which results in decreased Syk activity by increased c-Cbl activity [130]. On the other hand, association of Septin 9 with CIN85 reduces the CIN85-c-Cbl interaction, leading to a delay of EGFR degradation by decreased c-Cbl activity [34]. The only example for direct negative regulation of a protein function by CIN85 is its effect on the PI3K [55]. It was shown that the rat homolog of CIN85 can inhibit the PI3K activity *in vitro* by binding to the PI3K regulatory subunit p85 [55]. This interaction is mediated by the p85 SH3 domain and the CIN85-PRR. It was further demonstrated that the inhibition of PI3K by CIN85 can induce apoptosis in neurons. Interestingly, this effect was also exhibited by a CIN85 variant lacking the CC [55]. So this might be a functional different mechanism of CIN85, not mediated by protein clustering by the SH3 domains. In CIN85-deficient B cells, the loss of PI3K inhibiton by CIN85 could potentially compensate for missing clustering of activators of the BCR signaling. It might lead to higher Akt and Btk activity by increased PIP3 levels.

Some of the CIN85 interactors are activators for BCR signaling, like SLP65, some of them are inhibitors, like c-Cbl and SHIP1. Because CIN85 can potentially enhance the functions of all of them and because these enhancements are competitive, the overall outcome of CIN85 absence might mainly depend on the expression levels of the different interaction partners. This complicates the prediction of the effect of increased or decreased CIN85 expression. It would probably require an exact bioinformatic model and information of the concentration of all CIN85 interaction partners. In contrast, the specific loss of only one CIN85 interaction has a more straightforward effect. The disruption of the SLP65-CIN85 interaction in SLP65-deficient cells reconstituted with the CIN85 binding deficient variant SLP65-M2,3 shows a stronger phenotype than a complete CIN85 knockout. The explanation for this effect is that these cells lack only one positive, but not the negative, effects of CIN85 on BCR signaling. In addition, the SLP65-M2,3 variant cannot bind to the CIN85 homolog CD2AP which might partially compensate for this loss of CIN85.

The main readout in my experiments was the BCR-induced Ca^{2+} influx in DT40 B cells. In this model system, Ca^{2+} signaling can be regarded as an almost analog event. It will happen at a certain threshold of activation, but once the threshold is reached, the amount of Ca^{2+} influx into one cell seems to be always comparable, independent of the strength of the external stimulus (i.e. α-IgM concentration). Differences in the measured Ca^{2+} signals are generated by the different amount of cells reaching the threshold for Ca^{2+} influx. In this respect, CIN85 could act as modulator of this threshold. When positive regulators amongst CIN85 interactors dominate, CIN85 would increase Ca^{2+} signaling by lowering the threshold. When negative regulators amongst CIN85 interactors dominate, CIN85 would decrease Ca^{2+} signaling by raising the threshold. Nevertheless, the CIN85-deficient patient gives us the hint that CIN85 is a positive regulator of BCR signaling in a physiological situation. The patient displayed very low levels of IgM and IgG4 in the serum, indicating a defect in B cell activation, especially because his T cells seem to be activated normally (unpublished observations).

5.9 Conclusion

In this work, it could be shown that the interaction of CIN85 with SLP65 enables efficient BCR signaling due to CIN85-mediated multimerization of SLP65. The N-terminus of SLP65 is crucial for this multimerization. It can increase the local concentration of SLP65 on membranes which would allow the efficient formation of large SLP65-CIN85 complexes. SLP65 multimerization is essential for the recruitment of SLP65 to the BCR, probably by enhancing the avidity of the SLP65 SH2 domain and a hypothetical other function in the middle part of SLP65. The general concept of adaptor protein-mediated oligomerization can also be transferred to the SLP65 homolog in T cells, SLP76. SLP76 has been shown to oligomerize due to its interaction with the adaptor protein ADAP [30]. The oligomerization of SLP-adaptors seems to be a fundamental principle in lymphocyte signaling. With regards to SLP65, this thesis demonstrates this for the first time.

6 Bibliography

[1] Ababou, A., Pfuhl, M., and Ladbury, J. E. Novel insights into the mechanisms of cin85 sh3 domains binding to cbl proteins: solution-based investigations and in vivo implications. *Journal of molecular biology 387*, 5 (2009), 1120–1136.

[2] Abudula, A., Grabbe, A., Brechmann, M., Polaschegg, C., Herrmann, N., Goldbeck, I., Dittmann, K., and Wienands, J. Slp-65 signal transduction requires src homology 2 domain-mediated membrane anchoring and a kinase-independent adaptor function of syk. *Journal of Biological Chemistry 282*, 39 (2007), 29059–29066.

[3] Agou, F., Ye, F., Goffinont, S., Courtois, G., Yamaoka, S., Israël, A., and Véron, M. Nemo trimerizes through its coiled-coil c-terminal domain. *Journal of Biological Chemistry 277*, 20 (2002), 17464–17475.

[4] Antony, P., Petro, J. B., Carlesso, G., Shinners, N. P., Lowe, J., and Khan, W. N. B cell receptor directs the activation of nfat and nf-κb via distinct molecular mechanisms. *Experimental cell research 291*, 1 (2003), 11–24.

[5] Aronheim, A., Engelberg, D., Li, N., Al-Alawi, N., Schlessinger, J., and Karin, M. Membrane targeting of the nucleotide exchange factor sos is sufficient for activating the ras signaling pathway. *Cell 78*, 6 (1994), 949–961.

[6] Baba, T. W., Giroir, B. P., and Humphries, E. H. Cell lines derived from avian lymphomas exhibit two distinct phenotypes. *Virology 144*, 1 (1985), 139–151.

[7] Baba, Y., Hashimoto, S., Matsushita, M., Watanabe, D., Kishimoto, T., Kurosaki, T., and Tsukada, S. Blnk mediates syk-dependent btk activation. *Proceedings of the National Academy of Sciences 98*, 5 (2001), 2582–2586.

[8] Bao, M., Hanabuchi, S., Facchinetti, V., Du, Q., Bover, L., Plumas, J., Chaperot, L., Cao, W., Qin, J., Sun, S.-C., et al. Cd2ap/ship1 complex positively regulates plasmacytoid dendritic cell receptor signaling by inhibiting the e3 ubiquitin ligase cbl. *The Journal of Immunology 189*, 2 (2012), 786–792.

[9] Barua, D., Faeder, J. R., and Haugh, J. M. Computational models of tandem src homology 2 domain interactions and application to phosphoinositide 3-kinase. *Journal of Biological Chemistry 283*, 12 (2008), 7338–7345.

[10] Behrens, C., Binotti, B., Schmidt, C., Robinson, C. V., Chua, J. J. E., and Kühnel, K. Crystal structure of the human short coiled coil protein and insights into scoc-fez1 complex formation. *PloS one 8*, 10 (2013), e76355.

[11] Berridge, M. J. Inositol trisphosphate and calcium signalling. *Nature 361*, 6410 (1993), 315–325.

[12] Bethani, I., Lang, T., Geumann, U., Sieber, J. J., Jahn, R., and Rizzoli, S. O. The specificity of snare pairing in biological membranes is mediated by both proof-reading and spatial segregation. *The EMBO journal 26*, 17 (2007), 3981–3992.

[13] Bezsonova, I., Bruce, M. C., Wiesner, S., Lin, H., Rotin, D., and Forman-Kay, J. D. Interactions between the three cin85 sh3 domains and ubiquitin: Implications for cin85 ubiquitination. *Biochemistry 47*, 34 (2008), 8937–8949.

[14] Boerth, N. J., Judd, B. A., and Koretzky, G. A. Functional association between slap-130 and slp-76 in jurkat t cells. *Journal of Biological Chemistry 275*, 7 (2000), 5143–5152.

[15] Bögler, O., Furnari, F. B., Kindler-Roehrborn, A., Sykes, V. W., Yung, R., Huang, H.-J. S., and Cavenee, W. K. Seta: a novel sh3 domain-containing adapter molecule associated with malignancy in astrocytes. *Neuro-oncology 2*, 1 (2000), 6–15.

[16] Borinstein, S. C., Hyatt, M. A., Sykes, V. W., Straub, R. E., Lipkowitz, S., Boulter, J., and Bogler, O. Seta is a multifunctional adapter protein with three sh3 domains that binds grb2, cbl, and the novel sb1 proteins. *Cellular signalling 12*, 11 (2000), 769–779.

[17] Borthwick, E. B., Korobko, I. V., Luke, C., Drel, V. R., Fedyshyn, Y. Y., Ninkina, N., Drobot, L. B., and Buchman, V. L. Multiple domains of ruk/cin85/seta/cd2bp3 are involved in interaction with p85α regulatory subunit of pi 3-kinase. *Journal of molecular biology 343*, 4 (2004), 1135–1146.

[18] Bremes, V. *CIN85/CD2AP-based protein complexes in B cell antigen receptor signalling.* PhD thesis, Georg-August-Universität, Göttingen, 2012.

[19] Buchman, V. L., Luke, C., Borthwick, E. B., Gout, I., and Ninkina, N. Organization of the mouse ruk locus and expression of isoforms in mouse tissues. *Gene 295*, 1 (2002), 13–17.

[20] Büchse, T., Horras, N., Lenfert, E., Krystal, G., Körbel, S., Schümann, M., Krause, E., Mikkat, S., and Tiedge, M. Cin85 interacting proteins in b cells-specific role for ship-1. *Molecular & Cellular Proteomics 10*, 10 (2011), M110–006239.

[21] Campbell, K. S., Hager, E. J., Friedrich, R. J., and Cambier, J. C. Igm antigen receptor complex contains phosphoprotein products of b29 and mb-1 genes. *Proceedings of the National Academy of Sciences 88*, 9 (1991), 3982–3986.

[22] Cavaillon, J.-M. The historical milestones in the understanding of leukocyte biology initiated by elie metchnikoff. *Journal of leukocyte biology 90*, 3 (2011), 413–424.

[23] Chaineau, M., Danglot, L., and Galli, T. Multiple roles of the vesicular-snare ti-vamp in post-golgi and endosomal trafficking. *FEBS letters 583*, 23 (2009), 3817–3826.

[24] Chiu, C. W., Dalton, M., Ishiai, M., Kurosaki, T., and Chan, A. C. Blnk: molecular scaffolding through cis-mediated organization of signaling proteins. *The EMBO journal 21*, 23 (2002), 6461–6472.

[25] Chrambach, A., and Rodbard, D. Polyacrylamide gel electrophoresis. *Science 172*, 3982 (1971), 440–451.

[26] Constantine, R., Zhang, H., Gerstner, C. D., Frederick, J. M., and Baehr, W. Uncoordinated (unc) 119: coordinating the trafficking of myristoylated proteins. *Vision research 75* (2012), 26–32.

[27] Cooper, M. D. A life of adventure in immunobiology. *Annual review of immunology 28* (2009), 1–19.

[28] Cooper, M. D., and Alder, M. N. The evolution of adaptive immune systems. *Cell 124*, 4 (2006), 815–822.

[29] Coughlin, J. J., Stang, S. L., Dower, N. A., and Stone, J. C. Rasgrp1 and rasgrp3 regulate b cell proliferation by facilitating b cell receptor-ras signaling. *The Journal of Immunology 175*, 11 (2005), 7179–7184.

[30] Coussens, N. P., Hayashi, R., Brown, P. H., Balagopalan, L., Balbo, A., Akpan, I., Houtman, J. C., Barr, V. A., Schuck, P., Appella, E., et al. Multipoint binding of the slp-76 sh2 domain to adap is critical for oligomerization of slp-76 signaling complexes in stimulated t cells. *Molecular and cellular biology 33*, 21 (2013), 4140–4151.

[31] Da Silva, A. J., Li, Z., De Vera, C., Canto, E., Findell, P., and Rudd, C. E. Cloning of a novel t-cell protein fyb that binds fyn and sh2-domain-containing leukocyte protein 76 and modulates interleukin 2 production. *Proceedings of the National Academy of Sciences 94*, 14 (1997), 7493–7498.

[32] Dal Porto, J. M., Gauld, S. B., Merrell, K. T., Mills, D., Pugh-Bernard, A. E., and Cambier, J. B cell antigen receptor signaling 101. *Molecular immunology 41*, 6 (2004), 599–613.

[33] de Araújo, M. E., Stasyk, T., Taub, N., Ebner, H. L., Fürst, B., Filipek, P., Weys, S. R., Hess, M. W., Lindner, H., Kremser, L., et al. Stability of the endosomal scaffold protein lamtor3 depends on heterodimer assembly and proteasomal degradation. *Journal of Biological Chemistry 288*, 25 (2013), 18228–18242.

[34] Diesenberg, K., Beerbaum, M., Fink, U., Schmieder, P., and Krauss, M. Sept9 negatively regulates ubiquitin-dependent downregulation of egfr. *Journal of cell science 128*, 2 (2015), 397–407.

[35] Drew, D., Shimada, E., Huynh, K., Bergqvist, S., Talwar, R., Karin, M., and Ghosh, G. Inhibitor κb kinase β binding by inhibitor κb kinase γ. *Biochemistry 46*, 43 (2007), 12482–12490.

[36] Edelheit, O., Hanukoglu, A., and Hanukoglu, I. Simple and efficient site-directed mutagenesis using two single-primer reactions in parallel to generate mutants for protein structure-function studies. *BMC biotechnology 9*, 1 (2009), 61.

[37] Edry, E., and Melamed, D. Receptor editing in positive and negative selection of b lymphopoiesis. *The Journal of Immunology 173*, 7 (2004), 4265–4271.

[38] Engel, P., Zhou, L.-J., Ord, D. C., Sato, S., Koller, B., and Tedder, T. F. Abnormal b lymphocyte delevopment, activation, and differentiation in mice that lack or overexpress the cd19 signal transduction molecule. *Immunity 3*, 1 (1995), 39–50.

[39] Engelke, M., Oellerich, T., Dittmann, K., Hsiao, H.-H., Urlaub, H., Serve, H., Griesinger, C., and Wienands, J. Cutting edge: Feed-forward activation of phospholipase cγ2 via c2 domain–mediated binding to slp65. *The Journal of Immunology 191*, 11 (2013), 5354–5358.

[40] Engelke, M., Pirkuliyeva, S., Kühn, J., Wong, L., Boyken, J., Herrmann, N., Becker, S., Griesinger, C., and Wienands, J. Macromolecular assembly of the adaptor slp-65 at intracellular vesicles in resting b cells. *Science signaling 7*, 339 (2014), ra79–ra79.

[41] Engels, N., König, L. M., Heemann, C., Lutz, J., Tsubata, T., Griep, S., Schrader, V., and Wienands, J. Recruitment of the cytoplasmic adaptor grb2 to surface igg and ige provides antigen receptor–intrinsic costimulation to class-switched b cells. *Nature immunology 10*, 9 (2009), 1018–1025.

[42] Engels, N., Wollscheid, B., and Wienands, J. Association of slp-65/blnk with the b cell antigen receptor through a non-itam tyrosine of ig-α. *European journal of immunology 31*, 7 (2001), 2126–2134.

[43] Feng, L., Wang, J.-T., Jin, H., Qian, K., and Geng, J.-G. Sh3kbp1-binding protein 1 prevents epidermal growth factor receptor degradation by the interruption of c-cbl-cin85 complex. *Cell biochemistry and function 29*, 7 (2011), 589–596.

[44] Finniss, S., Movsisyan, A., Billecke, C., Schmidt, M., Randazzo, L., Chen, B., and Bögler, O. Studying protein isoforms of the adaptor seta/cin85/ruk with monoclonal antibodies. *Biochemical and biophysical research communications 325*, 1 (2004), 174–182.

[45] Flaswinkel, H., Barner, M., and Reth, M. The tyrosine activation motif as a target of protein tyrosine kinases and sh2 domains. *Seminars in immunology 7*, 1 (1995), 21–27.

[46] Fluckiger, A.-C., Li, Z., Kato, R. M., Wahl, M. I., Ochs, H. D., Longnecker, R., Kinet, J.-P., Witte, O. N., Scharenberg, A. M., and Rawlings, D. J. Btk/tec kinases regulate sustained increases in intracellular ca2+ following b-cell receptor activation. *The EMBO Journal 17*, 7 (1998), 1973–1985.

[47] Fu, C., Turck, C. W., Kurosaki, T., and Chan, A. C. Blnk: a central linker protein in b cell activation. *Immunity 9*, 1 (1998), 93–103.

[48] Gaidos, G., Soni, S., Oswald, D. J., Toselli, P. A., and Kirsch, K. H. Structure and function analysis of the cms/cin85 protein family identifies actin-bundling properties and heterotypic-complex formation. *Journal of cell science 120*, 14 (2007), 2366–2377.

[49] Gangi-Peterson, L., Peterson, S., Shapiro, L., Golding, A., Caricchio, R., Cohen, D., Margulies, D., and Cohen, P. bca: an activation-related b-cell gene. *Molecular immunology 35*, 1 (1998), 55–63.

[50] Geng, L., Raab, M., and Rudd, C. E. Cutting edge: Slp-76 cooperativity with fyb/fyn-t in the up-regulation of tcr-driven il-2 transcription requires slp-76 binding to fyb at tyr595 and tyr651. *The Journal of Immunology 163*, 11 (1999), 5753–5757.

[51] Goitsuka, R., Fujimura, Y.-i., Mamada, H., Umeda, A., Morimura, T., Uetsuka, K., Doi, K., Tsuji, S., and Kitamura, D. Cutting edge: Bash, a novel signaling molecule preferentially expressed in b cells of the bursa of fabricius. *The Journal of Immunology 161*, 11 (1998), 5804–5808.

[52] Good, M. C., Zalatan, J. G., and Lim, W. A. Scaffold proteins: hubs for controlling the flow of cellular information. *Science 332*, 6030 (2011), 680–686.

[53] Gorska, M. M., and Alam, R. A mutation in the human uncoordinated 119 gene impairs tcr signaling and is associated with cd4 lymphopenia. *Blood 119*, 6 (2012), 1399–1406.

[54] Gorska, M. M., Liang, Q., Karim, Z., and Alam, R. Uncoordinated 119 protein controls trafficking of lck via the rab11 endosome and is critical for immunological synapse formation. *The Journal of Immunology 183*, 3 (2009), 1675–1684.

[55] Gout, I., Middleton, G., Adu, J., Ninkina, N. N., Drobot, L. B., Filonenko, V., Matsuka, G., Davies, A. M., Waterfield, M., and Buchman, V. L. Negative regulation of pi 3-kinase by ruk, a novel adaptor protein. *The EMBO journal 19*, 15 (2000), 4015–4025.

[56] Graves, J., Draves, K., Craxton, A., Saklatvala, J., Krebs, E., and Clark, E. Involvement of stress-activated protein kinase and p38 mitogen-activated protein kinase in migm-induced apoptosis of human b lymphocytes. *Proceedings of the National Academy of Sciences 93*, 24 (1996), 13814–13818.

[57] Groth, S. F. d. S., Webster, R., and Datyner, A. Two new staining procedures for quantitative estimation of proteins on electrophoretic strips. *Biochimica et Biophysica Acta 71* (1963), 377–391.

[58] Haglund, K., Schmidt, M. H., Wong, E. S. M., Guy, G. R., and Dikic, I. Sprouty2 acts at the cbl/cin85 interface to inhibit epidermal growth factor receptor downregulation. *EMBO reports 6*, 7 (2005), 635–641.

[59] Haglund, K., Shimokawa, N., Szymkiewicz, I., and Dikic, I. Cbl-directed monoubiquitination of cin85 is involved in regulation of ligand-induced degradation of egf receptors. *Proceedings of the National Academy of Sciences 99*, 19 (2002), 12191–12196.

[60] Hao, S., and August, A. Actin depolymerization transduces the strength of b-cell receptor stimulation. *Molecular biology of the cell 16*, 5 (2005), 2275–2284.

[61] Hashimoto, A., Okada, H., Jiang, A., Kurosaki, M., Greenberg, S., Clark, E. A., and Kurosaki, T. Involvement of guanosine triphosphatases and phospholipase c-γ2 in extracellular signal–regulated kinase, c-jun nh2-terminal kinase, and p38 mitogen-activated protein kinase activation by the b cell antigen receptor. *The Journal of experimental medicine 188*, 7 (1998), 1287–1295.

[62] Hashimoto, S., Iwamatsu, A., Ishiai, M., Okawa, K., Yamadori, T., Matsushita, M., Baba, Y., Kishimoto, T., Kurosaki, T., and Tsukada, S. Identification of the sh2 domain binding protein of brutons tyrosine kinase as blnkfunctional significance of btk-sh2 domain in b-cell antigen receptor-coupled calcium signaling. *Blood 94*, 7 (1999), 2357–2364.

[63] Havrylov, S., Ichioka, F., Powell, K., Borthwick, E. B., Baranska, J., Maki, M., and Buchman, V. L. Adaptor protein ruk/cin85 is associated with a subset of copi-coated membranes of the golgi complex. *Traffic 9*, 5 (2008), 798–812.

[64] Havrylov, S., Jolanta Redowicz, M., and Buchman, V. L. Emerging roles of ruk/cin85 in vesicle-mediated transport, adhesion, migration and malignancy. *Traffic 11*, 6 (2010), 721–731.

[65] Havrylov, S., Rzhepetskyy, Y., Malinowska, A., Drobot, L., and Redowicz, M. J. Proteins recruited by sh3 domains of ruk/cin85 adaptor identified by lc-ms/ms. *Proteome science 7*, 1 (2009), 21.

[66] Hayden, M. S., and Ghosh, S. Nf-κb, the first quarter-century: remarkable progress and outstanding questions. *Genes & development 26*, 3 (2012), 203–234.

[67] Herrmann, N. *Kooperation funktioneller Domänen des Adaptorproteins SLP-65 für die Ca2+-Antwort in B-Lymphozyten.* PhD thesis, Georg-August-Universität, Göttingen, 2009.

[68] Higuchi, R., Krummel, B., and Saiki, R. A general method of in vitro preparation and specific mutagenesis of dna fragments: study of protein and dna interactions. *Nucleic acids research 16*, 15 (1988), 7351–7367.

[69] Homma, Y., Emori, Y., Shibasaki, F., Suzuki, K., and Takenawa, T. Isolation and characterization of a gamma-type phosphoinositide-specific phospholipase c (plc-gamma 2). *Biochem. J 269* (1990), 13–18.

[70] Huang, F., and Sorkin, A. Growth factor receptor binding protein 2-mediated recruitment of the ring domain of cbl to the epidermal growth factor receptor is essential and sufficient to support receptor endocytosis. *Molecular biology of the cell 16*, 3 (2005), 1268–1281.

[71] Hutchings, N. J., Clarkson, N., Chalkley, R., Barclay, A. N., and Brown, M. H. Linking the t cell surface protein cd2 to the actin-capping protein capz via cms and cin85. *Journal of Biological Chemistry 278*, 25 (2003), 22396–22403.

[72] Hutchins, J. R., Toyoda, Y., Hegemann, B., Poser, I., Hériché, J.-K., Sykora, M. M., Augsburg, M., Hudecz, O., Buschhorn, B. A., Bulkescher, J., et al. Systematic analysis of human protein complexes identifies chromosome segregation proteins. *Science 328*, 5978 (2010), 593–599.

[73] Huttlin, E., Ting, L., Bruckner, R., Paulo, J., Gygi, M., Rad, R., Kolippakkam, D., Szpyt, J., Zarraga, G., Tam, S., Gebreab, F., Colby, G., Pontano-Vaites, L., Obar, R., Guarani-Pereira, V., Harris, T., Artavanis-Tsakonas, S., Sowa, M., Harper, J., and Gygi, S. High-throughput proteomic mapping of human interaction networks via affinity-purification mass spectrometry (pre-publication). *Pre-publication* (2014).

[74] Inohara, N., Koseki, T., Lin, J., del Peso, L., Lucas, P. C., Chen, F. F., Ogura, Y., and Núñez, G. An induced proximity model for nf-κb activation in the nod1/rick and rip signaling pathways. *Journal of Biological Chemistry 275*, 36 (2000), 27823–27831.

[75] Ishiai, M., Kurosaki, M., Pappu, R., Okawa, K., Ronko, I., Fu, C., Shibata, M., Iwamatsu, A., Chan, A. C., and Kurosaki, T. Blnk required for coupling syk to plcγ2 and rac1-jnk in b cells. *Immunity 10*, 1 (1999), 117–125.

[76] Ishiai, M., Sugawara, H., Kurosaki, M., and Kurosaki, T. Cutting edge: association of phospholipase c-γ2 src homology 2 domains with blnk is critical for b cell antigen receptor signaling. *The Journal of Immunology 163*, 4 (1999), 1746–1749.

[77] Jiang, X., and Sorkin, A. Epidermal growth factor receptor internalization through clathrin-coated pits requires cbl ring finger and proline-rich domains but not receptor polyubiquitylation. *Traffic 4*, 8 (2003), 529–543.

[78] Jumaa, H., Wollscheid, B., Mitterer, M., Wienands, J., Reth, M., and Nielsen, P. J. Abnormal development and function of b lymphocytes in mice deficient for the signaling adaptor protein slp-65. *Immunity 11*, 5 (1999), 547–554.

[79] Kabak, S., Skaggs, B. J., Gold, M. R., Affolter, M., West, K. L., Foster, M. S., Siemasko, K., Chan, A. C., Aebersold, R., and Clark, M. R. The direct recruitment of blnk to immunoglobulin α couples the b-cell antigen receptor to distal signaling pathways. *Molecular and cellular biology 22*, 8 (2002), 2524–2535.

[80] Kaneko, T., Maeda, A., Takefuji, M., Aoyama, H., Nakayama, M., Kawabata, S., Kawano, Y., Iwamatsu, A., Amano, M., and Kaibuchi, K. Rho mediates endocytosis of epidermal growth factor receptor through phosphorylation of endophilin a1 by rho-kinase. *Genes to Cells 10*, 10 (2005), 973–987.

[81] Kassas, N., Tryoen-Tóth, P., Corrotte, M., Thahouly, T., Bader, M.-F., Grant, N. J., and Vitale, N. Genetically encoded probes for phosphatidic acid. *Methods Cell Biol 108* (2012), 445–459.

[82] Kay, B. K. Sh3 domains come of age. *FEBS letters 586*, 17 (2012), 2606–2608.

[83] Kirsch, K. H., Georgescu, M.-M., Ishimaru, S., and Hanafusa, H. Cms: an adapter molecule involved in cytoskeletal rearrangements. *Proceedings of the National Academy of Sciences 96*, 11 (1999), 6211–6216.

[84] Kirstein, J., Schlothauer, T., Dougan, D. A., Lilie, H., Tischendorf, G., Mogk, A., Bukau, B., and Turgay, K. Adaptor protein controlled oligomerization activates the aaa+ protein clpc. *The EMBO journal 25*, 7 (2006), 1481–1491.

[85] Kläsener, K., Maity, P. C., Hobeika, E., Yang, J., and Reth, M. B cell activation involves nanoscale receptor reorganizations and inside-out signaling by syk. *Elife 3* (2014), e02069.

[86] Klein, G., Giovanella, B., Westman, A., Stehlin, J., and Mumford, D. An ebv-genome-negative cell line established from an american burkitt lymphoma; receptor characteristics. ebv infectibility and permanent conversion into ebv-positive sublines by in vitro infection. *Intervirology 5*, 6 (1975), 319–334.

[87] Köhler, F., Storch, B., Kulathu, Y., Herzog, S., Kuppig, S., Reth, M., and Jumaa, H. A leucine zipper in the n terminus confers membrane association to slp-65. *Nature immunology 6*, 2 (2005), 204–210.

[88] Kometani, K., Yamada, T., Sasaki, Y., Yokosuka, T., Saito, T., Rajewsky, K., Ishiai, M., Hikida, M., and Kurosaki, T. Cin85 drives b cell responses by linking bcr signals to the canonical nf-κb pathway. *The Journal of experimental medicine 208*, 7 (2011), 1447–1457.

[89] Konishi, H., Tashiro, K., Murata, Y., Nabeshi, H., Yamauchi, E., and Taniguchi, H. Cfbp is a novel tyrosine-phosphorylated protein that might function as a regulator of cin85/cd2ap. *Journal of Biological Chemistry 281*, 39 (2006), 28919–28931.

[90] Koretzky, G. A., Abtahian, F., and Silverman, M. A. Slp76 and slp65: complex regulation of signalling in lymphocytes and beyond. *Nature Reviews Immunology 6*, 1 (2006), 67–78.

[91] Kowanetz, K., Husnjak, K., Höller, D., Kowanetz, M., Soubeyran, P., Hirsch, D., Schmidt, M. H., Pavelic, K., De Camilli, P., Randazzo, P. A., et al. Cin85 associates with multiple effectors controlling intracellular trafficking of epidermal growth factor receptors. *Molecular biology of the cell 15*, 7 (2004), 3155–3166.

[92] Kowanetz, K., Szymkiewicz, I., Haglund, K., Kowanetz, M., Husnjak, K., Taylor, J. D., Soubeyran, P., Engstrom, U., Ladbury, J. E., and Dikic, I. Identification of a novel proline-arginine motif involved in cin85-dependent clustering of cbl and down-regulation of epidermal growth factor receptors. *Journal of Biological Chemistry 278*, 41 (2003), 39735–39746.

[93] Kowanetz, K., Terzic, J., and Dikic, I. Dab2 links cin85 with clathrin-mediated receptor internalization. *FEBS letters 554*, 1 (2003), 81–87.

[94] Kurakin, A. V., Wu, S., and Bredesen, D. E. Atypical recognition consensus of cin85/seta/ruk sh3 domains revealed by target-assisted iterative screening. *Journal of Biological Chemistry 278*, 36 (2003), 34102–34109.

[95] Kurosaki, T. Regulation of b-cell signal transduction by adaptor proteins. *Nature Reviews Immunology 2*, 5 (2002), 354–363.

[96] Kurosaki, T., Maeda, A., Ishiai, M., Hashimoto, A., Inabe, K., and Takata, M. Regulation of the phospholipase C-γ2 pathway in b cells. *Immunological reviews 176* (2000), 19–29.

[97] Kurosaki, T., and Tsukada, S. Blnk: connecting syk and btk to calcium signals. *Immunity 12*, 1 (2000), 1–5.

[98] Laemmli, U. K., et al. Cleavage of structural proteins during the assembly of the head of bacteriophage t4. *nature 227*, 5259 (1970), 680–685.

[99] Lange, S., Sylvester, M., Schumann, M., Freund, C., and Krause, E. Identification of phosphorylation-dependent interaction partners of the adapter protein adap using quantitative mass spectrometry: Silac vs 18o-labeling. *Journal of proteome research 9*, 8 (2010), 4113–4122.

[100] Li, S. Specificity and versatility of sh3 and other proline-recognition domains: structural basis and implications for cellular signal transduction. *Biochem. J 390* (2005), 641–653.

[101] Liu, H., and May, K. Disulfide bond structures of igg molecules: structural variations, chemical modifications and possible impacts to stability and biological function. *MAbs 4*, 1 (2012), 17–23.

[102] Liu, H., Thaker, Y. R., Stagg, L., Schneider, H., Ladbury, J. E., and Rudd, C. E. Slp-76 sterile α motif (sam) and individual h5 α helix mediate oligomer formation for microclusters and t-cell activation. *Journal of Biological Chemistry 288*, 41 (2013), 29539–29549.

[103] Liu, S. K., Fang, N., Koretzky, G. A., and McGlade, C. J. The hematopoietic-specific adaptor protein gads functions in t-cell signaling via interactions with the slp-76 and lat adaptors. *Current Biology 9*, 2 (1999), 67–75.

[104] Lösing, M., Goldbeck, I., Manno, B., Oellerich, T., Schnyder, T., Bohnenberger, H., Stork, B., Urlaub, H., Batista, F. D., Wienands, J., et al. The dok-3/grb2 protein signal module attenuates lyn kinase-dependent activation of syk kinase in b cell antigen receptor microclusters. *Journal of Biological Chemistry 288*, 4 (2013), 2303–2313.

[105] Lyubchenko, T. Ca^{2+} signaling in b cells. *The Scientific World Journal 10* (2010), 2254–2264.

[106] Marienfeld, R. B., Palkowitsch, L., and Ghosh, S. Dimerization of the iκb kinase-binding domain of nemo is required for tumor necrosis factor alpha-induced nf-κb activity. *Molecular and cellular biology 26*, 24 (2006), 9209–9219.

[107] Marois, L., Vaillancourt, M., Paré, G., Gagné, V., Fernandes, M. J., Rollet-Labelle, E., and Naccache, P. H. Cin85 modulates the down-regulation of fcγriia expression and function by c-cbl in a pkc-dependent manner in human neutrophils. *Journal of Biological Chemistry 286*, 17 (2011), 15073–15084.

[108] Mayevska, O., Shuvayeva, H., Igumentseva, N., Havrylov, S., Basaraba, O., Bobak, Y., Barska, M., Volodko, N., Baranska, J., Buchman, V., et al. Expression of adaptor protein ruk/cin85 isoforms in cell lines of various tissue origins and human melanoma. *Exp. Oncol 28*, 4 (2006), 275–81.

[109] Medeiros, R. B., Burbach, B. J., Mueller, K. L., Srivastava, R., Moon, J. J., Highfill, S., Peterson, E. J., and Shimizu, Y. Regulation of nf-κb activation in t cells via association of the adapter proteins adap and carma1. *Science 316*, 5825 (2007), 754–758.

[110] Minegishi, Y., Rohrer, J., Coustan-Smith, E., Lederman, H. M., Pappu, R., Campana, D., Chan, A. C., and Conley, M. E. An essential role for blnk in human b cell development. *Science 286*, 5446 (1999), 1954–1957.

[111] Miyazaki, A., Yogosawa, S., Murakami, A., and Kitamura, D. Identification of cmtm7 as a transmembrane linker of blnk and the b-cell receptor. *PloS one 7*, 2 (2012), e31829.

[112] Molfetta, R., Belleudi, F., Peruzzi, G., Morrone, S., Leone, L., Dikic, I., Piccoli, M., Frati, L., Torrisi, M. R., Santoni, A., et al. Cin85 regulates the ligand-dependent endocytosis of the ige receptor: a new molecular mechanism to dampen mast cell function. *The Journal of Immunology 175*, 7 (2005), 4208–4216.

[113] Mor, A., and Philips, M. R. Compartmentalized ras/mapk signaling. *Annu. Rev. Immunol. 24* (2006), 771–800.

[114] Morita, S., Kojima, T., and Kitamura, T. Plat-e: an efficient and stable system for transient packaging of retroviruses. *Gene therapy 7*, 12 (2000), 1063–1066.

[115] Mullis, K., Faloona, F., Scharf, S., Saiki, R., Horn, G., and Erlich, H. Specific enzymatic amplification of dna in vitro: the polymerase chain reaction. *Cold Spring Harbor Symposia on Quantitative Biology* (1993), 263–273.

[116] Nakagawa, C., Nishimura, S., Senda-Murata, K., and Sugimoto, K. A rapid and simple method of evaluating the dimeric tendency of fluorescent proteins in living cells using a truncated protein of importin α as fusion tag. *Bioscience, biotechnology, and biochemistry 76*, 2 (2012), 388–390.

[117] Nam, J.-M., Onodera, Y., Mazaki, Y., Miyoshi, H., Hashimoto, S., and Sabe, H. Cin85, a cbl-interacting protein, is a component of amap1-mediated breast cancer invasion machinery. *The EMBO journal 26*, 3 (2007), 647–656.

[118] Niiro, H., and Clark, E. A. Regulation of b-cell fate by antigen-receptor signals. *Nature Reviews Immunology 2*, 12 (2002), 945–956.

[119] Niiro, H., Jabbarzadeh-Tabrizi, S., Kikushige, Y., Shima, T., Noda, K., Ota, S.-i., Tsuzuki, H., Inoue, Y., Arinobu, Y., Iwasaki, H., et al. Cin85 is required for cbl-mediated regulation of antigen receptor signaling in human b cells. *Blood 119*, 10 (2012), 2263–2273.

[120] Oancea, E., and Meyer, T. Protein kinase c as a molecular machine for decoding calcium and diacylglycerol signals. *Cell 95*, 3 (1998), 307–318.

[121] Oellerich, T., Bremes, V., Neumann, K., Bohnenberger, H., Dittmann, K., Hsiao, H.-H., Engelke, M., Schnyder, T., Batista, F. D., Urlaub, H., et al. The b-cell antigen

receptor signals through a preformed transducer module of slp65 and cin85. *The EMBO journal 30*, 17 (2011), 3620–3634.

[122] Oellerich, T., Grønborg, M., Neumann, K., Hsiao, H.-H., Urlaub, H., and Wienands, J. Slp-65 phosphorylation dynamics reveals a functional basis for signal integration by receptor-proximal adaptor proteins. *Molecular & Cellular Proteomics 8*, 7 (2009), 1738–1750.

[123] Ohta, Y., Haire, R. N., Litman, R. T., Fu, S. M., Nelson, R. P., Kratz, J., Kornfeld, S. J., de La Morena, M., Good, R. A., and Litman, G. W. Genomic organization and structure of bruton agammaglobulinemia tyrosine kinase: localization of mutations associated with varied clinical presentations and course in x chromosome-linked agammaglobulinemia. *Proceedings of the National Academy of Sciences 91*, 19 (1994), 9062–9066.

[124] Okabe, S., Tauchi, T., Ohyashiki, K., and Broxmeyer, H. E. Stromal-cell-derived factor-1/cxcl12-induced chemotaxis of a t cell line involves intracellular signaling through cbl and cbl-b and their regulation by src kinases and cd45. *Blood Cells, Molecules, and Diseases 36*, 2 (2006), 308–314.

[125] Onodera, Y., Hashimoto, S., Hashimoto, A., Morishige, M., Mazaki, Y., Yamada, A., Ogawa, E., Adachi, M., Sakurai, T., Manabe, T., et al. Expression of amap1, an arfgap, provides novel targets to inhibit breast cancer invasive activities. *The EMBO journal 24*, 5 (2005), 963–973.

[126] Ottinger, E. A., Botfield, M. C., and Shoelson, S. E. Tandem sh2 domains confer high specificity in tyrosine kinase signaling. *Journal of Biological Chemistry 273*, 2 (1998), 729–735.

[127] Pappu, R., Cheng, A. M., Li, B., Gong, Q., Chiu, C., Griffin, N., White, M., Sleckman, B. P., and Chan, A. C. Requirement for b cell linker protein (blnk) in b cell development. *Science 286*, 5446 (1999), 1949–1954.

[128] Park, J. H., Bae, J. Y., and Park, H. H. Self-oligomerization of the card domain prevents complex formation in the carma1 signalosome. *International journal of molecular medicine 31*, 5 (2013), 1280–1287.

[129] Patterson, H. C. K., Kraus, M., Kim, Y.-M., Ploegh, H., and Rajewsky, K. The b cell receptor promotes b cell activation and proliferation through a non-itam tyrosine in the igα cytoplasmic domain. *Immunity 25*, 1 (2006), 55–65.

[130] Peruzzi, G., Molfetta, R., Gasparrini, F., Vian, L., Morrone, S., Piccoli, M., Frati, L., Santoni, A., and Paolini, R. The adaptor molecule cin85 regulates syk tyrosine kinase level by activating the ubiquitin-proteasome degradation pathway. *The Journal of Immunology 179*, 4 (2007), 2089–2096.

[131] Petrelli, A., Gilestro, G. F., Lanzardo, S., Comoglio, P. M., Migone, N., and Giordano, S. The endophilin–cin85–cbl complex mediates ligand-dependent downregulation of c-met. *Nature 416*, 6877 (2002), 187–190.

[132] Petro, J. B., and Khan, W. N. Phospholipase c-γ2 couples bruton's tyrosine kinase to the nf-κb signaling pathway in b lymphocytes. *Journal of Biological Chemistry 276*, 3 (2001), 1715–1719.

[133] Philippe, D., Ababou, A., Yang, X., Ghosh, R., Daviter, T., Ladbury, J., and Pfuhl, M. Making ends meet: the importance of the n-and c-termini for the structure, stability, and function of the third sh3 domain of cin85. *Biochemistry 50*, 18 (2011), 3649–3659.

[134] Pierce, S. K., and Liu, W. The tipping points in the initiation of b cell signalling: how small changes make big differences. *Nature Reviews Immunology 10*, 11 (2010), 767–777.

[135] Pike, K. A., and Ratcliffe, M. J. Dual requirement for the igα immunoreceptor tyrosine-based activation motif (itam) and a conserved non-igα itam tyrosine in supporting ig$\alpha\beta$-mediated b cell development. *The Journal of Immunology 174*, 4 (2005), 2012–2020.

[136] Pirkuliyeva, S. *Structural and functional elucidation of the primary transducer module of the B cell antigen receptor*. PhD thesis, Georg-August-Universität, Göttingen, 2015.

[137] Poyet, J.-L., Srinivasula, S. M., Lin, J.-h., Fernandes-Alnemri, T., Yamaoka, S., Tsichlis, P. N., and Alnemri, E. S. Activation of the iκb kinases by rip via ikkγ/nemo-mediated oligomerization. *Journal of Biological Chemistry 275*, 48 (2000), 37966–37977.

[138] Qiao, Q., Yang, C., Zheng, C., Fontán, L., David, L., Yu, X., Bracken, C., Rosen, M., Melnick, A., Egelman, E. H., et al. Structural architecture of the carma1/bcl10/malt1 signalosome: nucleation-induced filamentous assembly. *Molecular cell 51*, 6 (2013), 766–779.

[139] Radaev, S., Zou, Z., Tolar, P., Nguyen, K., Nguyen, A., Krueger, P. D., Stutzman, N., Pierce, S., and Sun, P. D. Structural and functional studies of ig$\alpha\beta$ and its assembly with the b cell antigen receptor. *Structure 18*, 8 (2010), 934–943.

[140] Rajewsky, K. Clonal selection and learning in the antibody system. *Nature*, 381 (1996), 751–758.

[141] Rawlings, D. J. Bruton's tyrosine kinase controls a sustained calcium signal essential for b lineage development and function. *Clinical Immunology 91*, 3 (1999), 243–253.

[142] Rawlings, D. J., Saffran, D. C., Tsukada, S., Largaespada, D. A., Grimaldi, J. C., Cohen, L., Mohr, R. N., Bazan, J. F., Howard, M., Copeland, N. G., et al. Mutation of unique region of bruton's tyrosine kinase in immunodeficient xid mice. *Science 261*, 5119 (1993), 358–361.

[143] Rawlings, D. J., Scharenberg, A. M., Park, H., Wahl, M. I., Lin, S., Kato, R. M., Fluckiger, A.-C., Witte, O. N., and Kinet, J.-P. Activation of btk by a phosphorylation mechanism initiated by src family kinases. *Science 271*, 5250 (1996), 822–825.

[144] Rekas, A., Alattia, J.-R., Nagai, T., Miyawaki, A., and Ikura, M. Crystal structure of venus, a yellow fluorescent protein with improved maturation and reduced environmental sensitivity. *Journal of biological chemistry 277*, 52 (2002), 50573–50578.

[145] Reth, M. Antigen receptor tail clue. *Nature 338*, 6214 (1989), 383–384.

[146] Reth, M., Wienands, J., Tsubata, T., and Hombach, J. Identification of components of the b cell antigen receptor complex. In *Mechanisms of Lymphocyte Activation and Immune Regulation III*. Springer, 1991, pp. 207–214.

[147] Riebeling, C., Morris, A. J., and Shields, D. Phospholipase d in the golgi apparatus. *Biochimica et Biophysica Acta (BBA)-Molecular and Cell Biology of Lipids 1791*, 9 (2009), 876–880.

[148] Rincón, M., Flavell, R. A., and Davis, R. A. The jnk and p38 map kinase signaling pathways in t cell–mediated immune responses. *Free Radical Biology and Medicine 28*, 9 (2000), 1328–1337.

[149] Rodriguez, R., Matsuda, M., Storey, A., and Katan, M. Requirements for distinct steps of phospholipase cγ2 regulation, membrane-raft-dependent targeting and subsequent enzyme activation in b-cell signalling. *Biochem. J 374* (2003), 269–280.

[150] Rowley, R. B., Burkhardt, A. L., Chao, H.-G., Matsueda, G. R., and Bolen, J. B. Syk protein-tyrosine kinase is regulated by tyrosine-phosphorylated ig alpha/ig beta immunoreceptor tyrosine activation motif binding and autophosphorylation. *Journal of Biological Chemistry 270*, 19 (1995), 11590–11594.

[151] Salim, K., Bottomley, M. J., Querfurth, E., Zvelebil, M., Gout, I., Scaife, R., Margolis, R., Gigg, R., Smith, C., Driscoll, P., et al. Distinct specificity in the recognition of phosphoinositides by the pleckstrin homology domains of dynamin and bruton's tyrosine kinase. *The EMBO journal 15*, 22 (1996), 6241.

[152] Sambrook, J., and Russell, D. W. Molecular cloning: A laboratory manual . 2001, 2001.

[153] Sato, Y., Taoka, M., Sugiyama, N., Kubo, K.-i., Fuchigami, T., Asada, A., Saito, T., Nakajima, K., Isobe, T., and Hisanaga, S.-i. Regulation of the interaction of disabled-1 with cin85 by phosphorylation with cyclin-dependent kinase 5. *Genes to Cells 12*, 12 (2007), 1315–1327.

[154] Sauer, K., Liou, J., Singh, S. B., Yablonski, D., Weiss, A., and Perlmutter, R. M. Hematopoietic progenitor kinase 1 associates physically and functionally with the adaptor proteins

b cell linker protein and slp-76 in lymphocytes. *Journal of Biological Chemistry 276*, 48 (2001), 45207–45216.

[155] Scharenberg, A. M., and Kinet, J.-P. Ptdins-3, 4, 5-p3: a regulatory nexus between tyrosine kinases and sustained calcium signals. *Cell 94*, 1 (1998), 5–8.

[156] Schmalstieg, F. C., and Goldman, A. S. Birth of the science of immunology. *Journal of medical biography 18*, 2 (2010), 88–98.

[157] Schmidt, M. H., Chen, B., Randazzo, L. M., and Bögler, O. Seta/cin85/ruk and its binding partner aip1 associate with diverse cytoskeletal elements, including faks, and modulate cell adhesion. *Journal of cell science 116*, 14 (2003), 2845–2855.

[158] Schmidt, M. H., Dikic, I., and Bögler, O. Src phosphorylation of alix/aip1 modulates its interaction with binding partners and antagonizes its activities. *Journal of Biological Chemistry 280*, 5 (2005), 3414–3425.

[159] Schmidt, M. H., Hoeller, D., Yu, J., Furnari, F. B., Cavenee, W. K., Dikic, I., and Bögler, O. Alix/aip1 antagonizes epidermal growth factor receptor downregulation by the cbl-seta/cin85 complex. *Molecular and cellular biology 24*, 20 (2004), 8981–8993.

[160] Schroeder, B., Srivatsan, S., Shaw, A., Billadeau, D., and McNiven, M. A. Cin85 phosphorylation is essential for egfr ubiquitination and sorting into multivesicular bodies. *Molecular biology of the cell 23*, 18 (2012), 3602–3611.

[161] Schroeder, B., Weller, S. G., Chen, J., Billadeau, D., and McNiven, M. A. A dyn2–cin85 complex mediates degradative traffic of the egfr by regulation of late endosomal budding. *The EMBO journal 29*, 18 (2010), 3039–3053.

[162] Schroeder, H. W., and Cavacini, L. Structure and function of immunoglobulins. *Journal of Allergy and Clinical Immunology 125*, 2 (2010), S41–S52.

[163] Schulze-Luehrmann, J., and Ghosh, S. Antigen-receptor signaling to nuclear factor κb. *Immunity 25*, 5 (2006), 701–715.

[164] Shiue, L., Green, J., Green, O., Karas, J. L., Morgenstern, J. P., Ram, M. K., Taylor, M. K., Zoller, M. J., Zydowsky, L. D., and Bolen, J. B. Interaction of p72syk with the gamma and beta subunits of the high-affinity receptor for immunoglobulin e, fc epsilon ri. *Molecular and cellular biology 15*, 1 (1995), 272–281.

[165] Shyu, Y. J., Hiatt, S. M., Duren, H. M., Ellis, R. E., Kerppola, T. K., and Hu, C.-D. Visualization of protein interactions in living caenorhabditis elegans using bimolecular fluorescence complementation analysis. *Nature protocols 3*, 4 (2008), 588–596.

[166] Soubeyran, P., Kowanetz, K., Szymkiewicz, I., Langdon, W. Y., and Dikic, I. Cbl–cin85–endophilin complex mediates ligand-induced downregulation of egf receptors. *Nature 416*, 6877 (2002), 183–187.

[167] Srivastava, R., Burbach, B. J., and Shimizu, Y. Nf-κb activation in t cells requires discrete control of iκb kinase α/β (ikkα/β) phosphorylation and ikkγ ubiquitination by the adap adapter protein. *Journal of Biological Chemistry 285*, 15 (2010), 11100–11105.

[168] Stamenova, S. D., French, M. E., He, Y., Francis, S. A., Kramer, Z. B., and Hicke, L. Ubiquitin binds to and regulates a subset of sh3 domains. *Molecular cell 25*, 2 (2007), 273–284.

[169] Stork, B., Engelke, M., Frey, J., Horejsi, V., Hamm-Baarke, A., Schraven, B., Kurosaki, T., and Wienands, J. Grb2 and the non-t cell activation linker ntal constitute a ca 2+-regulating signal circuit in b lymphocytes. *Immunity 21*, 5 (2004), 681–691.

[170] Su, Y.-w., and Jumaa, H. Lat links the pre-bcr to calcium signaling. *Immunity 19*, 2 (2003), 295–305.

[171] Su, Y.-W., Zhang, Y., Schweikert, J., Koretzky, G. A., Reth, M., and Wienands, J. Interaction of slp adaptors with the sh2 domain of tec family kinases. *European journal of immunology 29*, 11 (1999), 3702–3711.

[172] Suzuki, H., Matsuda, S., Terauchi, Y., Fujiwara, M., Ohteki, T., Asano, T., Behrens, T. W., Kouro, T., Takatsu, K., Kadowaki, T., et al. Pi3k and btk differentially regulate b cell antigen receptor-mediated signal transduction. *Nature immunology 4*, 3 (2003), 280–286.

[173] Swamy, M., Kulathu, Y., Ernst, S., Reth, M., and Schamel, W. W. Two dimensional blue native-/sds-page analysis of slp family adaptor protein complexes. *Immunology letters 104*, 1 (2006), 131–137.

[174] Szymkiewicz, I., Kowanetz, K., Soubeyran, P., Dinarina, A., Lipkowitz, S., and Dikic, I. Cin85 participates in cbl-b-mediated down-regulation of receptor tyrosine kinases. *Journal of Biological Chemistry 277*, 42 (2002), 39666–39672.

[175] Takata, M., Sabe, H., Hata, A., Inazu, T., Homma, Y., Nukada, T., Yamamura, H., and Kurosaki, T. Tyrosine kinases lyn and syk regulate b cell receptor-coupled ca2+ mobilization through distinct pathways. *The EMBO Journal 13*, 6 (1994), 1341.

[176] Take, H., Watanabe, S., Takeda, K., Yu, Z.-X., Iwata, N., and Kajigaya, S. Cloning and characterization of a novel adaptor protein, cin85, that interacts with c-cbl. *Biochemical and biophysical research communications 268*, 2 (2000), 321–328.

[177] Tanner, M. J., Hanel, W., Gaffen, S. L., and Lin, X. Carma1 coiled-coil domain is involved in the oligomerization and subcellular localization of carma1 and is required for t cell receptor-induced nf-κb activation. *Journal of Biological Chemistry 282*, 23 (2007), 17141–17147.

[178] Tegethoff, S., Behlke, J., and Scheidereit, C. Tetrameric oligomerization of iκb kinase γ (ikkγ) is obligatory for ikk complex activity and nf-κb activation. *Molecular and cellular biology 23*, 6 (2003), 2029–2041.

[179] Tibaldi, E. V., and Reinherz, E. L. Cd2bp3, cin85 and the structurally related adaptor protein cms bind to the same cd2 cytoplasmic segment, but elicit divergent functional activities. *International immunology 15*, 3 (2003), 313–329.

[180] Titz, B., Low, T., Komisopoulou, E., Chen, S., Rubbi, L., and Graeber, T. The proximal signaling network of the bcr-abl1 oncogene shows a modular organization. *Oncogene 29*, 44 (2010), 5895–5910.

[181] Tossidou, I., Niedenthal, R., Klaus, M., Teng, B., Worthmann, K., King, B. L., Peterson, K. J., Haller, H., and Schiffer, M. Cd2ap regulates sumoylation of cin85 in podocytes. *Molecular and cellular biology 32*, 6 (2012), 1068–1079.

[182] Towbin, H., Staehelin, T., and Gordon, J. Electrophoretic transfer of proteins from polyacrylamide gels to nitrocellulose sheets: procedure and some applications. *Proceedings of the National Academy of Sciences 76*, 9 (1979), 4350–4354.

[183] Treanor, B., Depoil, D., Gonzalez-Granja, A., Barral, P., Weber, M., Dushek, O., Bruckbauer, A., and Batista, F. D. The membrane skeleton controls diffusion dynamics and signaling through the b cell receptor. *Immunity 32*, 2 (2010), 187–199.

[184] Tsuji, S., Okamoto, M., Yamada, K., Okamoto, N., Goitsuka, R., Arnold, R., Kiefer, F., and Kitamura, D. B cell adaptor containing src homology 2 domain (bash) links b cell receptor signaling to the activation of hematopoietic progenitor kinase 1. *The Journal of experimental medicine 194*, 4 (2001), 529–540.

[185] Tsukada, S., Rawlings, D. J., and Witte, O. N. Role of bruton's tyrosine kinase in immunodeficiency. *Current opinion in immunology 6*, 4 (1994), 623–630.

[186] Turvey, S. E., Durandy, A., Fischer, A., Fung, S.-Y., Geha, R. S., Gewies, A., Giese, T., Greil, J., Keller, B., McKinnon, M. L., et al. The card11-bcl10-malt1 (cbm) signalosome complex: Stepping into the limelight of human primary immunodeficiency. *Journal of Allergy and Clinical Immunology 134*, 2 (2014), 276–284.

[187] Venkitaraman, A. R., Williams, G. T., Dariavach, P., and Neuberger, M. S. The b-cell antigen receptor of the five immunoglobulin classes. *Nature*, 352 (1991), 777–781.

[188] Wang, W., Singh, S., Zeng, D. L., King, K., and Nema, S. Antibody structure, instability, and formulation. *Journal of pharmaceutical sciences 96*, 1 (2007), 1–26.

[189] Watanabe, S., Take, H., Takeda, K., Yu, Z.-X., Iwata, N., and Kajigaya, S. Characterization of the cin85 adaptor protein and identification of components involved in cin85 complexes. *Biochemical and biophysical research communications 278*, 1 (2000), 167–174.

[190] Wells, C. D., Fawcett, J. P., Traweger, A., Yamanaka, Y., Goudreault, M., Elder, K., Kulkarni, S., Gish, G., Virag, C., Lim, C., et al. A rich1/amot complex regulates the cdc42 gtpase and apical-polarity proteins in epithelial cells. *Cell 125*, 3 (2006), 535–548.

[191] Wienands, J., Freuler, F., and Baumann, G. Tyrosine-phosphorylated forms of ig β, cd22, tcr ζ and hoss are major ligands for tandem sh2 domains of syk. *International immunology 7*, 11 (1995), 1701–1708.

[192] Wienands, J., Schweikert, J., Wollscheid, B., Jumaa, H., Nielsen, P. J., and Reth, M. Slp-65: a new signaling component in b lymphocytes which requires expression of the antigen receptor for phosphorylation. *The Journal of experimental medicine 188*, 4 (1998), 791–795.

[193] Wilson, C. B., and Marcuse, E. K. Vaccine safety–vaccine benefits: science and the public's perception. *Nature Reviews Immunology 1*, 2 (2001), 160–165.

[194] Winding, P., and Berchtold, M. W. The chicken b cell line dt40: a novel tool for gene disruption experiments. *Journal of immunological methods 249*, 1 (2001), 1–16.

[195] Wollscheid, B., Wienands, J., and Reth, M. The adaptor protein slp-65/blnk controls the calcium response in activated b cells. In *Mechanisms of B Cell Neoplasia 1998*. Springer, 1999, pp. 283–289.

[196] Wong, J., Ishiai, M., Kurosaki, T., and Chan, A. C. Functional complementation of blnk by slp-76 and lat linker proteins. *Journal of Biological Chemistry 275*, 42 (2000), 33116–33122.

[197] Xu, S., Tan, J. E.-L., Wong, E. P.-Y., Manickam, A., Ponniah, S., and Lam, K.-P. B cell development and activation defects resulting in xid-like immunodeficiency in blnk/slp-65-deficient mice. *International immunology 12*, 3 (2000), 397–404.

[198] Yang, J., and Reth, M. Oligomeric organization of the b-cell antigen receptor on resting cells. *Nature 467*, 7314 (2010), 465–469.

[199] Yoon, H.-Y., Kales, S. C., Luo, R., Lipkowitz, S., and Randazzo, P. A. Arap1 association with cin85 affects epidermal growth factor receptor endocytic trafficking. *Biology of the Cell 103*, 4 (2011), 171–184.

[200] Zhang, J., Zheng, X., Yang, X., and Liao, K. Cin85 associates with endosomal membrane and binds phosphatidic acid. *Cell research 19*, 6 (2009), 733–746.

[201] Zheng, X., Zhang, J., and Liao, K. The basic amino acids in the coiled-coil domain of cin85 regulate its interaction with c-cbl and phosphatidic acid during epidermal growth factor receptor (egfr) endocytosis. *BMC biochemistry 15*, 1 (2014), 13.

7 Appendix

7.1 The Proteome of VAMP7$^+$ vesicles in DT40 B cells

Tab. 7.1: The Proteome of VAMP7-containing vesicles in DT40 cells. See 3.2.3.3 and the end of this table for experimental details.

Vesicular transport	Syntaxin-12
	Syntaxin-16
Vesicular coat	Syntaxin-binding protein 3
AP-1 β	Syntaxin-binding protein 5
AP-1 γ	t-SNARE domain-containing protein 1
AP-1 μ-1	
AP-1 AR	**other vesicular transport components**
AP-2 β	SCY1-like protein 2
AP-3 β-1	Vesicle-fusing ATPase
AP-3 δ	Synaptic vesicle membrane protein
AP-5 ζ-1	VAT-1 homolog
Clathrin heavy chain	Exocyst complex component 4
Clathrin heavy chain 2	
Clathrin light chain A	**ER**
Clathrin light chain B	All-trans-retinol 13,14-reductase
	α-mannosidase-like protein 3
Rab proteins	ER membrane complex subunit 1
Rab-4A	Hypoxia up-regulated protein 1
Rab-11A	Manganese-transporting ATPase 13A1
Rab-11B	PIEZO1
Rab-14	PIP3-phosphatase TPTE2
Rab3 GTPase-activating protein	Solute carrier family 2, member 3
catalytic subunit	Thioredoxin domain-containing protein 11
	Ubiquitin carboxyl-terminal hydrolase
SNAREs	
VAMP3	**Golgi apparatus / TGN**
VAMP4	α-mannosidase 2
VAMP7	Beta-soluble NSF attachment protein
VTI 1A	Calcium-transporting ATPase 2C member 1
VTI 1B	cGMP-inhibited 3',5'-cyclic
Syntaxin-6	phosphodiesterase B
Syntaxin-7	Coatomer subunit alpha
Syntaxin-8	Copper-transporting ATPase 1
	Endophilin-B1
	Fibronectin type-III
	domain-containing protein 3A
	γ-aminobutyric acid
	receptor-associated protein-like 2
	γ-soluble NSF attachment protein
	Golgin subfamily A member 2
	Golgin subfamily A member 4
	Golgin subfamily A member 5
	Golgin subfamily A member 7
	Golgin subfamily B member 1
	H(+)/Cl(-) exchange transporter 5
	HIP1
	HIP1R
	Kinesin-like protein KIF16B
	Maspardin
	Microtubule-actin cross-linking factor 1
	N-acetylglucosamine-1-phosphodiester
	α-N-acetylglucosaminidase
	Oxysterol-binding protein
	Oxysterol-binding protein L1A
	Phospholipase D4
	Probable phospholipid-transporting ATPase IB
	Probable phospholipid-transporting ATPase IIB
	Proprotein convertase subtilisin/kexin type 7
	Prostaglandin F2 receptor negative regulator
	Protein bicaudal D homolog 2
	Protein GPR107
	Protein transport protein Sec24A
	Protein XRP2
	Serine/threonine-protein kinase 16
	SNARE-associated protein Snapin
	Stathmin-3

Trafficking protein particle complex subunit 2
Trafficking protein particle complex subunit 5
Trafficking protein particle complex subunit 6B
Trafficking protein particle complex subunit 8
Trafficking protein particle complex subunit 9
Trafficking protein particle complex subunit 10
Trafficking protein particle complex subunit 11
Trafficking protein particle complex subunit 12
Tumor protein p63-regulated gene 1-like protein
UDP-glucuronic acid decarboxylase 1

Endosomal
1-phosphatidylinositol 3-phosphate 5-kinase
EH domain-containing protein 4
H(+)/Cl(-) exchange transporter 4
KIDINS220
KxDL motif-containing protein 1
Oxysterol-binding protein-related protein 10
Phosphatidylinositol 4-kinase type 2-α
Phosphatidylinositol 4-kinase type 2-β
Phosphatidylinositol 4-phosphate 3-kinase
C2 domain-containing subunit alpha
Phosphoinositide-binding protein 1
Polyphosphoinositide phosphatase
Probable phospholipid-transporting ATPase IF
RUN and SH3 domain-containing protein 1
Secretory carrier-associated membrane protein 2
Secretory carrier-associated membrane protein 4
Sodium/hydrogen exchanger
Sorting nexin-3
Sorting nexin-4
Sorting nexin-12
Sorting nexin-27
Spermatogenesis-defective protein 39
Target of Myb protein 1
TGF-beta-activated kinase 1 and
MAP3K7-binding protein 1
Transferrin receptor protein 1, CD71
Transmembrane 9 superfamily member 2
Transmembrane 9 superfamily member 2
Tyrosine-protein kinase JAK1
VAC14 homolog
VPS 11
VPS 18
VPS 26A
VPS 26B
VPS 29
VPS 29
VPS 33A
VPS 35
VPS 39
VPS 41
VPS 45
WAS protein family homolog 1
WASH complex subunit 7
WASH complex subunit CCDC53
WASH complex subunit FAM21A
WASH complex subunit strumpellin
Zinc finger FYVE domain-containing protein 21

Lysosomal
Acid ceramidase
ADP-ribosylation factor-like protein 8A
Aldo-keto reductase family 1 member B10
β-galactosidase
Cathepsin B
Cathepsin D
Cathepsin Z
Cation-independent
mannose-6-phosphate receptor
Cytochrome b ascorbate-dependent protein 3
DEP domain-containing
mTOR-interacting protein
Dipeptidyl peptidase 1
Dipeptidyl peptidase 2
DnaJ homolog subfamily C member 5
DnaJ homolog subfamily C member 13
DNAJC25
E3 ubiquitin-protein ligase RNF13
Ganglioside-induced
differentiation-associated protein 2
H(+)/Cl(-) exchange transporter 7
Heme transporter HRG1
Iduronate 2-sulfatase
LAMP-1
LAMP-2C
LAMP-3
LAMP-5
Legumain
Lipopolysaccharide-induced tumor
necrosis factor-alpha factor homolog
LMBR1 domain-containing protein 2
Lysosomal cholesteryl ester hydrolase

Lysosomal α-glucosidase
Lysosomal protective protein
Lysosome membrane protein 2
Mannose 6-Phosphate Receptor
N-acetylgalactosamine-6-sulfatase
N-acetylglucosamine-6-sulfatase
Niemann-Pick C1 protein
Nitrogen permease regulator 3-like protein
Palmitoyl-protein thioesterase 1
Patatin-like phospholipase
domain-containing protein 7
Probable lysosomal cobalamin transporter
Proton-coupled amino acid transporter 1
Ragulator complex protein LAMTOR1
Ragulator complex protein LAMTOR2
Ragulator complex protein LAMTOR3
Ragulator complex protein LAMTOR5
Ras-related GTP-binding protein B
Ras-related GTP-binding protein C
Saposin-A
Serine/threonine-protein kinase mTOR
Signal peptide peptidase-like 2A
Solute carrier family 35 member F6
Transmembrane protein 192
Uncharacterized protein C18orf8
Vesicle transport protein SFT2A
V-ATPase 116 kDa subunit a
V-ATPase 16 kDa proteolipid subunit
V-ATPase catalytic subunit A
V-ATPase subunit B
V-ATPase subunit C 1
V-ATPase subunit d 1
V-ATPase subunit E 1
V-ATPase subunit G 1
V-type proton ATPase subunit S1
WD repeat-containing protein 11
WD repeat-containing protein 59
WD repeat-containing protein mio

secreted
Adenosine deaminase CECR1
α/β hydrolase domain-containing
protein 17A
α/β hydrolase domain-containing
protein 17B
Attractin
β-galactosidase-1-like protein
Coiled-coil domain-containing protein 126
γ-glutamyl hydrolase
γ-interferon-inducible lysosomal thiol reductase
Glucose-6-phosphate isomerase
Insulin-degrading enzyme
Protein SZT2
Synaptogyrin

BCR complex components
B29/Ig-β
Ig heavy chain V-III region VH26
Lyn

Plasma membrane
ABC transporter A family member 2
ABC transporter C family member 3
ABC transporter C family member 4
activin like receptor kinase 5
Amyloid-like protein 2
ATP-binding cassette sub-family A member 3
B-cell differentiation antigen CD72
Bis(5'-adenosyl)-triphosphatase ENPP4
C2 domain-containing protein 5
Carboxypeptidase D
CD44-like protein
Cell cycle control protein 50A
CKLF-like MARVEL transmembrane
domain-containing protein 7
Common cytokine receptor g chain
Contactin-associated protein 1
DENN domain-containing protein 5B
Endothelin converting enzyme-1
EGFR substrate 15-like 1
Equilibrative nucleoside transporter 1
Formin-like protein 1
Guanine nucleotide-binding protein G(i) a-1
Guanine nucleotide-binding protein G(k) a
Guanine nucleotide-binding protein G(q) a
Guanine nucleotide-binding protein a-11
Guanine nucleotide-binding protein a-13
Guanine nucleotide-binding protein g
High affinity cationic amino acid transporter 1
Integral membrane protein 2A
Integral membrane protein GPR155
Integrin α FG-GAP repeat-containing protein 1
Integrin α FG-GAP repeat containing 3

Integrin β
Large neutral amino acids transporter small subunit 4
Leucyl-cystinyl aminopeptidase
Ldl receptor-related protein 8
Macrophage-expressed gene 1 protein
Monoacylglycerol lipase ABHD6
Monocarboxylate transporter 1
Neutral amino acid transporter A
Nicastrin
Nodal modulator 1
Nucleoside diphosphate kinase
Pituitary tumor-transforming gene 1 protein-interacting protein
Plasma membrane calcium-transporting ATPase 1
Prestin
Probable cation-transporting ATPase 13A3
Protein kinase C and casein kinase substrate in neurons protein 3
Protein MAL2
Protein RFT1 homolog
PX domain-containing protein kinase-like protein
Receptor-type tyrosine-protein phosphatase a
Receptor-type tyrosine-protein phosphatase S
Rho-related GTP-binding protein RhoG
Semaphorin-4D, CD100
Sn_1-specific diacylglycerol lipase beta
Sodium- and chloride-dependent glycine transporter 1
Sodium- and chloride-dependent taurine transporter
Sodium bicarbonate cotransporter 3
Sodium-coupled neutral amino acid transporter 1
Sodium-coupled neutral amino acid transporter 2
Sodium-dependent glucose transporter 1
Sodium-dependent phosphate transporter 2
Solute carrier family 12 member 4
Solute carrier family 12 member 5
Solute carrier family 12 member 7
Solute carrier family 15 member 4
Solute carrier family 22 member 16
Solute carrier family 43 member 3
Spatacsin
Tetraspanin-3
Toll-like receptor 2 type-2
Toll-like receptor 21
Transient receptor potential cation channel subfamily M member 7
Transmembrane 9 family member 4
Transmembrane protein 87A
Transmembrane protein 9B
Uncharacterized protein KIAA1467
UPF0505 protein C16orf62
Voltage-gated hydrogen channel 1
Zinc transporter 1

Cytosolic
Adenylosuccinate lyase
Alanine–tRNA ligase, cytoplasmic
ANKRD27
Casein kinase I γ-1
COMMD1
COMMD4
COMMD5
COMMD6
COMMD7
COMMD8
COMMD9
COMMD10
Ferritin heavy chain
Galectin 8
GTPase-activating Rap/RanGAP domain-like 1 protein
Guanylate cyclase
Major vault protein
N-α-acetyltransferase 25
NEDD4-like E3 ubiquitin-protein ligase WWP2
Peptidyl-prolyl cis-trans isomerase
Protein RUFY3
Ral GTPase-activating protein a-2
Serologically defined colon cancer antigen 3
STIP1 homology and U box-containing protein 1
TBC1 domain family member 5
TGF-β receptor-associated protein 1
Toll-interacting protein
Tyrosine-protein phosphatase non-receptor type 9
Ubiquitin conjugation factor E4 A

Cytoskeleton-associated	**Unknown localization**
CD2-binding protein 1	AMSH-like protease
Cytoplasmic dynein 1 heavy chain 1	Ankyrin repeat and IBR domain-containing protein 1
MAP7 domain-containing protein 2	Coiled-coil domain-containing protein 93
Myosin-Ic	Down syndrome critical region protein 3
Myosin-Id	Endonuclease/exonuclease/phosphatase
Myosin-Ig	family domain-containing protein 1
Myosin-Va	Kelch-like protein 6
Protein 4.1	Leucine-rich repeat and IQ domain-containing protein 1
Protein JTB	Protein FAM45A
	Protein FAM91A1
Mitochondrial	Protein MEF2BNB
Cysteine desulfurase, mitochondrial	SPRY domain-containing protein 7
δ-1-pyrroline-5-carboxylate synthase	UHRF1-binding protein 1-like
GRAM domain-containing protein 4	Uncharacterized protein C17orf59
NAD(P) transhydrogenase, mitochondrial	Uncharacterized protein CXorf21
NADH dehydrogenase [ubiquinone] 1 α 9	WD repeat and FYVE domain-containing protein 2
NADH dehydrogenase [ubiquinone] 1 α 10	WD repeat-containing protein 81
	WD repeat-containing protein 91
Nuclear	
Polymerase δ-interacting protein 2	

The proteome of VAMP7-containing vesicles in DT40 cells was determined by SILAC-based mass spectrometry. A plasmid coding for Cerulean-tagged VAMP7 was introduced inDT40 cells by retroviral transduction. The cells were labeled by growing them in SILAC medium containing the heavy isotope labeled amino acids lysine+4 and arginine+6. As a control, DT40 cells transduced with eGFP were grown in medium with light amino acids. The differently labeled cells were mechanically disrupted by passing them through a Balch homogenizer (Figure 4.5). The PNS subjected to affinity purification with α-GFP antibodies. In the end, the light and heavy labeled samples were pooled in a 1:1 ratio and subsequently analyzed by mass spectrometry. The experiment was repeated 4 times, proteins appearing at least 3 times at a heavy to light ratio of 2 or higher were regarded as component of the vesicular proteome.

7.2 Amino acid single letter code

A	Alanine
C	Cysteine
D	Aspartic acid
E	Glutamic acid
F	Phenylalanine
G	Glycine
H	Histidine
I	Isoleucine
K	Lysine
L	Leucine
M	Methionine
N	Asparagine
P	Proline
Q	Glutamine
R	Arginine
S	Serine
T	Theronine
V	Valine
W	Tryptophane
X	any amino acid
Y	Tyrosine

7.3 Deoxyribonucleotide single letter code

A	Deoxyadenosine monophosphate
C	Deoxycytidine monophosphate
G	Deoxyguanosine monophosphate
T	Deoxythymidine monophosphate

7.4 Abbreviations

α	anti
aa	amino acid
ADAP	adhesion and degranulation promoting adaptor protein
ADAP2	Arf-GAP with dual PH domain-containing protein 2
ADCC	antibody-dependent cellular cytotoxicity
Akt	AKR mouse transforming
Alix	ALG-2-interacting protein X
ALKBH2	α-ketoglutarate-dependent dioxygenase alkB homolog 2
AP	affinity purification
APC/C	anaphase promoting complex/cyclosome
APS	ammonium persulfate
ARAP1	Arf-GAP with Rho-GAP domain, ANK repeat and PH domain-containing protein 1
ARHGAP17	Rho GTPase-activating protein 17
ASAP1	Arf-GAP with SH3 domain, ANK repeat and PH domain-containing protein 1
ASC	apoptosis-associated speck-like protein containing a CARD
ATP	adenosine triphosphate
BASH	B cell adaptor containing SH2 domain
bca	B cell activation
BCL10	B-cell lymphoma/leukemia 10
BCR	B cell receptor
BiFC	Bimolecular fluorescence complementation
bleo	bleomycin resistance
BLNK	B cell linker
BSA	bovine serum albumin
Btk	Bruton's tyrosine kinase
C domain	constant domain
C2	Protein kinase C conserved region 2
Ca^{2+}	calcium^{2+} ion
CapZ	capping protein (actin filament) muscle Z-line
CARD11	caspase recruitment domain-containing protein 11
Cbl	Casitas B-lineage lymphoma
CBM	CARD11-BCL10-MALT1
CC	coiled-coil
C_C	C-terminal half of CIN85 coiled-coil domain

CCDC88B	coiled-coil domain-containing protein 88B
CD	cluster of differentiation
CD2AP	CD2-associated protein
CDC	complement-dependent cytotoxicity
CDC21	cell division cycle 21
CH	Ig heavy chain constant domain
CIN85	Cbl-interacting protein of 85 kDa
CIP	calf intestinal phosphatase
Cit	Citrine
CLEC17a	C-type lectin 17a
ClpC	ATP-dependent Clp protease subunit C
CMTM7	CKLF-like MARVEL transmembrane domain-containing protein 7
C_N	N-terminal half of CIN85 coiled-coil domain
COPI	coat protein complex I
Crk	CT10 Regulator of Kinase
Cyt	cytosol
D segment	diversifying segment
Dab2	disabled homolog 2
DAG	diacyl-glycerol
ΔN	devoid of the N-terminal region
DMEM	Dulbecco's modified Eagle's medium
DMSO	dimethyl sulfoxide
DNA	deoxyribonucleic acid
dNTP	deoxynucleoside triphosphate
DTT	dithiothreitol
E. coli	*Escherichia coli*
ECL	enhanced chemical luminescence
EDTA	ethylenediaminetetraacetic acid
EGF	epidermal growth factor
EGFR	epidermal growth factor receptor
eGFP	enhanced green fluorescent protein
ER	endoplasmic reticulum
ERK	extracellular signal-regulated kinase
ESCRT-I	endosomal sorting complex required for transport I
ESI	electrospray ionization
F(ab')2	bivalent antigen binding fragment

FBXO28	F-box only protein 28
Fc	fragment crystallizable
FcαR	Fc α Receptor
FcγR	Fc γ Receptor
FcϵR	Fc ϵ Receptor
FcR	Fc Receptor
FCS	fetal calf serum
fw	forward
FYB	FYN-binding protein
GADS	GRB2-related adaptor protein 2
GAP	GTPase activating protein
GFP	green fluorescent protein
GM130	130 kDa cis-Golgi matrix protein
Grb2	growth factor receptor-bound protein 2
GTP	guanosine triphosphate
HA	hemaglutinin
HEPES	4-(2-hydroxyethyl)-1-piperazineethanesulfonic acid
His6	hexahistidine tag
HRP	horseradish peroxidase
HUS1	checkpoint protein HUS1
Ig	immunoglobulin
IgSF	immunoglobulin super-family
IKK	Inhibitor of κB kinase
INDO-1 AM	INDO-1 acetoxymethylester
IP3	inositol trisphosphate
IPTG	isopropyl-β-D-thiogalactopyranoside
ITAM	immunoreceptor tyrosine-based activation motif
ITT	immunoreceptor tail tyrosine
J segment	joining segment
JNK	c-Jun N-terminal kinase
kB	kilobasepair
kDa	kilodalton
LAMP1	lysosome-associated membrane glycoprotein 1
LAT	linker of activated T cells
LB	lysogeny broth
LEW	Lysis-Equilibration-Wash

Lyn	Lck/yes-related novel protein tyrosine kinase
M2,3	CIN85 binding motifs 2 and 3
MALLS	multiangle laser light scattering
MALT1	mucosa-associated lymphoid tissue lymphoma translocation protein 1
MAPK	mitogen activated protein kinase
MecA	methicillin resistance determinant A
MIRab13	molecule interacting with Rab13
MIRR	multichain immune recognition receptor
mRNA	messenger ribonucleic acid
mTOR	mechanistic target of rapamycin
MVB12A	multivesicular body subunit 12A
N-BAR	N-terminal Bin-Amphiphysin-Rvs
NEMO	NFκB essential modulator
NFAT	nuclear factor of activated T cells
NfκB	nuclear factor of κ light polypeptide gene enhancer in B cells
NLRP3	NACHT, LRR and PYD domains-containing protein 3
NMR	nuclear magnetic resonance
OSBP1	oxysterol-binding protein 1
p110	phosphatidylinositol 3-kinase 110 kDa catalytic subunit
p38	mitogen-activated protein kinase p38
p85	phosphatidylinositol 3-kinase 85 kDa regulatory subunit
PA	phosphatidic acid
PAGE	polyacrylamide gel electrophoresis
PBS	phosphated buffered saline
PCR	polymerase chain reaction
PH	pleckstrin-homology
PI3K	phosphatidylinositol-3-kinase
PIP_2	phosphatidylinositol-4,5-bisphosphate
PIP_3	phosphatidylinositol-3,4,5-trisphosphate
PKC-β	protein kinase C-β
PLC	phospholipase C
PNS	postnuclear supernatant
PRR	proline-rich region
puro	puromycin resistance
pY	phosphorylated tyrosine residue
Rab5	Ras-related protein Rab5

Raf1	rat fibrosarcoma proto-oncogene serine/threonine-protein kinase
Raf-PA	Raf1 phosphatidic acid binding motif
RAG	recombination activating gene
Ras	GTPase rat sarcoma
RASAL2	Ras GTPase-activating protein nGAP
rev	reverse
RIP1	receptor-interacting serine/threonine-protein kinase 1
RL	arginine-to-leucine exchange in the SLP65 SH2 domain
RNA	ribonucleic acid
RPMI	Roswell Park Memorial Institute
RSS	recombination signal sequences
RT	room temperature
Ruk	regulator of ubiquitous kinase
SAM	sterile α motif
SCOC	short coiled-coil protein
SDS	sodium dodecyl sulfate
SETA	SH3 domain containing gene expressed in tumorigenic astrocytes
SH2	src homology 2
SH3	src homology 3
SH3BP1	SH3 domain-binding protein 1
SHP2	SH2 domain-containing phosphatase 2
SHIP1	SH2 domain-containing inositol phosphatase 1
SHKBP1	SH3KBP1-binding protein 1
SILAC	stable isotope labeling by amino acids in cell culture
SIPA1	signal-induced proliferation-associated protein 1
SLP65	SH2-domain containing leukocyte protein of 65 kDa
SLP76	SH2-domain containing leukocyte protein of 76 kDa
SNARE	soluble NSF attachment protein receptor
SOC	store-operated Ca^{2+} channel
SOS	son of sevenless
Src	rous sarcoma oncogene
STAP1	signal-transducing adaptor protein 1
STIM	stromal interaction module
Syk	spleen tyrosine kinase
TAE	Tris acetate EDTA buffer
TBC	Tre-2, Bub2p, and Cdc16p

TBS	Tris buffered saline
TBS-T	Tris buffered saline-Tween
TCR	T cell receptor
TdT	terminal deoxynucleotidyl transferase
Tec	tyrosine kinase expressed in hepatocellular carcinoma
TEMED	tetramethylethylenediamine
TGN	trans-Golgi network
TIRAP	Toll-interleukin 1 receptor domain-containing adaptor protein
TRIM62	tripartite motif-containing protein 62
Tris	tris(hydroxymethyl)-aminomethane
tSH2	tandem SH2
V domain	variable domain
V segment	variable segment
VAMP7	vesicle-associated membrane protein 7
VC	Venus C-terminal part
VN	Venus N-terminal part
VSV	vesicular stomatitis virus
wt	wild-type
X-gal	5-bromo-4-chloro-3-indolyl-β-D-galactopyranoside
XLA	X-linked agammaglobulinemia
ZAP70	ζ-associated protein of 70 kDa

7.5 Figures

7.6 Tables

8 Acknowledgements

First of all, I want to express my gratitude towards my supervisor Prof. Jürgen Wienands for giving me the opportunity to create this thesis in his group and discovering the fascinating world of B cell immunology. I appreciated especially his ubiquitous willingness to discuss results and his openess to new ideas and suggestions. This influenced my picture of scientific work a lot. I also thank him for providing me the opportunity to do a great research internship in Paris which was a very valuable experience. Thanks to Dr. Barbara Bertocci for enabling my stay in France.
I am grateful for the help of the two other members of my thesis committee, Prof. Blanche Schwappach and Prof. Henning Urlaub for their interest in my project and the remunerating suggestions they came up with during the thesis committee meetings. Thanks also to Prof. M. Thumm, Prof. D. Kube and Prof. U. Großfor taking part in my thesis defense as members of the examination board.
Furthermore, I want to thank the members of the Wienands lab for their support, scientifically and non-scientifically. I want to emphasize my thanks to Michael, for sharing his knowledge and expertise of at least ten years of work on SLP65, and especially to Sona. I want to thank her for the really good collaboration during the whole three years and for the many, many discussions about our projects and the mutual motivations we could gain from this. I liked the nice working atmosphere in our group due to Christoffer, Caren, Kanika, Vanessa, Kathrin, Kai, Lars and Niklas. We formed a good running team at several occasions (Altstadtlauf, Frühjahrslauf). I always enjoyed the interesting conversations with Johannes about all kind of topics, thanks to him for making the lab life less monotonous. I also want to express my thanks to Gabi and Ines for organizing the lab and keeping things running by endless preparation of buffers, media, pipette tips Just as important for me was the support of Annika and Ingrid Teuteberg regarding all the administrative stuff.

I really appreciated the collaboration with our NMR co-workers, Prof. Christian Griesinger, Stefan, Luigi , and Leo. We had always interesting meetings, fruitfully exchanging ideas from two different corners of biology. Leo invested a lot of effort in the successful elucidation of the CIN85 coiled-coil structure. This progress helped our project a lot. The membership of our group within the SFB860 brought many great scientific meetings and interesting ideas because it connected us with other groups in Göttingen working on macromolecular complexes. Janina Boyken shared her excellent knowledge concerning the technique of subcellular fractionation with me which was were helpful. Mariana Guimaraes de Araujo taught me the technique of cell homogenization by cavitation. I acknowledge also the help of Sabrina Beckmann and Dr. Karin Kühnel who provided the plasmids for split Venus respectively SCOC. I thank Prof. Carsten Lüder for the access to the confocal microscope and the group of Prof. R. Jahn for access to their ultracentrifuges.

Thanks to Elena and Carina, Kai, Katharina and Amina for the nice chats, motivations and friendship I could get from the other side of immunology, from people working wiht T(!!!) cells and even with mice I thank also my long-term friends from the Frankfurt area, especially Michael and Stefan. They have the ability to cheer me up by funny discussions, even after long days in the lab. I thank my flatmate since one and a half year, Anja, and her boyfriend Lars, for making our flat in Göttingen a real home to me by their patience, help in all every day situations and even for directing my nutrition towards more healthy stuff like salad.
Nearly last, but probably most of all, I want to thank Anna for giving me the energy to write this thesis. Finally, I am so grateful to my family, my parents, my brother Koni, my sister Biri, Ömi and Großmutter for the ever-lasting support a got and still get from them.